ORANGE COUNTY FLOOD CONTROL DISTRICT

SANTA ANA, CALIFORNIA
92702

EXPERIMENTAL AND MATHEMATICAL INVESTIGATION OF FLOW OVER SIDE-WEIRS IN OPEN CHANNELS

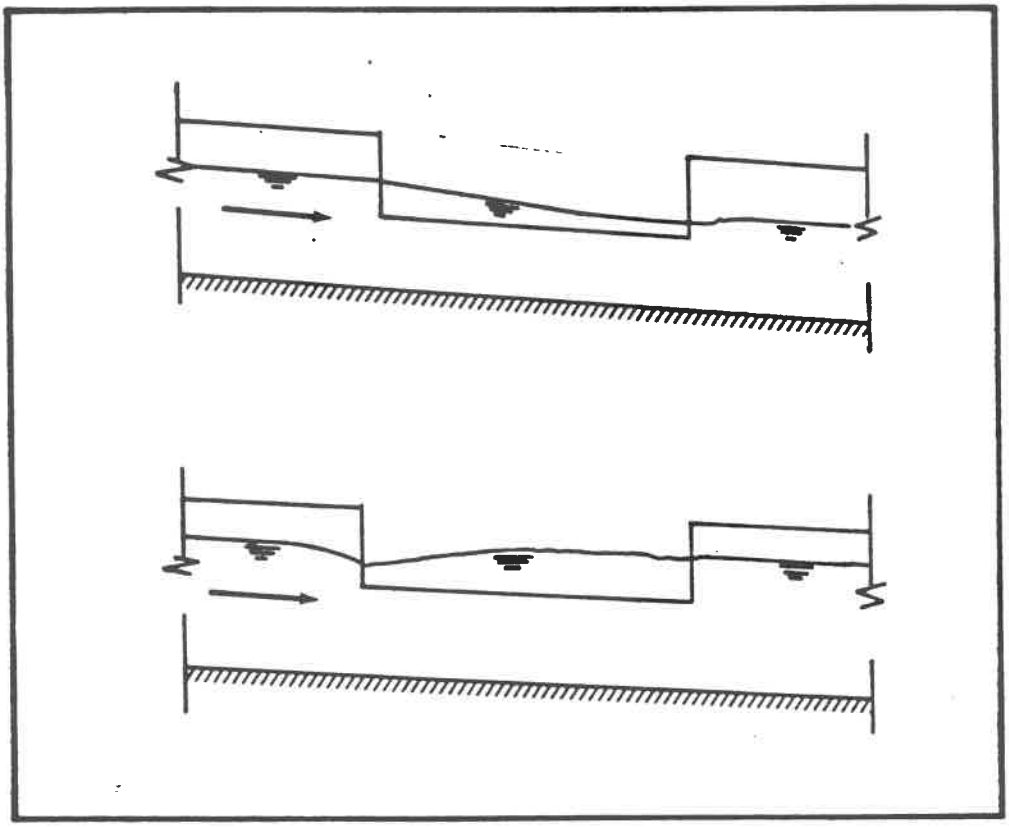

Prepared by

M. Gamal Mostafa, Principal Investigator

and

Gene H. Chu, Research Associate

ENGINEERING RESEARCH CENTER

CALIFORNIA STATE UNIVERSITY LONG BEACH FOUNDATION

90840

cfa] ORANGE COUNTY FLOOD CONTROL DISTRICT
SANTA ANA, CALIFORNIA
92702

EXPERIMENTAL AND MATHEMATICAL INVESTIGATION OF FLOW OVER SIDE-WEIRS IN OPEN CHANNELS

Final Report No. ERC-74-012-F
June 15, 1974

Prepared by
M. Gamal Mostafa, Principal Investigator
and
Gene H. Chu, Research Associate

ENGINEERING RESEARCH CENTER
CALIFORNIA STATE UNIVERSITY LONG BEACH FOUNDATION
90840

ACKNOWLEDGEMENTS

This research was carried out at the hydraulics laboratory of California State University, Long Beach, with the financial support of Orange County Flood Control District (OCFCD). Mr. H. G. Osborne, Chief Engineer, and many other engineers of the District visited the laboratory and the flumes during the study. In particular, Mr. Joe Natsuhara who represented OCFCD in liaison with the research group followed and discussed every step of the research and made very helpful suggestions.

The following Civil Engineering Department personnel contributed to the study in various capacities:

Faculty:	Ali Eshett
Technicians:	John Bartley Tony Vandagriff Jim Compton
Graduate Students:	Omer Zeki Kayiran Dorothy Weisz Kuang Liu
Undergraduate Students:	Valerie DaSilva Al Mikinka

Thanks are also due to Mrs. Helen Tyler for typing the final manuscript.

M. Gamal Mostafa
Principal Investigator

Gene Chu
Research Associate

K = constant in equation 5 and equals 1 when computations proceed downstream and -1 when computations proceed upstream

L = length

M_i = function for simulating the momentum equation when applied to block i

n = Manning's coefficient of friction

P = wetted perimeter

Q = discharge in the channel

Q_w = discharge over the side-weir

q = lateral discharge per unit weir length

S_o = bed slope

S_f = friction slope

S_m = minor-loss slope

T = top width

t = time

V = average velocity of flow

x = distance along the channel

y = depth of flow

y_a = depth of water at the mid-point of a block

y_w = weir height

Z = height above an arbitrary horizontal datum

$\not{z}$ = side-slope (1 vertical on $\not{z}$ horizontal)

α = energy correction factor

θ = angle between the streamlines over the weir and a line normal to the channel centerline at the beginning of the weir

LIST OF FIGURES

ABSTRACT

Extensive experimental and theoretical research on flow over side-weirs in open channels has led to computer solutions which can be effectively used for design purposes. Programs OCFCD4A and OCFCD4B, dealing with steady and unsteady flow conditions respectively, are introduced in this report. The steady flow mathematical model which led to Program OCFCD4A was verified experimentally by two physical models, a rectangular and a trapezoidal channel. The coefficient for side-weir discharge was found to depend on the ratio of weir discharge to total discharge and on channel side-slope. A relation between these variables was established through numerous verification tests (equation 20).

Several characteristics of flow over side-weirs were analyzed by theory and observed by experiment, leading to some design guidelines for the side-weirs and their stilling basins which are given in Chapter

VIII and to the conclusions which are given in Chapter IX. Although this research has covered a wide range of variables for side-weir flow, it only dealt with the case of sharp-crested side-weirs. It is recommended that further research be carried out to derive and verify appropriate modifications to the mathematical models which would extend their applicability to other means of diversion such as broad-crested weirs and chute drops.

TABLE OF CONTENTS

SYMBOLS

Symbols are defined in the report when they first appear and are also listed below for the reader's convenience.

A = Cross-sectional area of flow

B = Channel bed width

B_1&B_2 = functions to describe first and second boundary conditions, respectively

C_1,C_2 C_3&C_4 = constants

C_d = discharge coefficient for the side-weir

C_{de} = discharge coefficient computed from relation of the experimental water surface profile and side-weir discharge

C_{dm} = discharge coefficient computed by the numerical model to verify measured side-weir discharge

C_{dl} = discharge coefficient for the weir in case of longitudinal flow

C_{ds} = discharge coefficient under submerged conditions

C_i = function for simulating continuity equation at subreach i

d = differential

g = acceleration due to gravity

H = Head of water above weir-crest in the channel

$= y-y_w$

H_1 = Height of water above weir crest in the stilling basin

i = channel block; also used for station number

j = time level

I. INTRODUCTION

When severe storms of infrequent recurrance occur, the peak discharge in a channel can be appreciably reduced by means of diversion of excess flood waters into a retarding basin. Automatic gates, inlet spillways, siphon spillways or lateral spillways are some of the means of diversion commonly used. Lateral spillways or side-weirs are usually preferred because they require the least maintenance.

The effects of the 1969 flood, which was similar to a 30-year flood, demonstrated the need for further flood protection projects at several locations in Orange County. For this reason, Orange County Flood Control District (OCFCD) has been carrying out extensive studies leading to the design and construction of flood control improvements in several channels. The channels in some cases are provided with means of diversion of excess flood waters into retarding basins for the purpose of reducing peak discharge of the standard project flood.

During the summer of 1972, Mostafa (1) prepared a report for OCFCD describing the state-of-the-art on the subject of flow over side-weirs. Then, OCFCD engaged the services of the Hydraulics Laboratory of the Engineering Research Center at California State University, Long Beach to carry out theoretical and experimental research leading to a verified mathematical model for the general solution of flow over

side-weirs. The research was to consider and seek answers to the following items:

(a) Determination of the discharge rate over the side-weir when the main channel, either rectangular or trapezoidal, flows in supercritical or subcritical velocity;

(b) Relative locations of transitions in side-weirs;

(c) Effect of imposition of subcritical condition in the upstream, in the downstream or at locations of the weir;

(d) Effect of ascending and descending flood stages;

(e) Submergence of side-weir due to rising of water level in the stilling basin;

(f) Comparison of mathematical model to physical model.

This report describes the findings of the research regarding these and other parameters that seemed pertinent during the study, and introduces verified computer programs capable of computing the discharge over a side-weir under various conditions.

Starting from the basic concepts of conservation of mass, energy and momentum, differential equations for determining the water surface profile and the discharge over a side-weir have been derived by many investigators over the years. A chronological presentation of the development of theory is given in reference 1. The exact analytical solution of these

differential equations is not available. By neglecting the friction loss, De Marchi (2) developed a method for determining the approximate solution of the equations which can only apply to steady flow in a prismatic rectangular channel with a horizontal bottom slope.

In the past decade due to the availability of high speed digital computers, numerical techniques have been introduced for solving steady gradually-varied flow equations and several computer programs (3) have been developed. However, these programs are for the purpose of computing water surface profiles in channels with no spatial variation such as the case of a side-weir. Not until recently was a numerical procedure which enables the computation of steady gradually-varied spatially decreasing flow in an open channel presented by Smith (4). The procedure is limited, however, to the case of channels with constant bed slope and no upstream or downstream control. Smith applied his program for computing subcritical and supercritical water surface profiles in the weir reach with the consideration of possible hydraulic jumps and assumed a constant side-weir coefficient of discharge in his application.

For practical use of side-weirs in channels, the slopes of the channel upstream, along, and downstream of the side-weir may be different. Water depth controls may also be expected at the beginning and/or at the end of the channel.

Only a mathematical model which can handle the computation of flow profiles in channels with or without boundary controls and with different bottom slopes upstream, along, and downstream of the side-weir may be used to determine the side-weir discharge of such cases. The development of such a mathematical model was therefore one of the main objectives of this study.

For the design of flood control channels with side-weirs to release excess flood waters, the concept of using a peak flow rate to determine extreme conditions of water surface profile and side-weir discharge satisfies most of the engineering design needs. However, for some special cases, in which accurate design data are needed, it is important to predict the variation in the water depth and discharge along the channel when the flood wave in the form of a storm hydrograph at the upstream end propogates downstream. This information can only be obtained by investigating the behavior of the unsteadiness of the side-weir flow and the flow along the channel. The equations governing the unsteady-gradually varied flow in a channel with no side-weir have been solved numerically and have been applied successfully by Amein (5) and several other investigators using various finite difference methods. But very little material is known regarding the unsteady spatially-varied flow computations in open channels with side-weirs. In this study a mathematical model

using the implicit finite difference method for solving the governing equation for unsteady spatially-varied flow is developed to investigate the unsteadiness of flow in channels with side-weirs. The advantage of using the implicit method over other finite difference methods for this application is that it can be applied to subreaches with different lengths and to relatively large time intervals without affecting the stability of the solution. Since in channel flow computations the steady solution represents one case of the unsteady solution, results obtained from the unsteady model can be used to verify the results obtained from the steady model.

The accuracy of applying the mathematical models for predicting side-weir discharge and water surface profile depends mostly on whether or not an appropriate side-weir coefficient of discharge can be chosen. Many factors can affect the value of this coefficient and the most reliable method for its determination is by experimental work.

Side-weirs are usually constructed in channels with either trapezoidal or rectangular cross-sections. Some experimental data are available (6) on flow behaviour over side-weirs for rectangular channels. Hardly any experimental information is known for trapezoidal channels. For this reason, two flumes, one rectangular and one trapezoidal, were used in this study. The main objective of the experimental investigation was to verify the mathematical solutions

experimentally, and to determine the appropriate coefficients of discharge which should be used in applying the mathematical models.

II. BASIC EQUATIONS OF THE MATHEMATICAL MODELS

STEADY FLOW EQUATIONS

Spatially-varied flow can be analyzed by proper application of either the momentum or the energy principle whether it is the case of a decreasing discharge in a channel or an increasing discharge in a channel. Either principle will lead to the same dynamic equation. For prismatic channels, the water surface profile equation can be represented by

$$\frac{dy}{dx} = \frac{S_o - S_f - (\alpha Q/gA^2)\frac{dQ}{dx} + (\alpha Q^2/gA^2)\frac{\partial A}{\partial x}}{1 - \alpha Q^2 T/gA^3} \qquad ..(1)$$

in which S_o = bed slope, S_f = friction slope; α = energy correction factor, g = acceleration due to gravity; A = cross-sectional area of flow, T = top width, Q = discharge in the channel, x = distance along the channel, $\partial A/\partial x$ = partial derivative of cross-sectional area with respect to x, when flow depth y is constant and $dQ/dx = -\frac{2}{3}Cd\sqrt{2g}\ H^{3/2}$, dQ being the discharge over the side-weir along an incremental distance dx, H = height of water above the weir-crest and C_d = coefficient of discharge.

For a channel with nonprismatic sections, the slope of minor loss due to contraction or expansion is added and the water surface profile equation becomes

$$\frac{dy}{dx} = \frac{S_o - S_f - S_m - (\alpha Q/gA^2)dQ/dx + (\alpha Q^2/gA^3)\partial A/\partial x}{1 - \alpha Q^2 T/gA^3} \qquad ..(2)$$

in which S_m is the minor loss slope.

UNSTEADY FLOW EQUATIONS

The mathematical equations governing unsteady flow in an open channel with side weirs may be written as

$$\frac{\partial A}{\partial t} + \frac{\partial (AV)}{\partial x} + q = 0 \qquad ..(3)$$

and

$$\frac{\partial (AV)}{\partial t} + \frac{\partial}{\partial x}(AV^2) + gA\frac{\partial y}{\partial x} + gA(S_f - S_o) + qV = o \qquad ..(4)$$

In the above equations, A is the channel section area, V is the average velocity of the flow, q is the lateral discharge per unit length of the side-weir, y is the channel water depth, S_f is the frictional slope and may be expressed by Manning's formula, S_o is the channel bottom slope, x is the distance along the channel, and t is the time.

Equation 3 is known as the equation of continuity and is the mathematical expression for the law of conservation of mass, while Equation 4 is the momentum equation and is the mathematical expression for the law of conservation of momentum rate. Derivation of these equations can be found in reference (1). Since steady flow is a special case of unsteady flow, Equation 1 which governs the steady spatially-varied flow with lateral discharge can also be derived from Equations 3 and 4 by deleting terms associated with time t.

Equations 3 and 4 serve as the basis for constructing

mathematical models for the study of unsteady spatially-varied flow with a decreasing discharge due to a side-weir. Mathematical application of unsteady flow conditions in fact consists of finding solutions of the two equations in conformance with the necessary boundary conditions. The boundary conditions may consist of known changes in water levels, discharges or discharge-depth relationships at two ends of the channel reach. By using an appropriate numerical method for finding the solutions of Equations 3 and 4 with the associated boundary conditions, the water depths, discharges and velocities at all sections of a channel reach can be determined as functions of time.

III. FINITE DIFFERENCE SCHEMES

THE STEADY FLOW CASE

To solve equation 1 or equation 2 numerically for computing the water surface profile, an iteration process has been used. This process is similar to the one used by Prased (7) and by Smith (4) with some minor modifications. A block of water along the channel between stations i and i + 1 as shown in figure 1 is considered. When the depth of flow y_i at station i is known, either an assumed value of dy/dx or the value of dy/dx calculated for the previous step is used to compute an approximate depth of flow y_{i+1} at station i + 1 as follows:

$$y_{i+1} = y_i + K(dy/dx)\Delta x \qquad ..(5)$$

where K is a constant which is 1 when computations proceed downstream and is -1 when computations proceed upstream. For achieving the same degree of accuracy in the computation process along the channel, the incremental step Δx in the above equation is taken inversely proportional to the absolute value of the slope of the water surface profile dy/dx of the previous station. The head over the side-weir is

$$H = y_a - y_w$$

where y_w is the height of weir crest above the channel bottom and y_a is the depth of water at the midpoint of the block and is expressed by

$$y_a = (y_i + y_{i+1})/2$$

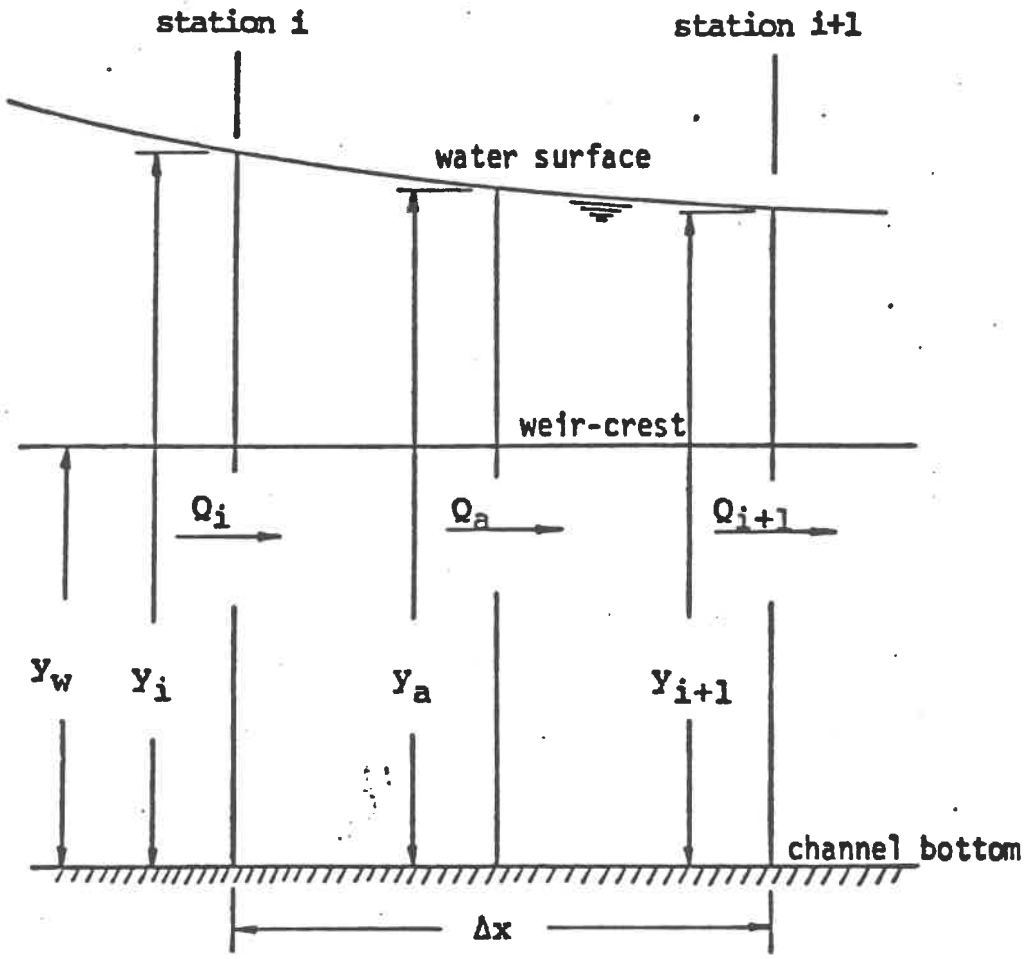

Figure 1

Definition Sketch of the Numerical Process
for Computing Water Surface Profile

The lateral discharge over the side-weir dQ/dx depends on H and for a channel with a rectangular side-weir,

$$dQ/dx = -(2/3)\, C_d \sqrt{2g}\, H^{3/2} \qquad ..(6)$$

where C_d is the discharge coefficient. The change of discharge (Q) with distance (x) for a channel with a trapezoidal side-weir reach is different from the change for a channel with a rectangular side-weir reach. When the channel cross section in the side-weir reach is trapezoidal, flow not only discharges laterally over the weir length into the retarding basin but also longitudinally at both the beginning and the end of the side-weir. For this case equation 6 should be modified as follows:

$$dQ/dx = -(2/3)\, C_d \sqrt{2g}\, H^{3/2} - (4/15)\, C_{d1}\, Z \sqrt{2g}\, H^{5/2} \qquad ..(7)$$

in which Z is the side slope of the trapezoidal section, C_{d1} is a discharge coefficient equivalent to the coefficient of a V-notch weir with side slope Z. In the above equation, the second term exists only at the beginning and at the end of the side-weir. It has little effect upon the flow except in the case of very short weir length.

With the aid of equation 6 or 7 the discharge at the midpoint of the block can be obtained as follows:

$$Q_a = Q_i + K(dQ/dx)\, \Delta x/2$$

where Q_i is the discharge at station i. Knowing Q_a and y_a the velocity of flow V and the variation in A for a fixed

depth ($\partial A/\partial x$) are found. Substituting these values in equation 1 or equation 2, whichever case may be, a new value of water depth variation dy/dx is obtained. The new values of water depth and discharge at station i + 1 can be computed as follows:

$$Y_{i+1} = Y_i + K\,(dy/dx)\,\Delta x$$

and

$$Q_{i+1} = Q_a + K(dQ/dx)\Delta x/2$$

If the new y_{i+1} is close to the original y_{i+1} within a pre-specified tolerable limit, computations proceed to the next channel block. Otherwise, the value of the depth of flow y_{i+1} at station i + 1 is taken as the average of the new and the previously found values and the same iteration process is repeated until the difference is within tolerable limits.

THE UNSTEADY FLOW CASE

Numerical methods for solving unsteady flow partial differential equations are based on replacing the derivatives in the equations by the corresponding finite difference counterparts. In recent years several finite difference numerical methods have been introduced and applied successfully to artificial and natural channels (5, 8). The most commonly used methods are the methods of characteristics by finite difference, the explicit finite difference method and the implicit finite difference method. In the method of characteristics by finite difference, equations are first transformed into the characteristics form and then finite difference representation is introduced to the characteristic curves on the time-distance plane. In the explicit method, the equations are directly transformed into finite difference counterparts forming linear algebraic equations from which the unknowns can be evaluated explicitly at a given time interval. On the other hand, in the implicit finite difference method the finite difference representation is introduced to the equations in such a way that the equations become nonlinear algebraic equations and the unknowns appear implicitly in the equations. Solutions to these unknowns can be found by the application of Newton-Raphson iteration method or any other method capable of solving nonlinear system of algebraic equations.

A numerical procedure developed by Chu (9) for formulating the finite difference equations by the implicit method is used in this study. Equations 3 and 4 are first transformed to their integral counterparts and applied to a channel block (as shown in figure 2) between two adjacent sections x and x + Δx as follows:

$$\frac{d}{dt'}\left[\frac{1}{\Delta x}\int_x^{x+\Delta x} A(x',t')dx'\right] + \frac{d}{dx'}\left[A(x',t')V(x',t')\right] - \frac{1}{\Delta x}\int_x^{x+\Delta x} q(x',t')dx' = 0 \qquad ..(8)$$

$$\frac{d}{dt'}\left[\frac{1}{\Delta x}\int_x^{x+\Delta x} A(x',t')V(x',t')dx'\right] + \frac{d}{dx'}\left[A(x',t')V^2(x',t')\right] - g\frac{1}{\Delta x}\int_x^{x+\Delta x}\left\{\frac{d}{dx'}\left[y(x',t') + Z(x')\right]A(x',t')\right\}dx' + g\frac{1}{\Delta x}\left(\frac{n}{1.49}\right)^2\int_x^{x+\Delta x} V(x',t')\left|V(x',t')\right|\left[\frac{P(x',t')}{A(x',t')}\right]^{4/3}A(x',t')dx' + \frac{1}{\Delta x}\int_x^{x+\Delta x} v(x',t')q(x',t')dx' = 0 \qquad ..(9)$$

In the above two equations, x' (distance) and t' (time) are independent variables within the channel block, S_0 is expressed in terms of Z(x') which is the channel bottom elevation with respect to a horizontal datum, and S_f is given by Manning's formula.

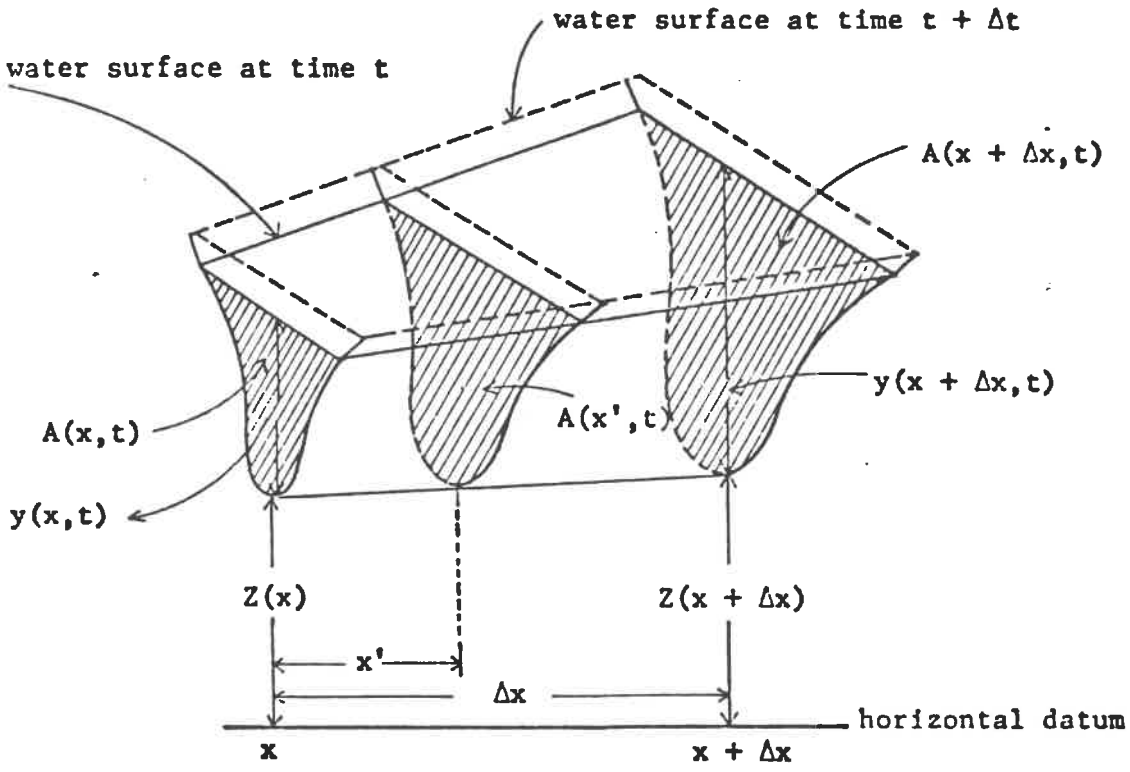

Figure 2

Definition Sketch for Equations 8 and 9

When variables in the above two equations are considered to vary linearly with both time (t) and distance (x), these two equations can be converted to:

$$[\int_x^{x+\Delta x} A(x',t+\Delta t)dx' - \int_x^{x+\Delta x} A(x',t)dx']$$

$$+ \int_t^{t+\Delta t} [A(x+\Delta x,t')V(x+\Delta x,t') - A(x,t')V(x,t')]dt'$$

$$- \int_t^{t+\Delta t}\int_x^{x+\Delta x} q(x,'t')dx'dt' = 0 \qquad ..(10)$$

$$[\int_x^{x+\Delta x} A(x',t+\Delta t)V(x',t+\Delta t)dx' - \int_x^{x+\Delta x} A(x',t)V(x',t)dx']$$

$$+ \int_t^{t+\Delta t} [A(x+\Delta x,t')V^2(x+\Delta x,t') - A(x,t')V^2(x,t')]dt'$$

$$- g\int_t^{t+\Delta t} \{[y(x+\Delta x,t') + Z(x+\Delta x) - y(x,t') - Z(x)]\forall(t')\}dt'$$

$$+ g(\frac{n}{1.49})^2 \int_t^{t+\Delta t} \{\int_x^{x+\Delta x} [A(x',t')V(x',t')]|A(x',t')V(x',t')|$$

$$\frac{P^{4/3}(x',t')}{A^{4/3}(x',t')}dx'\}dt' + \int_t^{t+\Delta t}\int_x^{x+\Delta x} v(x',t')q(x',t')dx'dt' = 0$$

$$..(11)$$

Equations 10 and 11 can also be written in the form:

$$[V(t+\Delta t) - V(t)] + \frac{1}{2}\frac{\Delta t}{\Delta x}[Q(x+\Delta x,t+\Delta t) + Q(x+\Delta x,t) - Q(x,t+\Delta t) - Q(x,t)] - \frac{1}{2}\frac{\Delta t}{\Delta x}\int_x^{x+\Delta x}[q(x',t) + q(x',t+\Delta t)]dx' = 0 \quad ..(12)$$

$$[Q(x+\Delta x,t+\Delta t) + Q(x,t+\Delta t) - Q(x+\Delta x,t) - Q(x,t)] + \frac{\Delta t}{\Delta x}\left[\frac{Q^2(x+\Delta x,t+\Delta t)}{A(x+\Delta x,t+\Delta t)} + \frac{Q^2(x+\Delta x,t)}{A(x+\Delta x,t)} - \frac{Q^2(x,t+\Delta t)}{A(x,t+\Delta t)} - \frac{Q^2(x,t)}{A(x,t)}\right]$$
$$-\left(g\frac{\Delta t}{\Delta x}\right)\{[y(x+\Delta x,t+\Delta t) + Z(x+\Delta x) - y(x,t+\Delta t) - Z(x)]V(t+\Delta t) - [y(x+\Delta x,t) + Z(x+\Delta x) - y(x,t) - Z(x)]V(t)\} \quad ..(13)$$
$$+ \left(g\frac{\Delta t}{\Delta x}\right)\left(\frac{n}{1.49}\right)^2\{\int_x^{x+\Delta x}\left[Q(x',t+\Delta t)\,|Q(x',t+\Delta t)|\frac{P^{4/3}(x',t+\Delta t)}{A^{7/3}(x',t+\Delta t)}\right]dx' + \int_x^{x+\Delta x}\left[Q(x',t)\,|Q(x',t)|\frac{P^{4/3}(x',t)}{A^{7/3}(x',t)}\right]dx'\}$$
$$+ \frac{\Delta t}{\Delta x}\int_x^{x+\Delta x}[V(x',t)q(x',t) + V(x',t+\Delta t)q(x',t+\Delta t)]\,dx' = 0$$

Where $Q(x,t) = A(x,t)V(x,t)$ is the discharge at location (x) and time (t) and $\forall(t)$ is the volume of flow of the channel block at time (t).

To convert the above two equations into the finite-difference forms, the variables at locations x and x + Δx are expressed by using superscripts i and i + 1 respectively; the variables at t and t + Δt are expressed by using subscripts j and j + 1 respectively. The continuity equation in the finite-difference form becomes

$$[\forall_i^{j+1} - \forall_i^j] + \frac{1}{2}\frac{\Delta t}{\Delta x}[Q_{i+1}^{j+1} + Q_i^j - Q_{i+1}^{j+1} - Q_i^j] \qquad ..(14)$$
$$- \frac{1}{2}\frac{\Delta t}{\Delta x}[\text{Ł}_i^{j+1} + \text{Ł}_i^j] = 0$$

where $\text{Ł}_i^j = \int_x^{x+\Delta x} q(x',t)\,dx'$ = volume of lateral flow in the channel block and the equation of motion in the finite-difference form becomes

$$[Q_{i+1}^{j+1} + Q_i^{j+1} - Q_{i+1}^j - Q_i^j] + \frac{\Delta t}{\Delta x}\left[\frac{(Q_{i+1}^{j+1})^2}{A_{i+1}^{j+1}} + \frac{(Q_{i+1}^j)^2}{A_{i+1}^j}\right.$$
$$\left. + \frac{(Q_i^{j+1})^2}{A_i^{j+1}} + \frac{(Q_i^j)^2}{A_i^j}\right] - \left(g\frac{\Delta t}{\Delta x}\right)\{[y_{i+1}^{j+1} + z_{i+1} - y_i^{j+1} - z_i]\forall_i^{j+1}$$
$$- [y_{i+1}^j + z_{i+1} - y_i^j - z_i]\forall_i^j\} + \left(g\frac{\Delta t}{\Delta x}\right)\left(\frac{n}{1.49}\right)^2(F_i^{j+1} + F_i^j)$$

$$+ \frac{\Delta t}{\Delta x}(R_i^{j+1} + R_i^j) = 0 \qquad ..(15)$$

where $F_i^j = \int_x^{x+\Delta x}[Q(x',t)|Q(x',t)|\frac{P^{4/3}(x',t)}{A^{7/3}(x',t)}\,dx']$

and is the momentum (excluding density) due to the frictional force in the channel block, and $R_i^j = \int_x^{x+\Delta x} v(x',t)q(x',t)dx'$ is the momentum (excluding density) due to lateral flow into or out of the channel block. L_i^j, F_i^j and R_i^j can be evaluated by numerical integration techniques.

The finite-difference scheme as expressed by equations 14 and 15 can be programmed to handle any combination of the following upstream and downstream boundary conditions; two possible upstream boundary conditions are

1. stage or depth hydrograph at upstream is given, or
2. discharge hydrograph at upstream is given,

while three possible downstream boundary conditions are

1. stage or depth hydrograph at downstream is given,
2. discharge hydrograph at downstream is given, or
3. rating curve (stage-discharge relationship) is given.

For simplicity, equations 14 and 15 are represented by:

$$C\ (y_i,\ y_{i+1},\ V_i,\ V_{i+1}) = 0 \qquad ..(16)$$

$$M\ (y_i,\ y_{i+1},\ V_i,\ V_{i+1}) = 0 \qquad ..(17)$$

where function C denotes the continuity equation in finite difference form and function M denotes the momentum equation in finite difference form as applied to a channel block i. Note that each of the above two equations consists of four unknowns.

To apply the implicit finite difference method, the channel reach under consideration is divided into n sub-reaches with (n-1) channel blocks. Equations 16 and 17 are then introduced to each of the (n-1) channel blocks forming 2(n-1) equations. Although there are four unknowns in each equation, two of them appear also in the neighboring equations. In other words, when equations 16 and 17 are applied to all the (n-1) channel blocks, only 2n unknowns are implicitly contained in the 2(n-1) nonlinear algebraic equations. Since 2(n-1) equations are not sufficient to solve 2n unknowns, two additional equations are needed and usually can be provided by the upstream and/or the downstream boundary conditions.

For a subcritical unsteady channel flow case, the upstream boundary condition can be either a discharge hydrograph which describes a discharge Q versus time t relationship or a stage hydrograph which expresses the depth y versus time t relationship at the upstream end of the channel reach; the downstream boundary condition usually is given by a rating curve which provides the relationship between discharge Q versus depth y.

For a supercritical unsteady channel flow case, flow is controlled at the upstream end and normally two upstream boundary conditions are required. The first upstream boundary condition may be a discharge or stage hydrograph while the second upstream boundary condition may be a rating curve such as a Q versus y relationship expressed by the uniform flow criteria.

In summary the 2n equations applying to a channel with (n-1) subreaches for a subcritical channel flow case can be written:

$$B_1 (y_1, V_1) = 0$$
$$C_1 (y_1, V_1, y_2, V_2) = 0$$
$$M_1 (y_1, V_1, y_2, V_2) = 0$$
$$\vdots$$
$$C_i (y_i, V_i, y_{i+1}, V_{i+1}) = 0$$
$$M_i (y_i, V_i, y_{i+1}, V_{i+1}) = 0$$
$$\vdots$$
$$C_{n-1} (y_{n-1}, V_{n-1}, y_n, V_n) = 0$$
$$M_{n-1} (y_{n-1}, V_{n-1}, y_n, V_n) = 0$$
$$B_2 (y_n, V_n) = 0$$

while for a supercritical channel flow case they can be written as:

$$B_1 (y_1, V_1) = 0$$
$$B_2 (y_1, V_1) = 0$$

$$C_1 (y_1, V_1, y_2, V_2) = 0$$
$$M_1 (y_1, V_1, y_2, V_2) = 0$$
$$\vdots$$
$$C_i (y_i, V_i, y_{i+1}, V_{i+1}) = 0$$
$$M_i (y_i, V_i, y_{i+1}, V_{i+1}) = 0$$
$$\vdots$$
$$C_{n-1} (y_{n-1}, V_{n-1}, y_n, V_n) = 0$$
$$M_{n-1} (y_{n-1}, V_{n-1}, y_n, V_n) = 0$$

In the above equations, B_1 is a function to describe the first boundary condition, B_2 is a function to describe the second boundary condition, C_i and M_i are functions for simulating continuity equation and momentum equation at subreach i respectfully.

Direct methods for the solution of the above nonlinear algebraic system of equations are not available. Among the available indirect methods, Newton-Raphson's iteration method proved to be effective and powerful for the solution of this system. In general this method consists of assigning trial values into the equations for computing a residual for each equation. A correction procedure consisting of a series of iteration steps is then followed to adjust the trial values until each residual approaches zero or is reduced to a tolerable quantity.

IV. DESCRIPTION OF THE PHYSICAL MODELS

A rectangular and a trapezoidal flume were used for the purpose of experimental verification of the numerical models developed for this study. Each of these flumes utilized the laboratory circulating flow facility which could handle discharges up to 2.5 cfs (the laboratory new circulating flow facility which will be available by August, 1974 will be able to handle up to 6 cfs).

THE RECTANGULAR FLUME

The rectangular flume shown diagramatically in figure 3, is approximately 60' long with glass sides and steel bottom. Its cross section is 10" wide and 18" deep. The flume is mounted on a steel frame supported by jacks which are used to adjust the slope of the flume. A 6' panel near the center reach was removed from one side of the flume and replaced by a sharp-edged steel plate which acted as the side-weir. Plates of 1", 2", 3", 4", and 5" height were alternately used in the experiments. Water was supplied from the constant-level tank on the laboratory roof through a 6" pipeline into the inlet box of the flume. Water discharged from the downstream end of the flume and from the side-weir, into tanks leading to V-notch weirs for discharge measurement before returning to the underground reservoir to be pumped up to the constant-level tank and so on.

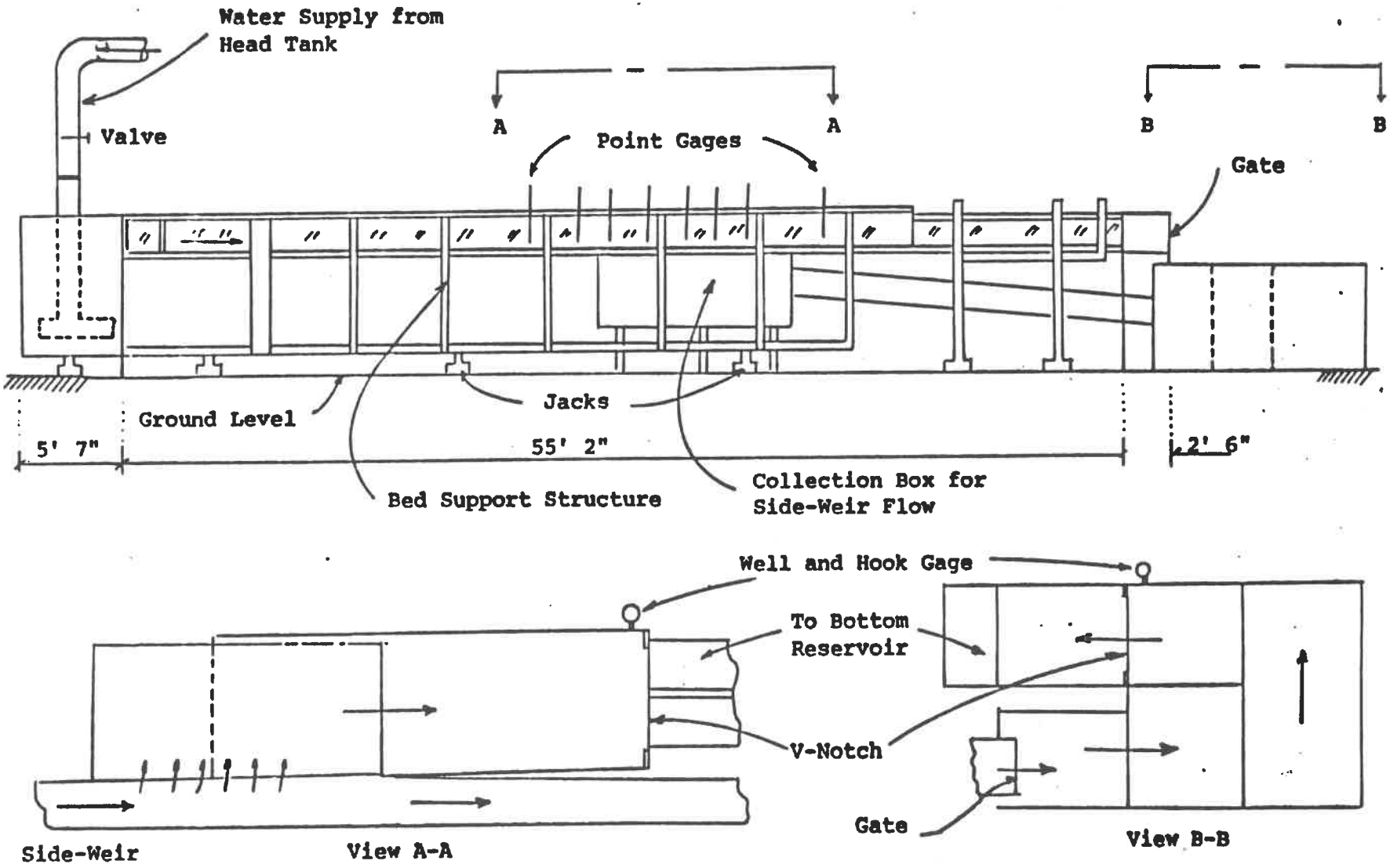

Figure 3 The Rectangular Flume

THE TRAPEZOIDAL FLUME

A trapezoidal flume 46' long, 1' deep with 10" bottom width and 1 vertical to 1.5 horizontal side-slope was specially constructed for this study. The flume shown diagramatically in figure 4, is carried by a steel-reinforced wooden frame with adjustable supports for setting different channel slopes. A sharp-edged side-weir was provided on one side of the flume by cutting the upper portion of a 5' panel of the flume side. The same circulating flow system as for the rectangular flume was used. Water was supplied from the constant-level tank through a 6" pipeline into a wooden intake structure 6' x 6' in base area and 6' in depth. The beginning of the side-weir was located 25 feet downstream of intake structure. Flow over the side-weir discharged into a short side channel and then through a 4" pipeline leading into the underground reservoir. A Venturi-meter was placed in the 4" line to measure the side-weir flow, and another Venturi-meter was mounted on the 6" inlet pipeline to monitor the flow rate into the main channel.

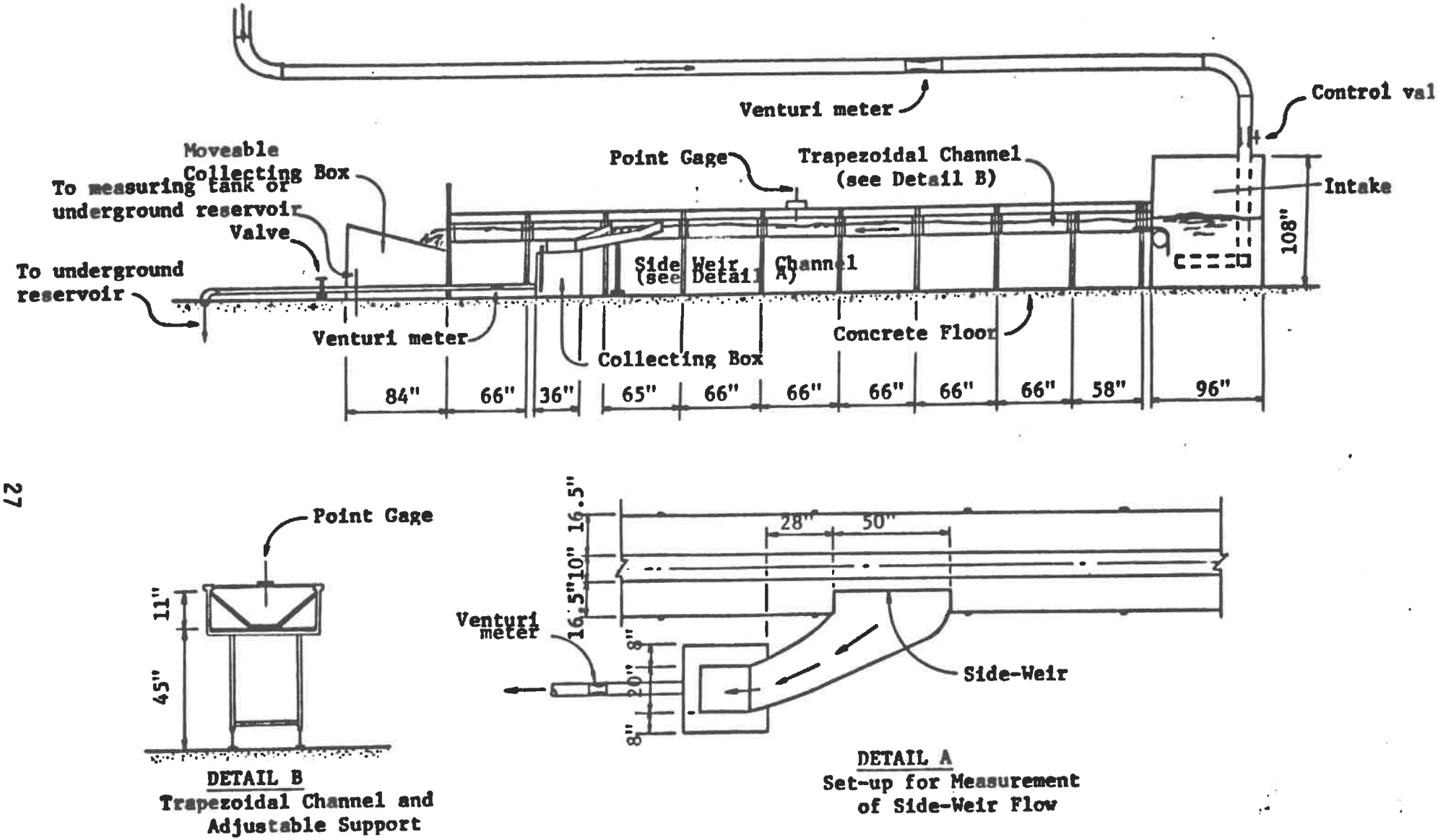

Figure 4 The Trapezoidal Flume

V. ANALYSIS OF THE EXPERIMENTAL DATA

SCOPE OF THE EXPERIMENTS

For the rectangular flume a total of seventy (70) experiments were conducted covering four (4) slopes (.000338, .000781, .00663, 00864), six (6) weir heights (0", 1", 2", 3", 4", 5") and five (5) weir lengths (1.1125', 2.2250', 3.3375', 4.45', 5.5625') with discharge in the upstream main channel varying from 0.45 cfs to 2.30 cfs. Investigated flow cases in the side-weir reach were ten (10) subcritical, fifty (50) critical and supercritical and ten (10) supercritical with hydraulic jumps. Most of the subcritical flow cases were obtained by means of adjusting the downstream gate height thus imposing a downstream boundary control.

For the trapezoidal channel twenty-one (21) experiments were conducted to date, covering two (2) slopes (.00645, .00119), four (4) weir lengths (1.25', 2.083', 2.9166', 4.1667') and two (2) weir heights (0.25', 0.375') with the same discharge range used in the rectangular channel. All types of flow were investigated through the test-runs.

The side-weir discharge and the discharge upstream and/or downstream were carefully measured in each test-run after the readings became stable which usually took about 15 to 20 minutes. Thirteen point gages located as shown in figure 5 were used in each of the two channels for measurement of the water surface levels at appropriate locations. Manning's coefficients of 0.0089 and 0.0127 were formed for the

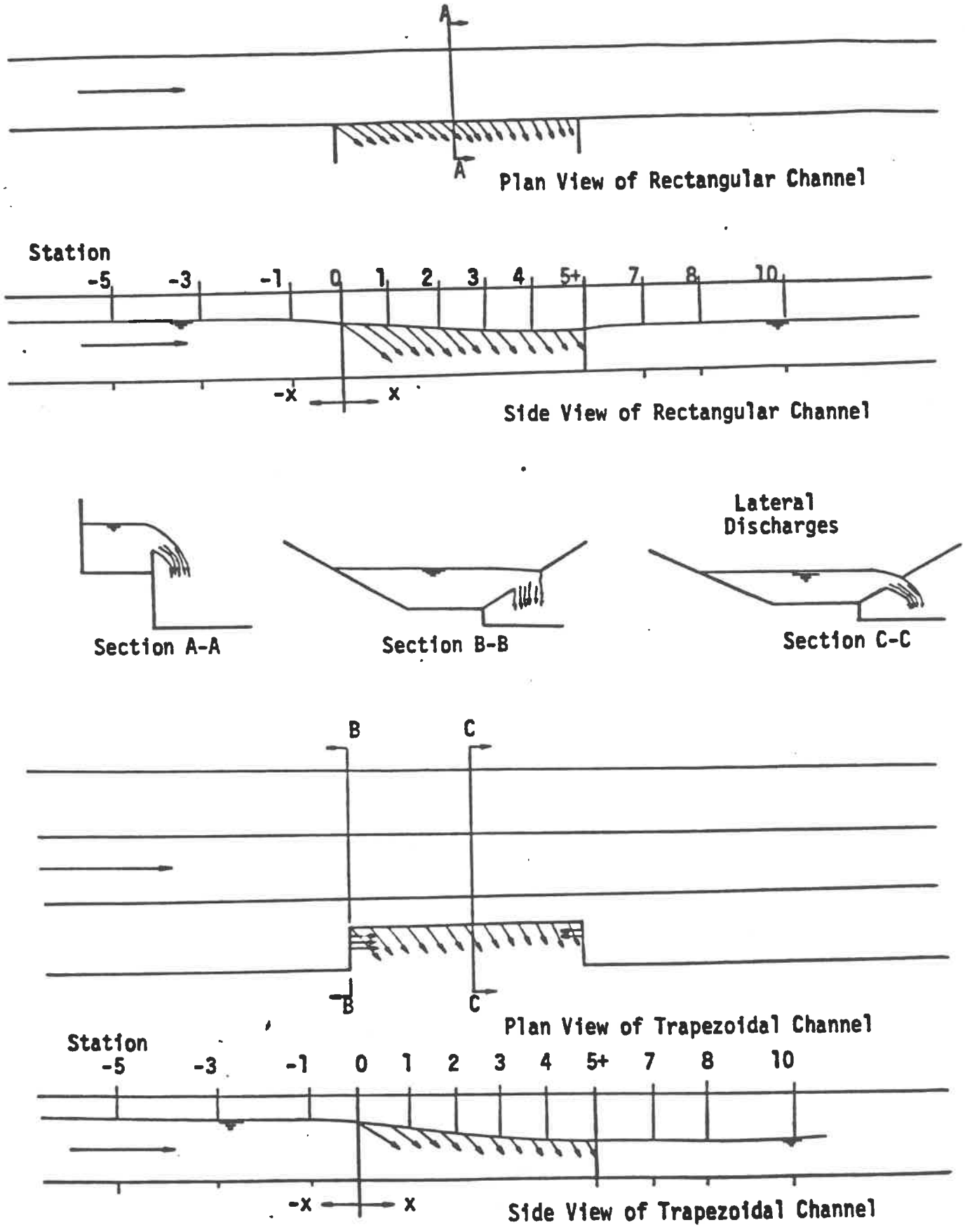

Figure 5. Definition Sketch for the Experimental Data

rectangular and the trapezoidal flumes respectively through several uniform flow experiments.

A complete set of experimental data for all phases of this study that have been completed to date is included in the Appendix. Parts of the data have been presented in a Thesis by Weisz (10) and in a Directed Study Report by Liu (11). A version of the mathematical model for steady flow has been presented in a Thesis by Kayiran (12).

THE COEFFICIENT OF DISCHARGE

Experimental results from each test-run on the rectangular flume were introduced into a steady flow computer program for the purpose of determining the appropriate coefficient of discharge C_d for use in the mathematical model. This was achieved by using a successive iteration process to correct an assumed C_d until the side-weir discharges resulting from the experimental test-run and the computer run were closely matched.

Three approaches for investigating the coefficient of discharge were used in the analysis. The first assumed an unvaried coefficient along the entire reach of the side-weir as asserted and applied by de Marchi (2) and others (13, 14 and 15). Attempts were then made to correlate this coefficient to several dimensionless parameters including the Froude number in the upstream reach, the ratio of length of side-weir discharge to total discharge in the upstream, the

ratio of length of side-weir to channel top width, and several combinations thereof. Results of the analysis indicated that no apparent relationship could be found to express the coefficient of discharge in terms of any of the above mentioned parameters with the exception of the discharge ratio Q_w/Q_1. From the trend of the data it was evident that C_d increased with the increase of Q_w/Q_1 and that C_d reached its maximum value of about 0.62 when the flow over the side-weir was as high as 60% of the total flow in the upstream channel, and that C_d reached a minimum of about 0.25 when the side-weir flow was as low as 1% of the total flow in the upstream channel. By means of logarithmic plot of the data (figure 6) it was concluded that for the case of falling profiles (supercritical or critical flow conditions at the beginning of the side-weir) or rising profiles (subcritical flow condition) in rectangular channels and provided no hydraulic jump occurs in the weir reach, the discharge coefficient may be expressed in terms of the ratio of the side-weir discharge Q_w to the upstream discharge Q_1, as follows:

$$C_d = 0.64\ (Q_w/Q_1)^{0.206} \qquad ..(18)$$

In the second approach for the analysis of experimental data variation of the coefficient of discharge C_d along the side-weir was taken into consideration. As for the case of longitudinal flow over a sharp crested weir, C_d depends on

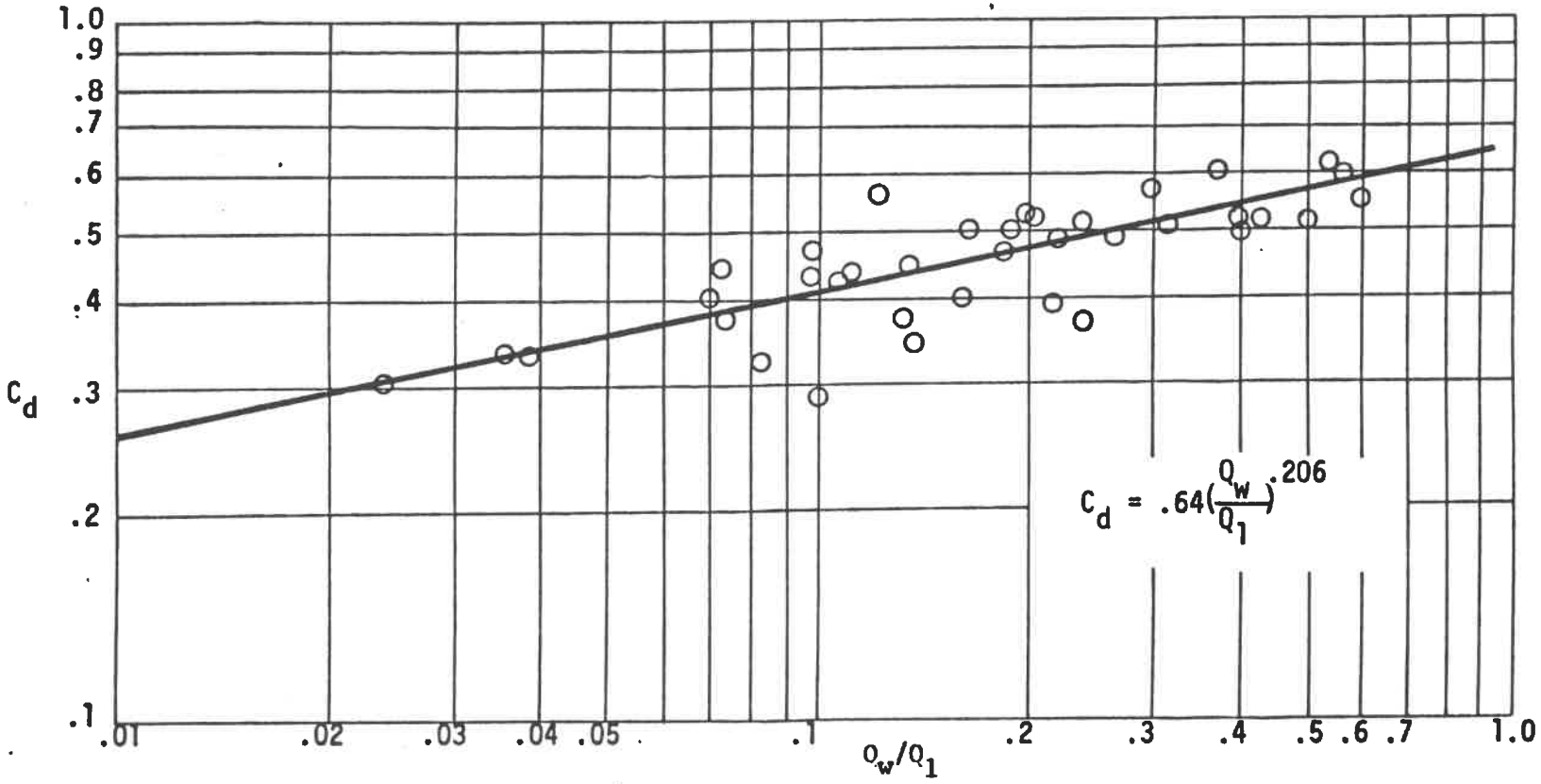

Figure 6. Discharge Coefficient for Side-Weirs in a Rectangular Channel Related to the Ratio of Weir Discharge to Upstream Discharge

the ratio of water depth above the weir ($y-y_w$) to the total water depth (y). Following this approach, the coefficient C_d can be expressed as:

$$C_d = C_1 + C_2 \left(1 - \frac{y_w}{y}\right) C_3 \qquad ..(19)$$

After several trials to determine appropriate values for the constants in this equation from the available experimental data, it was decided to abandon this approach for the time being. It seems that more experimental data are needed for proper statistical analysis leading to the determination of appropriate values for C_1, C_2 and C_3.

The third approach was meant to investigate the validity of the assumptions used in deriving equations leading to the mathematical model. In other words, this approach was to find out whether or not the approximations inherent in these assumptions were of smaller or larger order of magnitude than the errors of measurement in the physical model. The coefficient of discharge was computed from the weir discharge and water surface profile measurements taken during an experiment then compared with the coefficient arrived at by the first approach (figure 7). Results of this analysis show that the experimental coefficient of discharge over the weir is sometimes a little lower and sometimes a little higher than the coefficient which verifies the mathematical model. Calling the former C_{de} and the latter C_{dm} (both so far have

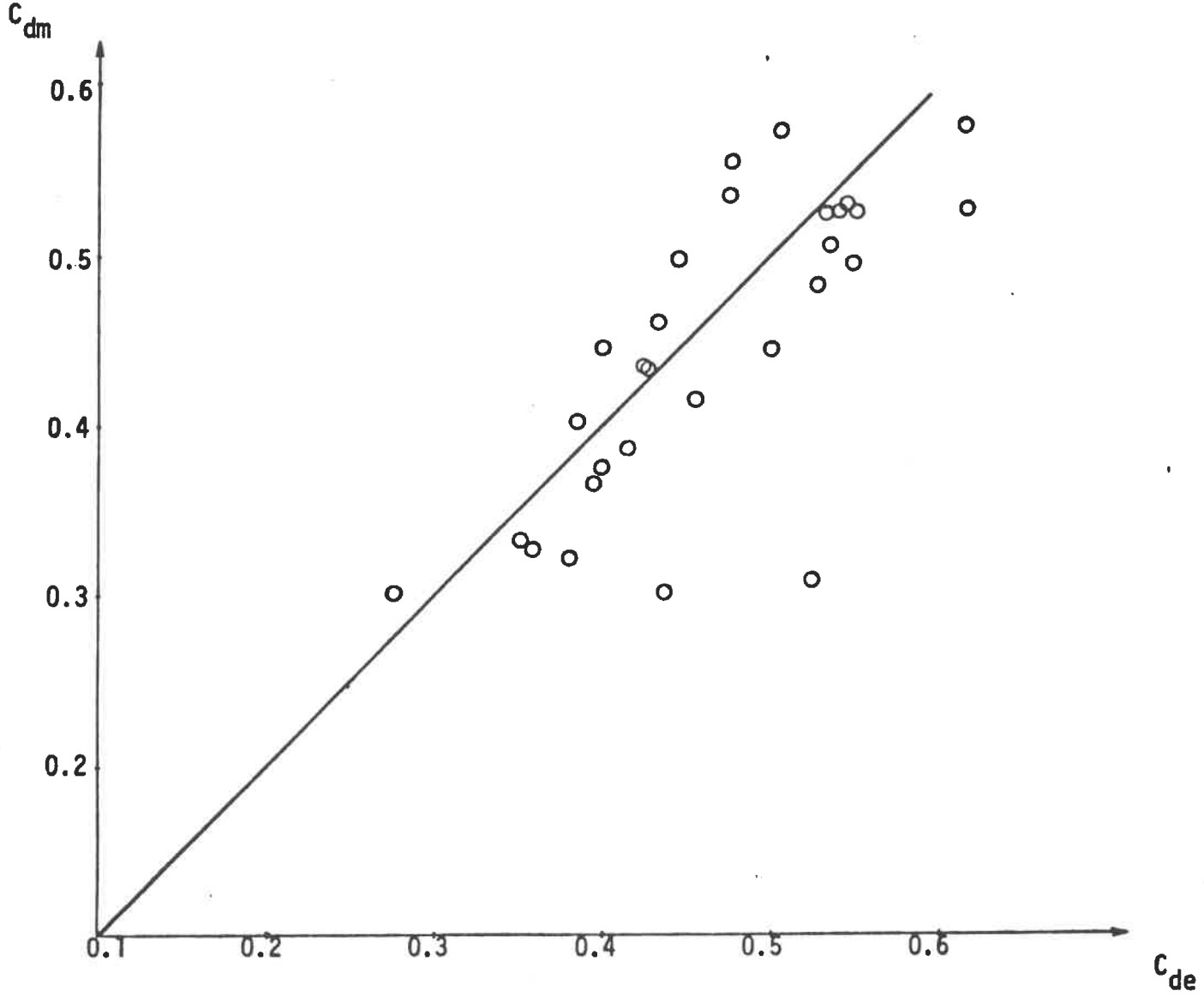

Figure 7. Comparison Between Discharge Coefficients Obtained from Experiments (C_{de}) and from Mathematical Model (C_{dm}) for the Rectangular Channel

been called C_d), no consistent relation was found between Q_w/Q_1 and $(C_{de}-C_{dm})/(C_{de}+C_{dm})$ for the data of the rectangular flume. This indicates that differences between C_{de} and C_{dm} were due to normal errors of measurement and normal errors in theoretical assumptions. The fact that the accumulated error of both experimental and theoretical sources was still within ±10%, makes it possible to conclude that for design purpose, C_d as given by equation (18) may be assumed equal to C_{dm} which should be used in the application of the mathematical model. The weir discharge can then be computed by the mathematical model provided other needed data such as the upstream discharge and boundary conditions are known.

WATER SURFACE PROFILE VERIFICATION

Water surface profiles obtained from the physical models usually agreed closely with the corresponding profiles from the numerical models. Figure 8 shows an example of two corresponding falling profiles, one obtained experimentally and the other obtained from the numerical model assuming a constant C_d over the side-weir. As can be seen from this example, along the portion of the side-weir reach where the water depth above the side-weir was large, the physical model showed a little higher water depth than that of the mathematical model, while along the portion of the reach where the water depth above the side-weir was small, the

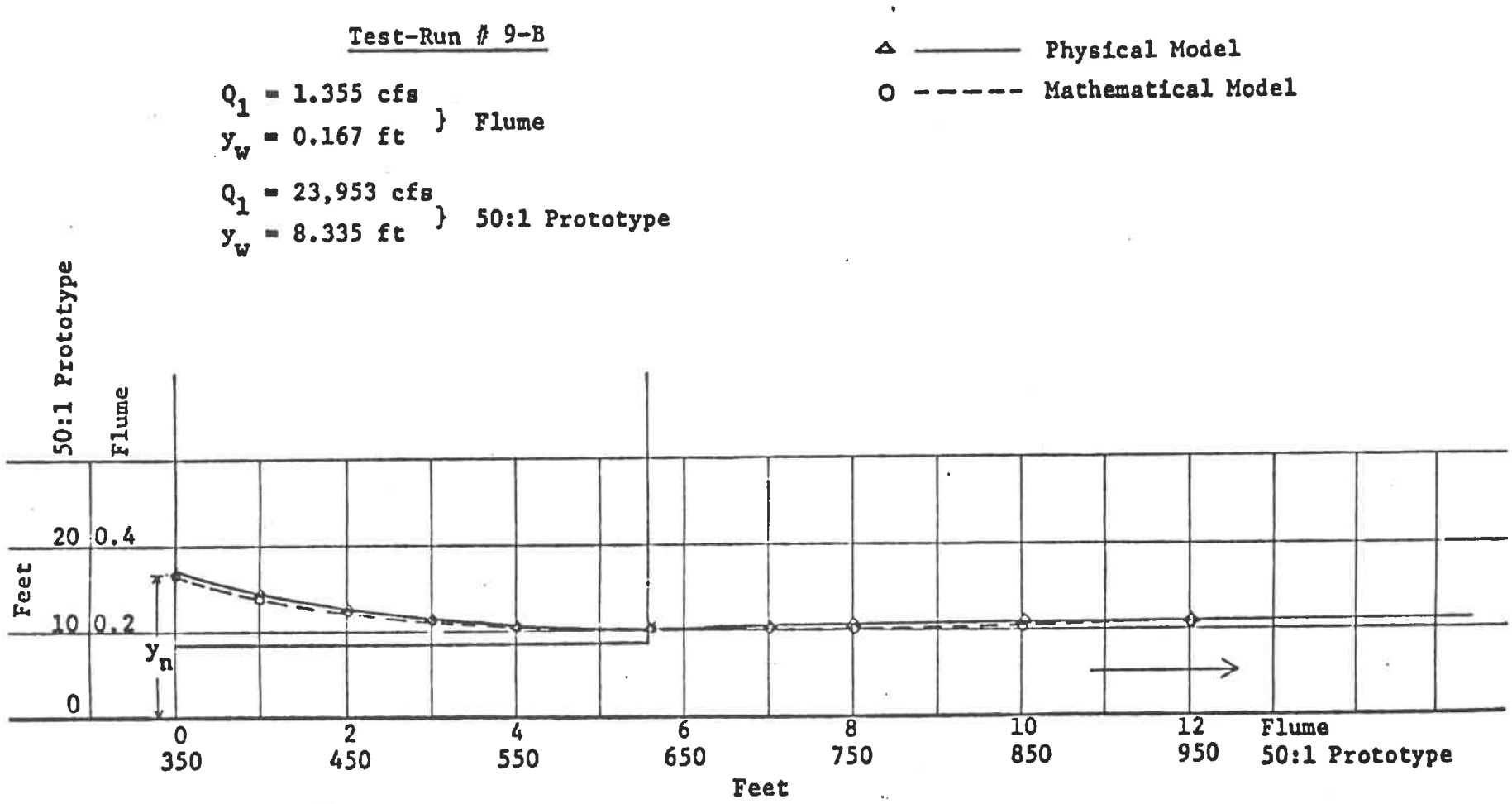

Figure 8

Typical Water Surface Profiles for the Physical and the Mathematical Model
(Test-Run # 9-B)

water level in the physical model was slightly lower than that of the mathematical model. This phenomenon was typical of most of the test-runs and seemed to suggest that the coefficient of discharge over the side-weirs should vary with the water depth above the side-weir, resembling the well-known trend in the variation of the coefficient of discharge over sharp-crested weirs with longitudinal flow. As mentioned earlier, the investigation of the coefficient of discharge by the second approach led to the conclusion that more experiments are needed if a reliable estimate of C_1, C_2, and C_3 of equation 19 is to be pursued. However, for the purpose of arriving at a practical mathematical model to enable an engineering estimate of side-weir discharge, it is felt that pursuing the research in this direction would only be of academic value, and was therefor temporarily abandoned.

Some other minor differences were observed, between the flow profiles in the physical and corresponding numerical models. For rising profiles, the minimum water depth in the physical model did not occur at the beginning of the side-weir as assumed in the theoretical analysis, but rather a short distance downstream. For falling profiles when the flow in the upstream channel was supercritical in the side-weir reach, the profile started falling before it reached the beginning of the side-weir while the theory considers the profile starting to fall just at the beginning

of the weir. For the case of subcritical flow in the upstream reach and supercritical flow along the side-weir reach, test results showed that the flow became critical a short distance before it reached the side-weir rather than at the beginning of the side-weir as indicated by the theoretical analysis. However, each and every one of these differences can be easily explained by the secondary flow process which is created by the disturbance to the flow caused by the existence of a side-weir and which has been completely ignored in the theoretical analysis. Measurements show that water leaves the channel at an angle which was always less than 45 degrees with the main channel flow (within the range of the experiments this angle varied between 40 and 30 degrees). This suggests that the centerline of the stilling basin should be inclined at a similar angle to the direction of flow in the main channel. The length of the stilling basin and any blocks that may be needed will depend upon the ratio of weir height to critical depth of flow, the critical depth, and the conditions downstream of the basin.

CASE OF HYDRAULIC JUMP

For cases where a hydraulic jump occurred in the side-

weir reach, the coefficient of discharge was found to be scattered in the range from 0.1 to 0.5. The location of the jump in the physical model was in most cases different from the location of the jump as per the numerical model. There are several reasons for this discrepancy and for the inconsistency of the variation in C_d when a hydraulic jump occurred in the weir reach. The location of the hydraulic jump is very sensitive to any change in roughness, bed slope, or upstream Froude number. Several assumptions were made in deriving the equations which led to the numerical model. One of these assumptions was that the kinetic energy correction factor α varies with the Manning n as found by Hulsing, Smith and Cobl (16). Another was that the pressure distribution at all sections of the flow remains hydrostatic. Effects of inaccuracy in assumptions such as these two were insignificant when the flow was strictly supercritical or subcritical. However, they became quite significant in the case of the hydraulic jump.

Another assumption, which was made in the mathematical model was that the jump can be represented by a vertical line. In other words, the jump length which is known to be several times the subcritical depth, was considered equal to zero in the mathematical model. This assumption together with the others mentioned above make it difficult to accept results of computer runs in case of a hydraulic jump in the

weir reach. The output of the numerical model as far as the location of the hydraulic jump is concerned largely depends on the value of C_d used in the input. If C_d is estimated from equation 18 errors of ±30% may be included in the output value for the weir discharge. For this reason, it is suggested that when better accuracy is needed, the designer should either avoid the situation when a jump would be produced in the weir reach, or use a physical model for this special case. The hydraulic model should give a more reliable answer than the numerical.

CASE OF TRAPEZOIDAL CHANNEL

The coefficient of discharge for the longitudinal flow C_{dl} as used in equation 7 in the case of trapezoidal sideweir reaches was found to be close to 0.60 which is similar to the value of the coefficient of discharge for a sharp-crested V-notch. Otherwise, the variation of the coefficient C_d followed a trend similar to that of the rectangular channel.

Contrary to the case of the rectangular flume, differences between corresponding values of C_{dm} and C_{de} for the case of the trapezoidal flume, were significant. In most cases as shown in figure 9 $(C_{de}-C_{dm})/C_{dm}+C_{de})$ was positive indicating that the use of the water surface elevations at the channel centerline in computing the head over the sideweir led to values for the coefficient higher than should

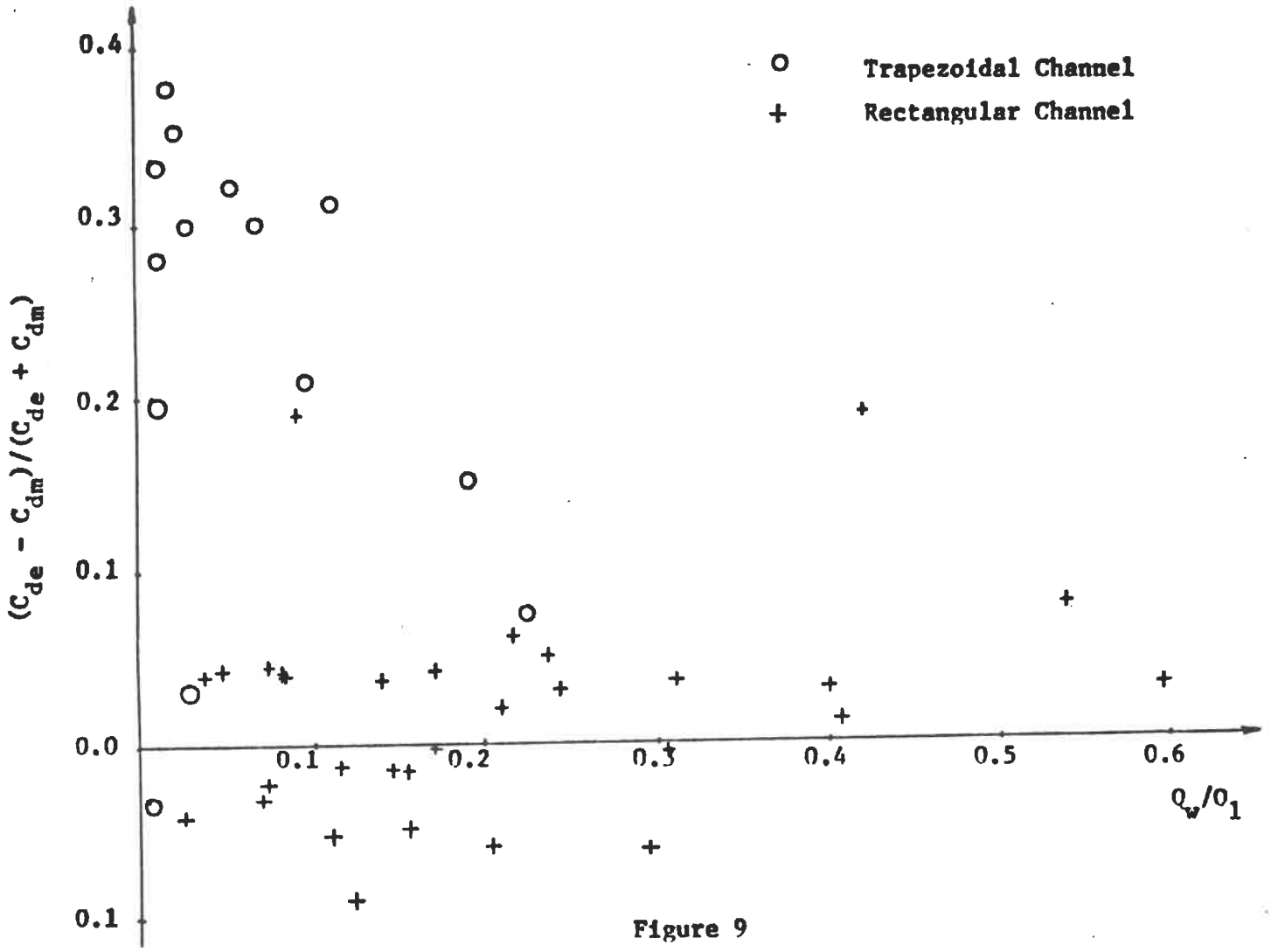

Figure 9

$(C_{de} - C_{dm})/(C_{de} + C_{dm})$ Plotted Against Q_w/Q_1

be. Most probably the coefficient which should be used in the numerical model does not only depend on the ratio (Q_w/Q_1), but also on other dimensionless parameters describing the geometry of the channel. In other words, C_d is a function of (Q_w/Q_1), (y_w/B) and $\bar{z}$, where B is the bottom width of the trapezoidal channel whose side-slope is 1 vertical on $\bar{z}$ horizontal. When $\bar{z}$ was zero (case of rectangular channels), it was established that C_d depended only on (Q_w/Q_1) as per equation 18. Experimental data from the trapezoidal flume, however, suggest the modification of equation 18 to include the effect of the side-slope. One way of modifying equation 18 is to include a term $(1+\bar{z})^{C_5}$ where C_5 is a constant. Following this procedure in the analysis of the results of the test-runs on the trapezoidal flume, C_5 was found to be about 0.263. Equation 20 is therefore recommended for computing the discharge coefficient for side-weirs in open channels.

$$C_d=0.64(Q_w/Q_1)^{0.206}\ (1+\bar{z})^{0.263} \qquad ...(20)$$

This equation is reduced to equation 18 when $\bar{z}=0$ (case of rectangular channels).

EFFECT OF SUBMERGENCE

Tests were run on the rectangular flume to determine the change of the coefficient of discharge due to the submergence of the side-weir resulting from rising of water

level in the stilling basin. No effect occurred until the water in the stilling basin reached the level of the weir crest. Test results indicated that the ratio of the coefficient of discharge of a submerged weir to that of a free weir can be expressed by:

$$\frac{C_{ds}}{C_d} = \left[1-\left(\frac{H_1}{H} \right)^{3/2} \right] C_4 \qquad ..(21)$$

where C_{ds} is the coefficient of discharge for the submerged weir, C_d is the corresponding coefficient when the side-weir is not submerged, H is the water depth above the weir crest in the channel and H_1 is the water depth above the weir crest in the stilling basin, and C_4 is a constant ranging from 0.30 to 0.40. While H_1 may be constant for a certain case, H is usually varying along the weir and therefore C_{ds}/C_d is expected to be also varying along the weir. However, an average value of H and C_4 may be used in applying the above-mentioned equation without too much error.

VI. AN APPROXIMATE METHOD FOR UNSTEADY FLOW COMPUTATIONS

For computing the quantity of flow discharging over a side-weir in a channel in which a flood wave in the form of a hydrograph propagates, the application of the unsteady numerical model should produce reasonably accurate results except for the case where a hydraulic jump occurs. The unsteady numerical model application is usually very complicated requiring appropriate initial and boundary conditions and a large-capacity computer for running the program.

For practical purposes, an approximate method utilizing the steady model for computing the flow over side-weirs due to unsteadiness of flow in the main channel with or without hydraulic jumps is needed for engineering design. If the base of a given hydrograph is simply divided into a finite number of time intervals, the average discharge for each interval can be assumed constant during the incremental time interval. The steady numerical model is then applied to each interval and flow over the side-weir corresponding to each average discharge is computed. Finally, the total volume of flow over the side-weir due to a flood wave propagation in the channel is obtained and is equal to the summation of the individual side-weir discharges multiplied by the corresponding time intervals.

The procedure can be summarized in the following:

1. If the original known hydrograph (Hydrograph 1) is for a station far from the proposed site of the side-weir, the unsteady numerical model should be used to route the flood from the original station to a station close to the side-weir location where a new hydrograph (Hydrograph 2) can thus be obtained. The new hydrograph usually would have a lower peak and a wider time base as compared to the original hydrograph (Hydrograph 1), the degree of subsidence depending on the flow conditions and the slope of the channel.

2. Determine the capacity of the retarding basin. This can be achieved by plotting a stage versus storage curve.

3. Choose a side-weir length and a side-weir height and compute the discharge in the main channel when the normal depth is equal to the side-weir height.

4. Divide hydrograph 2 into a number of parts according to the degree of variation of discharge Q with respect to time t, the larger the rate of discharge variation, the smaller should be the time intervals used in the computation.

5. Apply the steady numerical model using the average Q at each interval obtained in Step 4 to determine the side-weir discharge Q_w.

6. Plot the side-weir discharge Q_w versus time t curve. The area under this curve represents the total volume of water discharged over the side-weir. Composite Simpsons rule can be applied for obtaining this area.

If the volume obtained is equal to or slightly greater than the design volume, then the chosen side-weir height and length is appropriate. Otherwise another trial design should be adopted and the procedure repeated until the design requirements are met.

VII. APPROXIMATE SOLUTION OF UNSTEADY CASE COMPARED TO APPLICATION OF THE UNSTEADY FLOW MATHEMATICAL MODEL

To illustrate the difference between the results of applying an approximate method based on the steady flow mathematical model (PROGRAM OCFCD4A) and the results of applying the unsteady flow mathematical model (PROGRAM OCFCD4B), an example will be worked out by both methods. However, in this example, for simplicity, the coefficient of discharge will be assumed constant. Variation of C_d with Q_w/Q_1 as per equation 18, may be of significant effect in actual design but is considered insignificant for the purpose of comparing the two procedures.

Data for the channel:

Channel shape and roughness: Concrete lined rectangular channel, 10 ft. wide, Manning's Coefficient = 0.013

Channel slope: 0.009

Channel length: 8000 ft.

Design Hydrograph: The hydrograph is triangular in shape; it rises from 400 cfs linearly to a peak flow of 2000 cfs at the end of the first hour and then drops down linearly to 400 cfs at the end of the second hour.

time (hours)	0	0.25	1.25	2.25	2.5
discharge (cfs)	400	400	2000	400	400

Side-weir: 2.5 ft. high and 200 ft. long starting at station 4000 ft. and ending at station 4200 ft.

Discharge Coefficient = 0.47

Required:

1. Determine the discharge hydrograph and the total side-weir discharge using the unsteady numerical method.

2. Compute the discharges downstream of the side-weir corresponding to upstream discharges of 400, 600, 800, 1000, 1200, 1400, 1600, and 2000 cfs, respectively, using the steady numerical method and determine the total side-weir discharge.

3. Compare the total side-weir discharges obtained from steady numerical method and unsteady numerical method.

Solution: By applying the computer program OCFCD4B the discharge hydrographs at the beginning of the side-weir, at the end of the side-weir and at the end of the channel reach were found and plotted as shown in figure 10. The total volume of side-weir discharge was 4,073,850 cubic feet as given in the computer printout. By applying the computer program OCFCD4A to a number of discharges ranging from 400 cfs to 2000 cfs, the hydrographs upstream of the side-weir and downstream of the side-weir were plotted as shown in figure 10. The area between these two hydrographs represents the total volume of side-weir discharge and was found to be approximately 4,070,000 cubic feet.

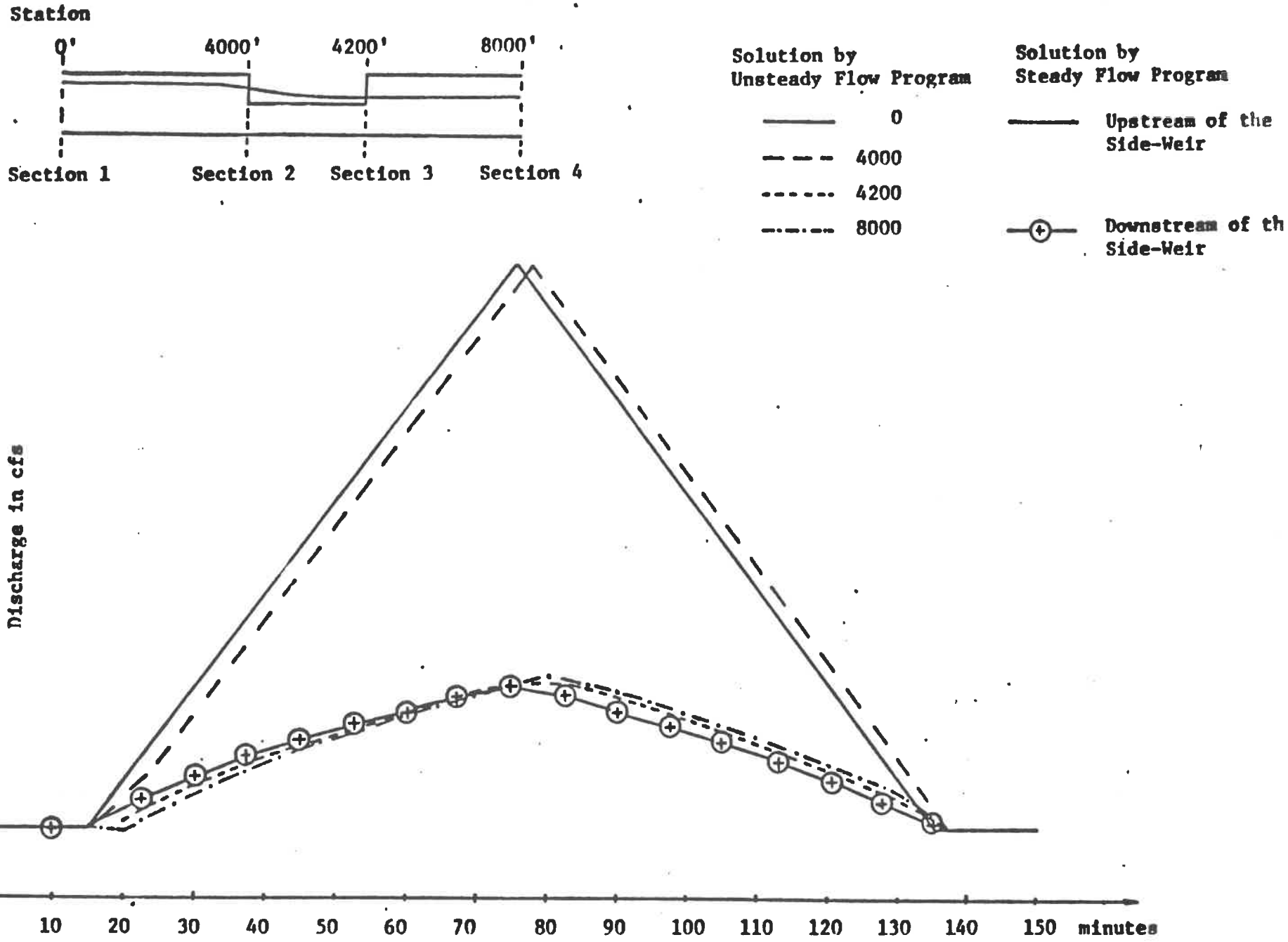

Figure 10 Example on the Application of the
Approximate Method for Unsteady Flow Computation

It is therefore concluded that the approximate method for unsteady flow computations provides reliable solutions for practical applications.

VIII. SOME DESIGN GUIDELINES

SIDE-WEIR DIMENSIONS

For a given value of the discharge $Q_{2\ max}$ that should not be exceeded in the downstream channel, the side-weir height is first assumed equal to the depth of flow in the weir reach at a steady discharge equal to this $Q_{2\ max}$. The side-weir discharge will gradually vary from zero to a maximum at the peak of the flood then gradually decreases back to zero. The weir length should be able to spill the maximum excess of flow (at flood peak) which means that $Q_{w\ max}=Q_{1\ max}$ minus given $Q_{2\ max}$. For this side-weir discharge, the ratio Q_w/Q_1 is established, then C_d is computed from equation 20. Several lengths are then tried with Program OCFCD4A until Q_w is verified. Program OCFCD4B or simply the procedure outlined in Chapter VII will enable the computation of the required volume for the retarding basin.

LOCATION OF TRANSITIONS

Unless the design is going to be checked by a hydraulic model, it is not advisable to locate the side-weir in a transition reach. The mathematical model needed to solve such a case would be terribly complicated. Computer Programs OCFCD4A and OCFCD4B given in the Appendix do not handle this case.

Transitions should be located downstream of the side-weir reach in case of supercritical flow in order to avoid

the effect of cross waves produced by the transition upon the performance of the side-weir. In subcritical flow, transitions may be located upstream or downstream of the weir reach.

RELATIVE LOCATION OF SIDE-WEIRS

In general, two short side-weirs situated across the channel from each other are more efficient than one long side-weir as long as the height of the weir is less than the critical depth (or the normal depth if the flow upstream is supercritical). Theoretically, among the cases shown in figure 11, case a is the most efficient, followed by case b then case c and d.

STILLING BASIN FOR THE SIDE-WEIR FLOW

Flow over the side-weir leaves the channel at an angle of 20 to 40 degrees depending on the conditions of the flow and the ratio of the weir discharge to the upstream discharge. In the design of the stilling basin, it is suggested that irrespective of flow conditions or discharge ratios, the stilling basin centerline be set at an angle 45 degrees with the direction of flow in the main channel. The length of the stilling basin should be enough to allow the flow to become more or less uniformly distributed across the basin and to provide enough resistance to dissipate some of the energy in the flow through a free or a submerged

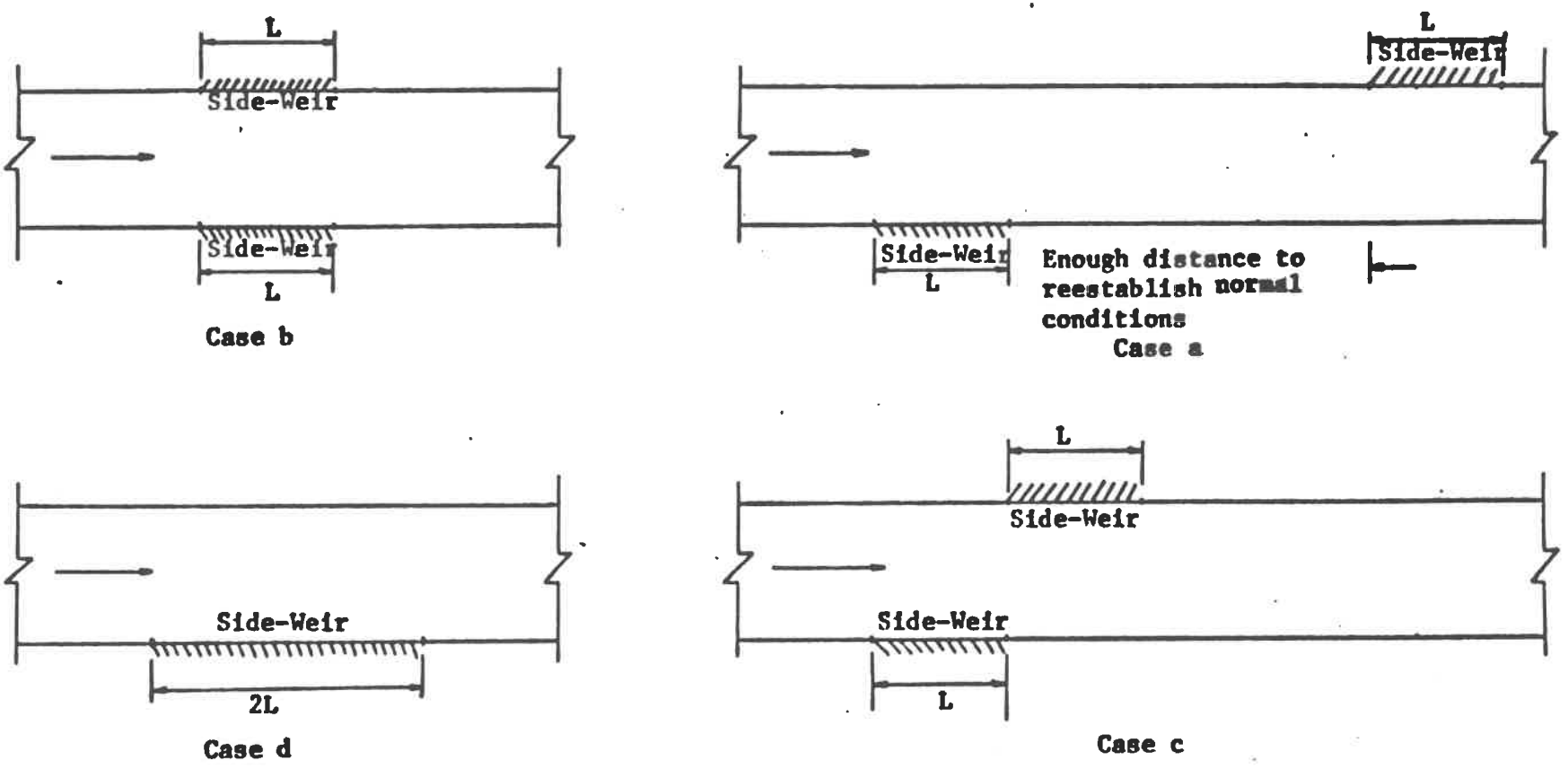

Figure 11 Side-Weir Locations

jump depending on the configuration of the surrounding area of the retarding basin and the expected water levels downstream of the stilling basin. It is suggested that in general no baffle blocks are needed in the stilling basin. Treating the weir as a low drop, its stilling basin should have a length of 7 to 10 times $\sqrt{y_w\ y_{cb}}$ where y_{cb} is the critical depth in the basin and may be taken as $(Q_w/B_w)^{2/3}/g^{1/3}$ (where B_w is the width of the basin. It may be advisable to use the upper limit for the case of side-weirs because of the uneven distribution of flow in the side-weir basin. Accordingly, the minimum length for the stilling basin is given by:

$$L_{b\ min} = 10\ y_w^{1/2}(Q_w/B_w)^{1/3}/g^{1/6} \qquad ..(22)$$

As an example, if the weir height is 4 feet and its length is 100 feet, the minimum design length for the stilling basin when the maximum weir discharge is 1400 cfs will be

$$10(4)^{1/2}\left(\frac{1400}{70}\right)^{1/3}/\ (\ 32.2\ )^{1/6} = 30\ \text{ft.}$$

IX. CONCLUSIONS

The following conclusions take into account all the findings of the theoretical and experimental study which has been carried out for flow over side-weirs in open channels.

1. The steady numerical model which was developed in this study enables the computation of water surface profiles and side-weir discharges for all flow cases with or without hydraulic jumps. The computer program developed from this model (Program OCFCD4A) proved to be very efficient; it handles all types of flow conditions in prismatic channels with or without boundary controls. With minor modifications, it can also be used to treat special flow problems in non-prismatic channels.

2. The unsteady numerical model is capable of handling both subcritical and supercritical flows in prismatic channels with or without side-weirs. For each application, appropriate boundary conditions and accurate initial conditions must be introduced. The initial conditions can usually be obtained from results of the steady numerical model. Accuracy of the unsteady numerical model depends on the number of stations chosen and the time intervals used. Improper choice of the distance interval Δx and the time interval Δt may result in obtaining scattering numerical values between adjacent stations or time intervals. The

application of unsteady model requires a large size computer.

The program developed from the unsteady model (Program OCFCD4B) can also be used for routing the flood from a remote station to a station close to the location of the side-weir. This enables the development of a new hydrograph at a site near the side-weir and increases the effectiveness of using a simulation method for unsteady flow computation.

3. The simulation method, which applies the steady model repeatedly using a sequence of discharges from the hydrograph to compute corresponding quantities of side-weir discharges due to the unsteadiness of flow in the main channel, proved to be effective and applicable to all cases of flow including cases with hydraulic jumps. A comparison of results in several applications using the unsteady numerical model and the simulation method indicated that solutions by the simulation method are reasonably accurate and usually satisfy engineering applications.

4. Experimental investigation of the performance of side-weirs on the rectangular and the trapezoidal flumes established a relation for the determination of the weir coefficient of discharge when the coefficient was assumed constant along the weir (equation 20). Application of equation (20) in estimating C_d for use as a part of the input data for Program OCFCD4A proved to be satisfactory

when no hydraulic jump occurred in the weir reach.

5. In the case of hydraulic jump occurring in the weir reach, the physical and the numerical models usually differed in the location of the jump. Since the jump location significantly influenced the value of C_d which would verify the measured weir discharge, and since this location is sensitive to factors which were not accounted for in the mathematical model (such as change in friction coefficient and the momentum correction factor), the difference between measured and computed weir discharges in the jump case reached 30% (compared to a maximum of 10% when there was no jump). Equation (20) is therefore less reliable in the case of a hydraulic jump occurring in the weir reach than in the case of strictly supercritical or strictly subcritical flow.

6. The study led to some guidelines for the design of side-weirs and their stilling basins.

7. It is recommended that the experimental and theoretical study be continued with the following objectives:

   a. to test the accuracy of equation (20) for various side slopes.
   b. to study the variation in the weir discharge coefficient along the weir as suggested by the second approach equation (19).
   c. To determine the appropriate modifications for the mathematical models if the weir was broad-crested instead of sharp-crested.

APPENDIX

A. CASES OF FLOW PROFILES WHICH MAY BE SOLVED BY THE COMPUTER PROGRAM OCFCD4A

The computer program developed for the steady numerical model applies to a channel which consists of 3 reaches. Section 1 is the beginning of the first reach in the upstream end of the channel; section 2 is at the beginning of the side-weir reach; section 3 is at the end of the side-weir reach and section 4 is at the end of the channel. The side-weir is located along the second reach between section 2 and section 3 on one side of the channel, or there could be two weirs. The bed slopes of the three reaches are expressed by S_{o1}, S_{o2}, S_{o3}. The first and/or the third reaches may be nonprismatic provided that the expansion or contraction is linear.

The computer program has been tested for numerous possible practical cases. Kayiran (12) provided a detailed description of the cases which have been tested. Different flow profiles produced in prismatic channels are shown in figure 12 through figure 20. Figures 12, 13, 14 show the flow profiles with no control at either the upstream or the downstream sections. Figure 15 shows the profiles with control at section 1; figures 16, 17 and 18 show profiles with control at section 4 and figure 19 shows the flow profiles with controls at both the upstream and downstream sections.

Flow profiles produced in nonprismatic channels are shown in figures 20 through 25. Flow profiles for the case of nonprismatic first reach with control at section 1 are shown in figure 20, and with control at sections 1 and 4 are given in figure 21. Flow profiles for the case of nonprismatic third reach with control at section 4 are given in figures 22, 23, and 24. Flow profiles for the case of nonprismatic first and third reaches with control at sections 1 and 4 are shown in figure 25.

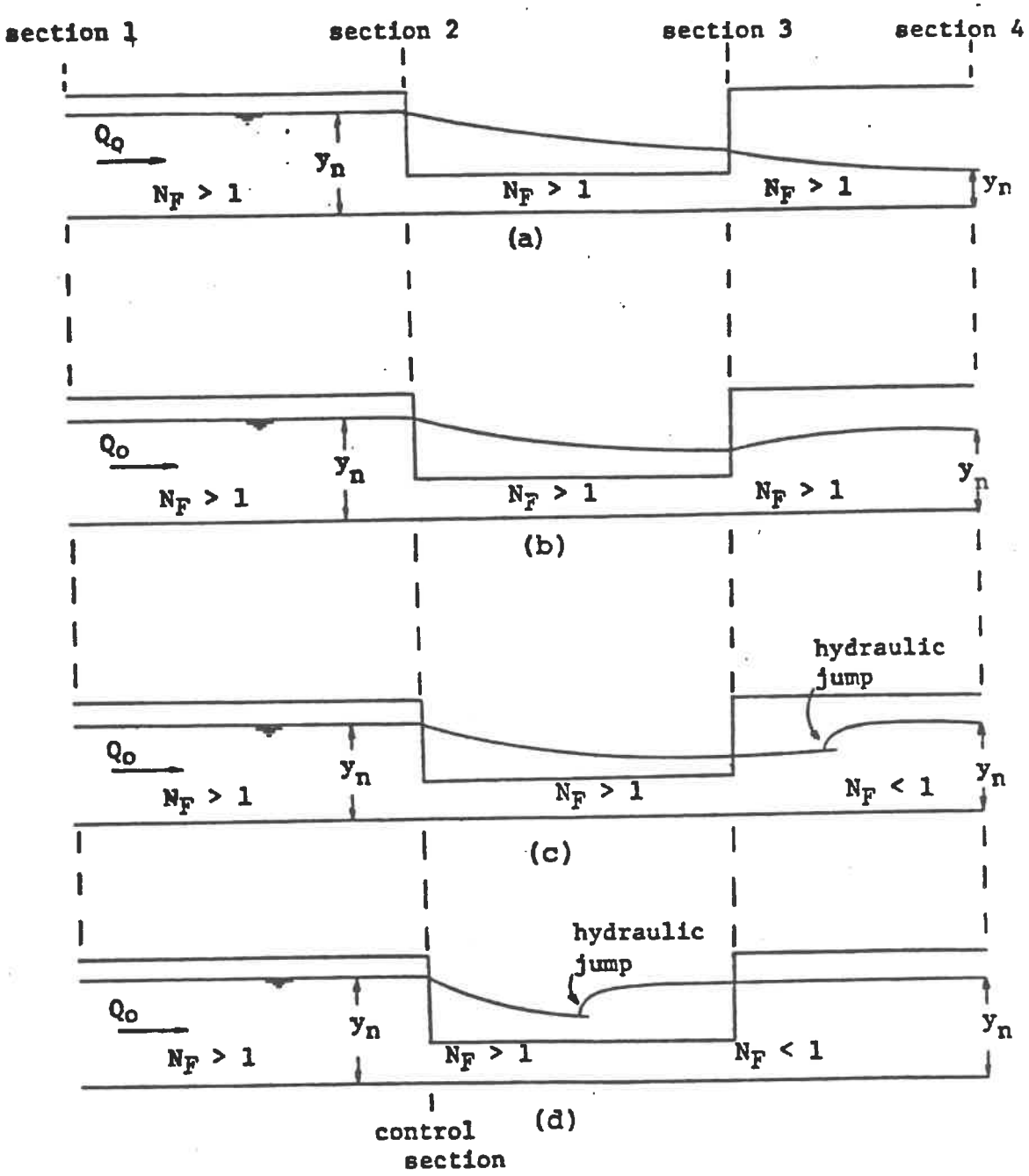

Figure 12

Flow Profiles for the Case of Prismatic Channel Reaches with $y_c > y_n > y_w$ for the First Reach

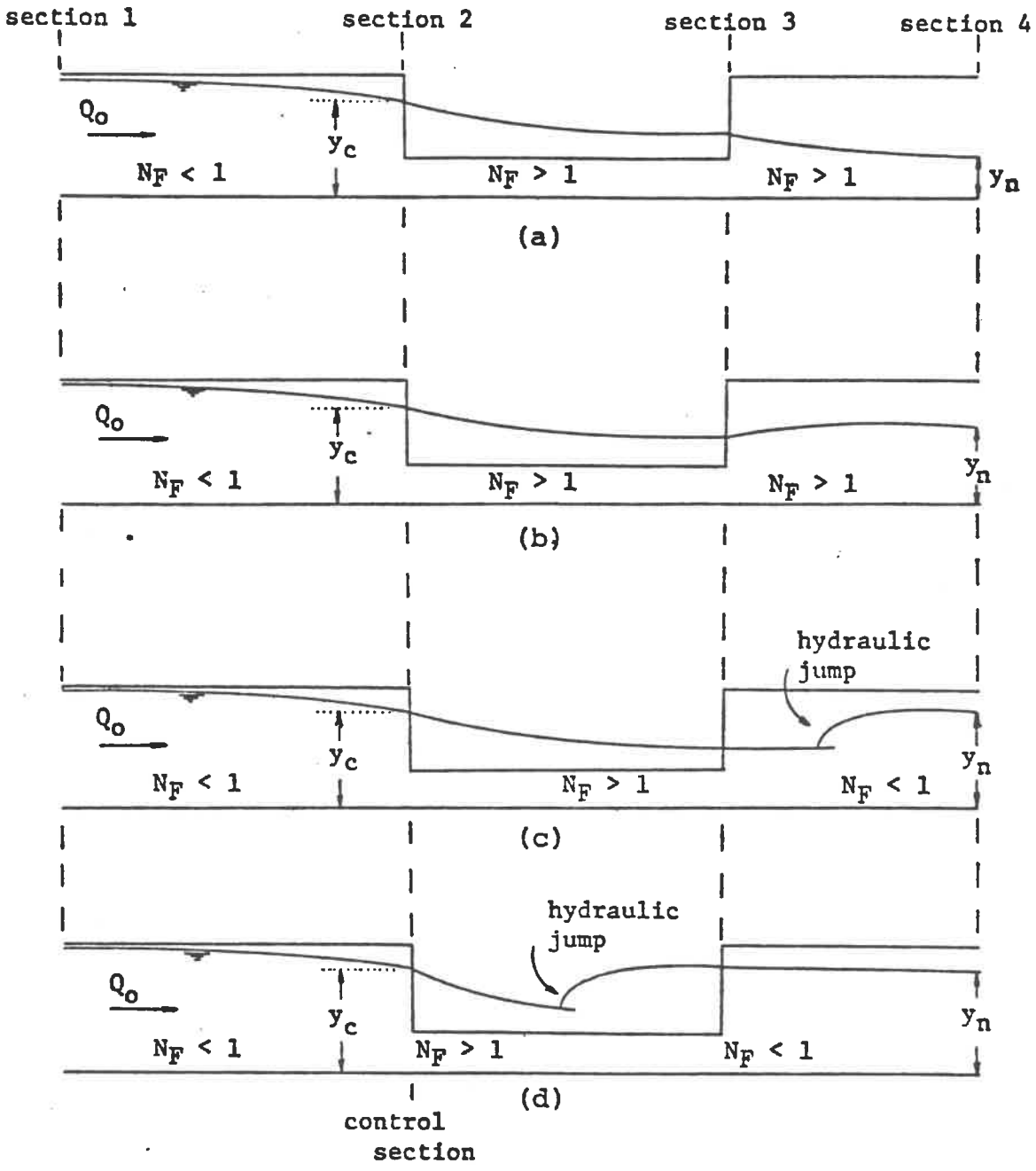

Figure 13

Flow Profiles for the Case of Prismatic Channel Reaches with $y_n > y_c > y_w$ for the First Reach

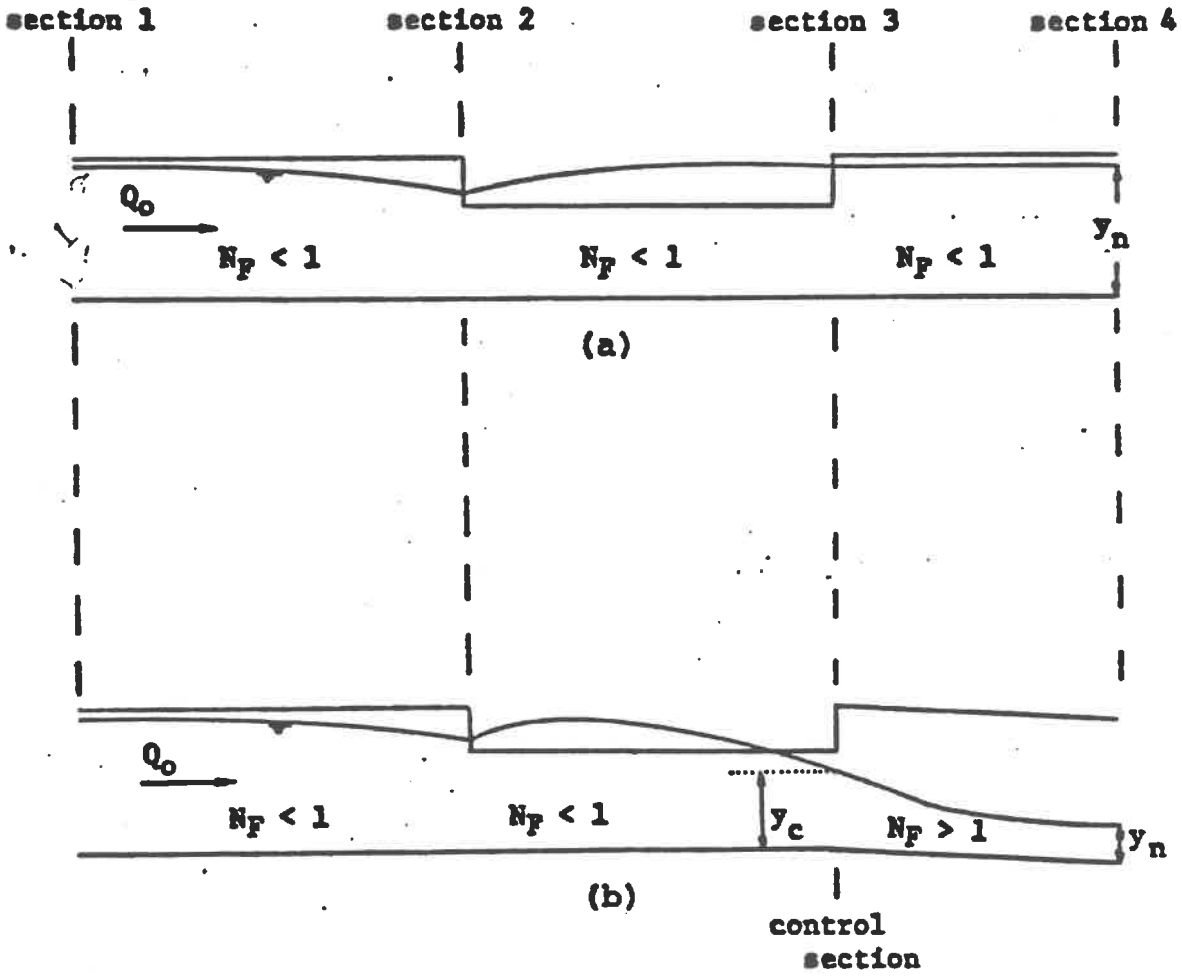

Figure 14

Flow Profiles for the Case of Prismatic Channel Reaches with $y_n > y_w > y_c$ for the First Reach

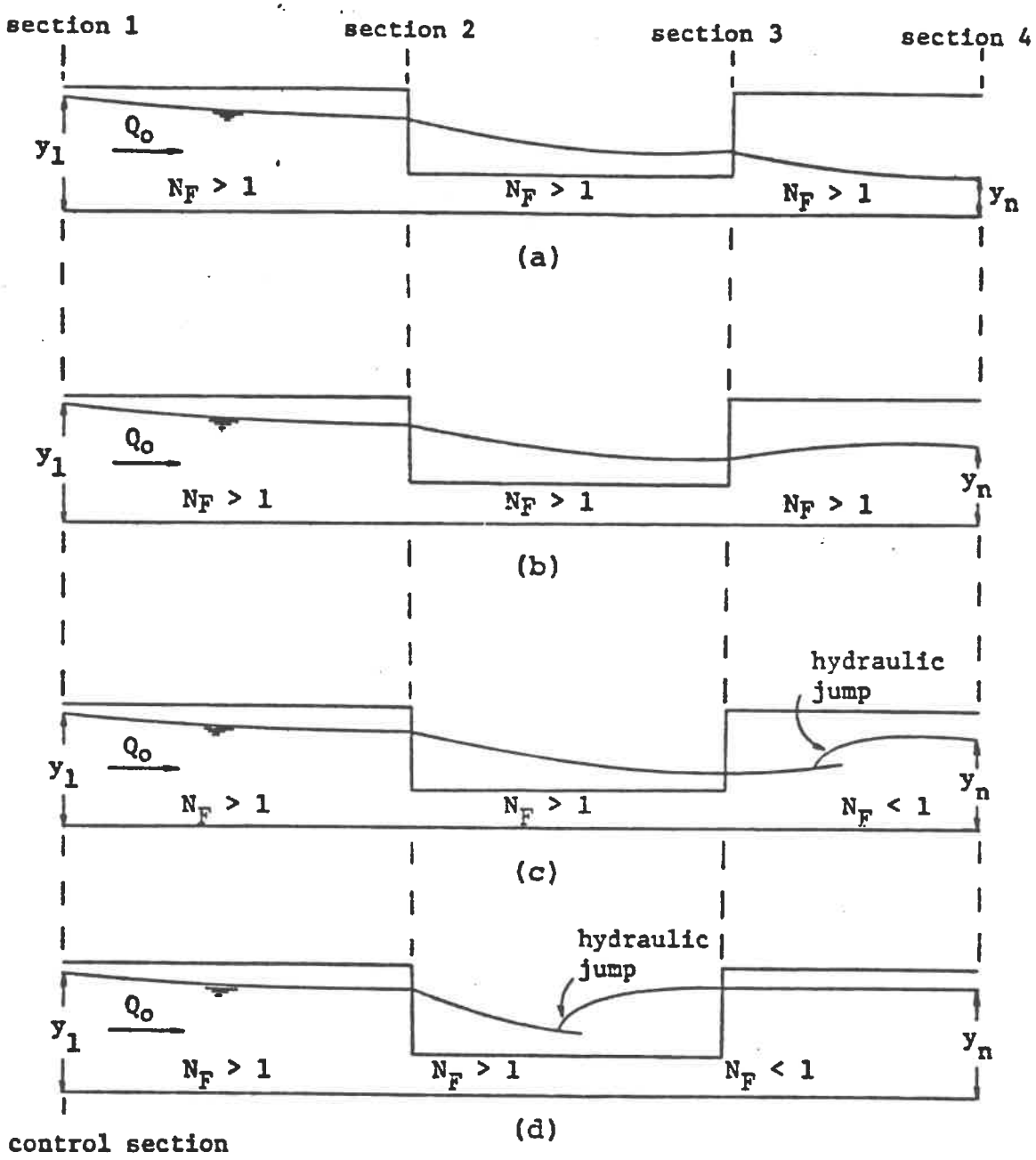

Figure 15

Flow Profiles for the Case of Prismatic Channel Reaches with Control at Section 1

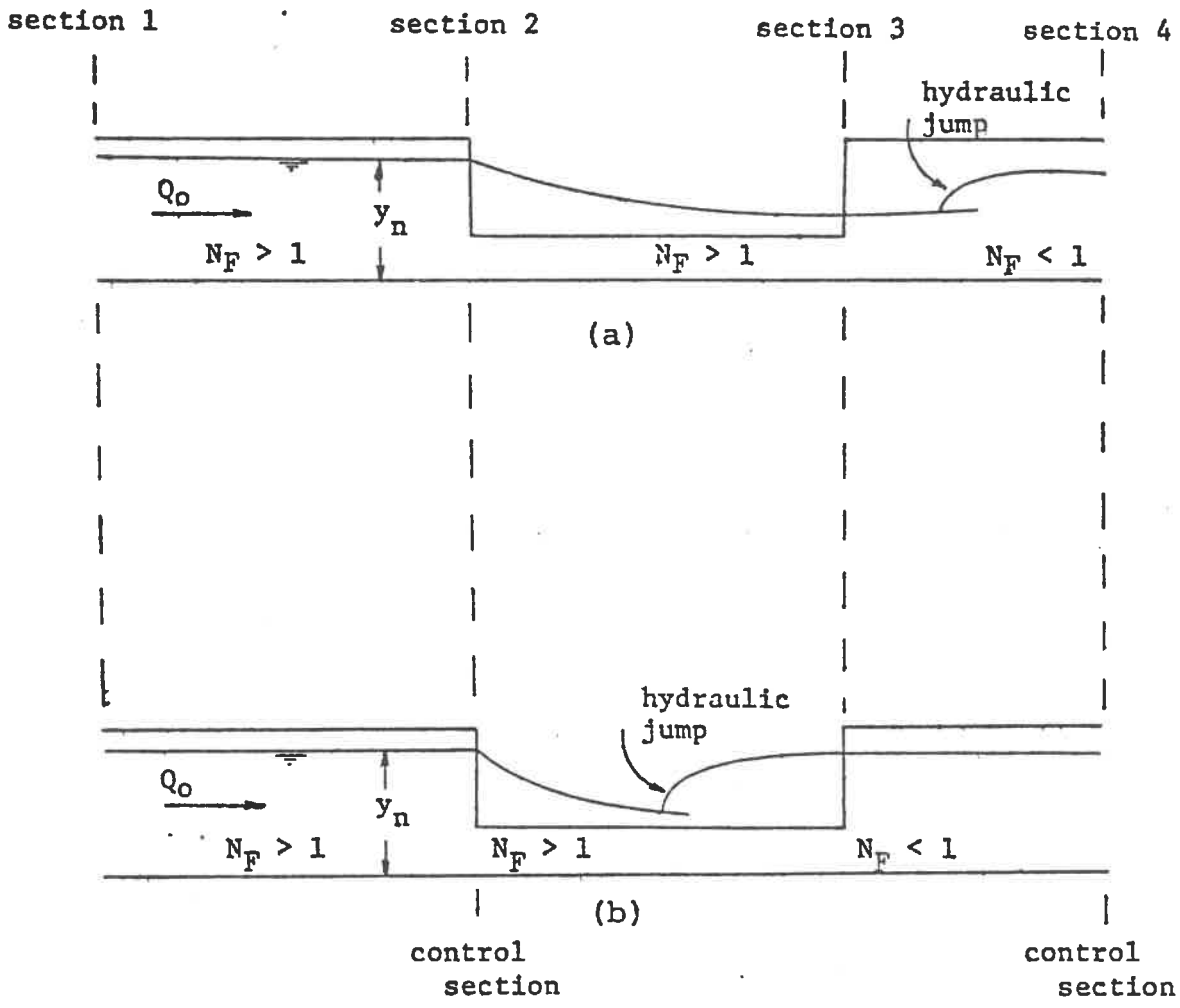

Figure 16

Flow Profiles for the Case of Prismatic Channel Reaches with Control at Section 4 and $y_c > y_n > y_w$ for the First Reach

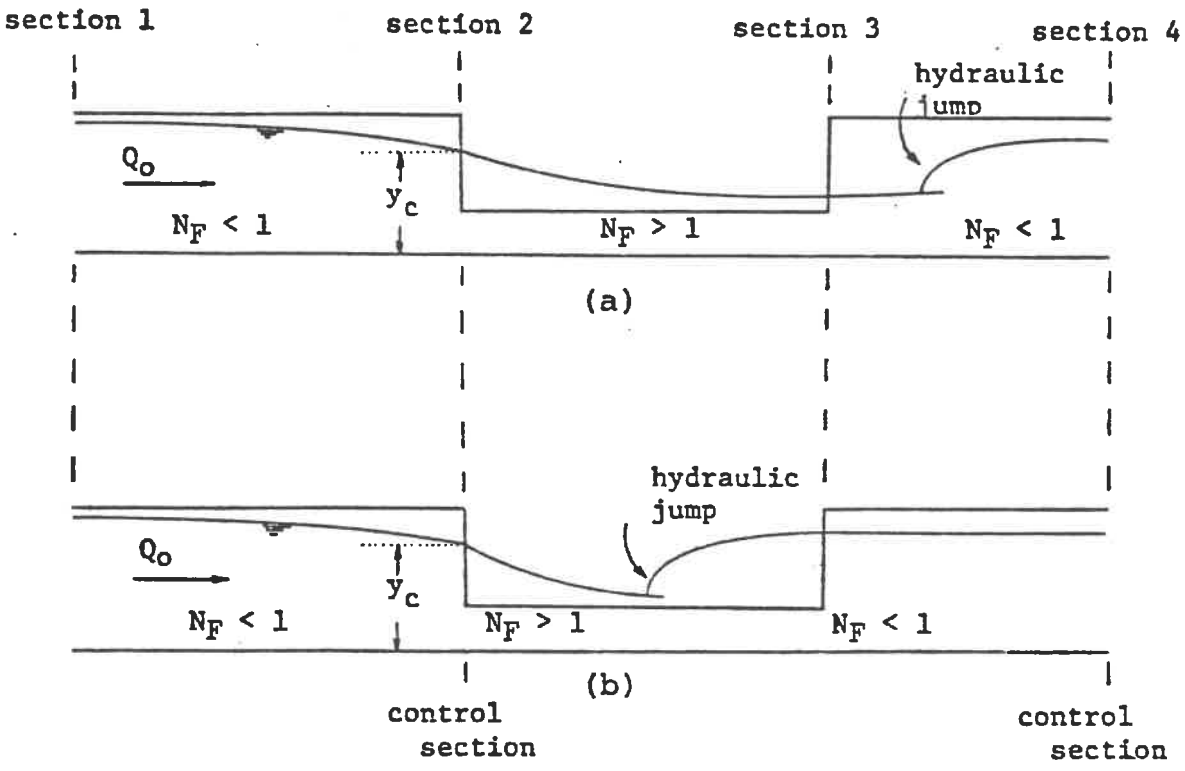

Figure 17

Flow Profiles for the Case of Prismatic Channel Reaches with Control at Section 4 and $y_n > y_c > y_w$ for the First Reach

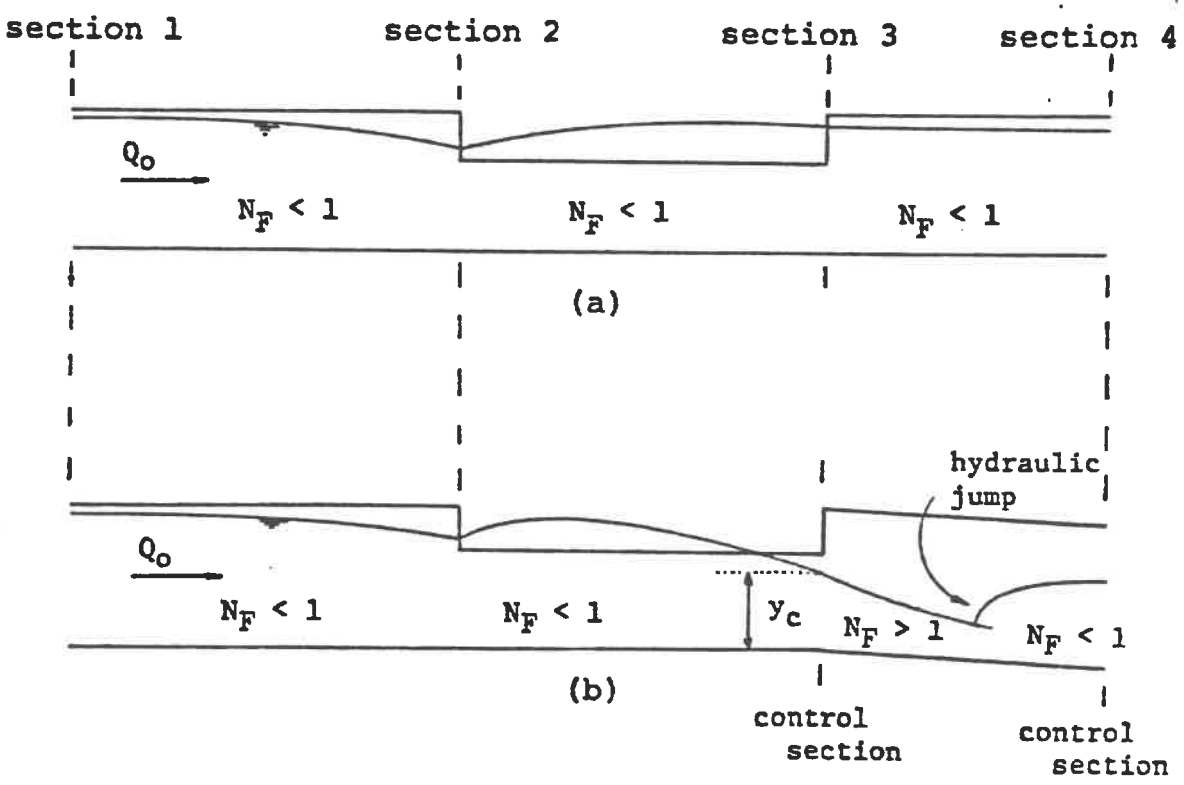

Figure 18

Flow Profiles for the Case of Prismatic Channel Reaches with Control at Section 4 and $y_n > y_w > y_c$ for the First Reach

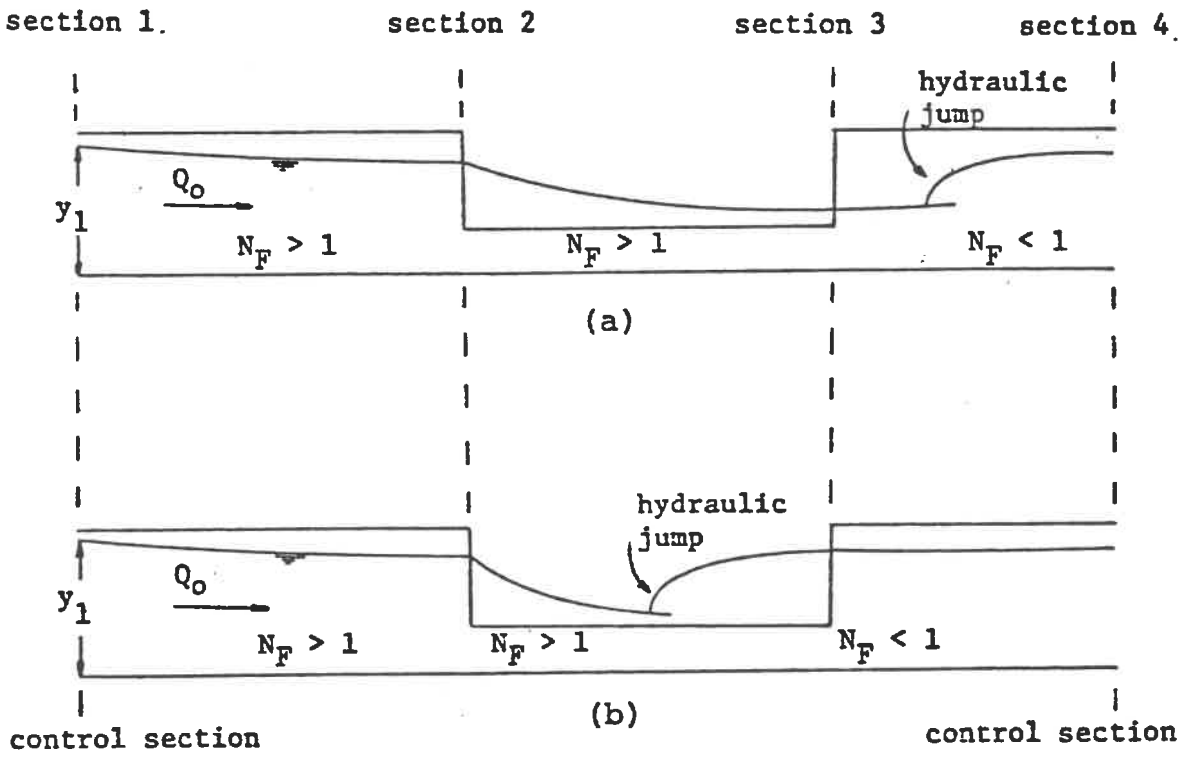

Figure 19

Flow Profiles for the Case of Prismatic Channel Reaches with Control at Sections 1 and 4

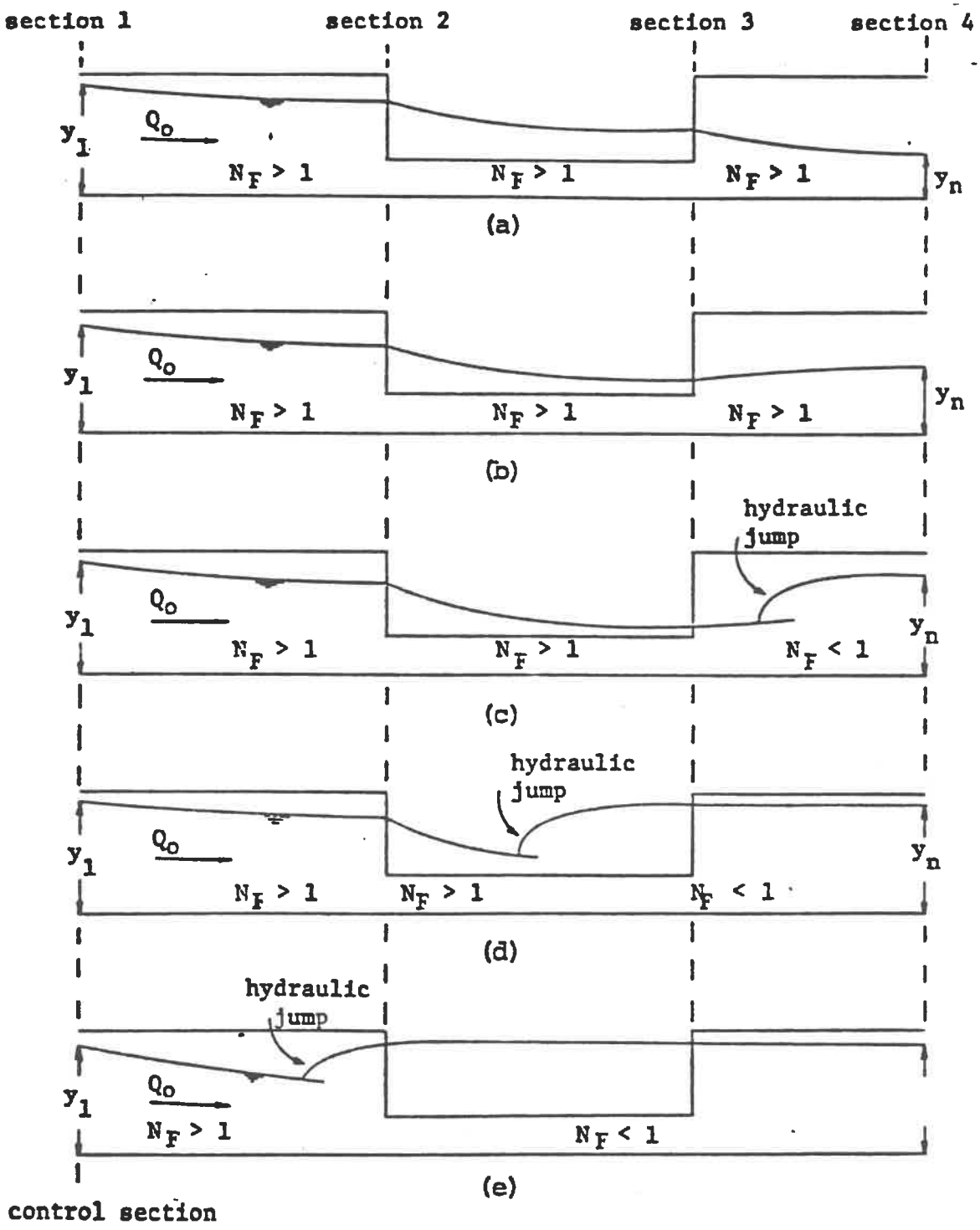

Figure 20

Flow Profiles for the Case of Nonprismatic First Reach with Control at Section 1

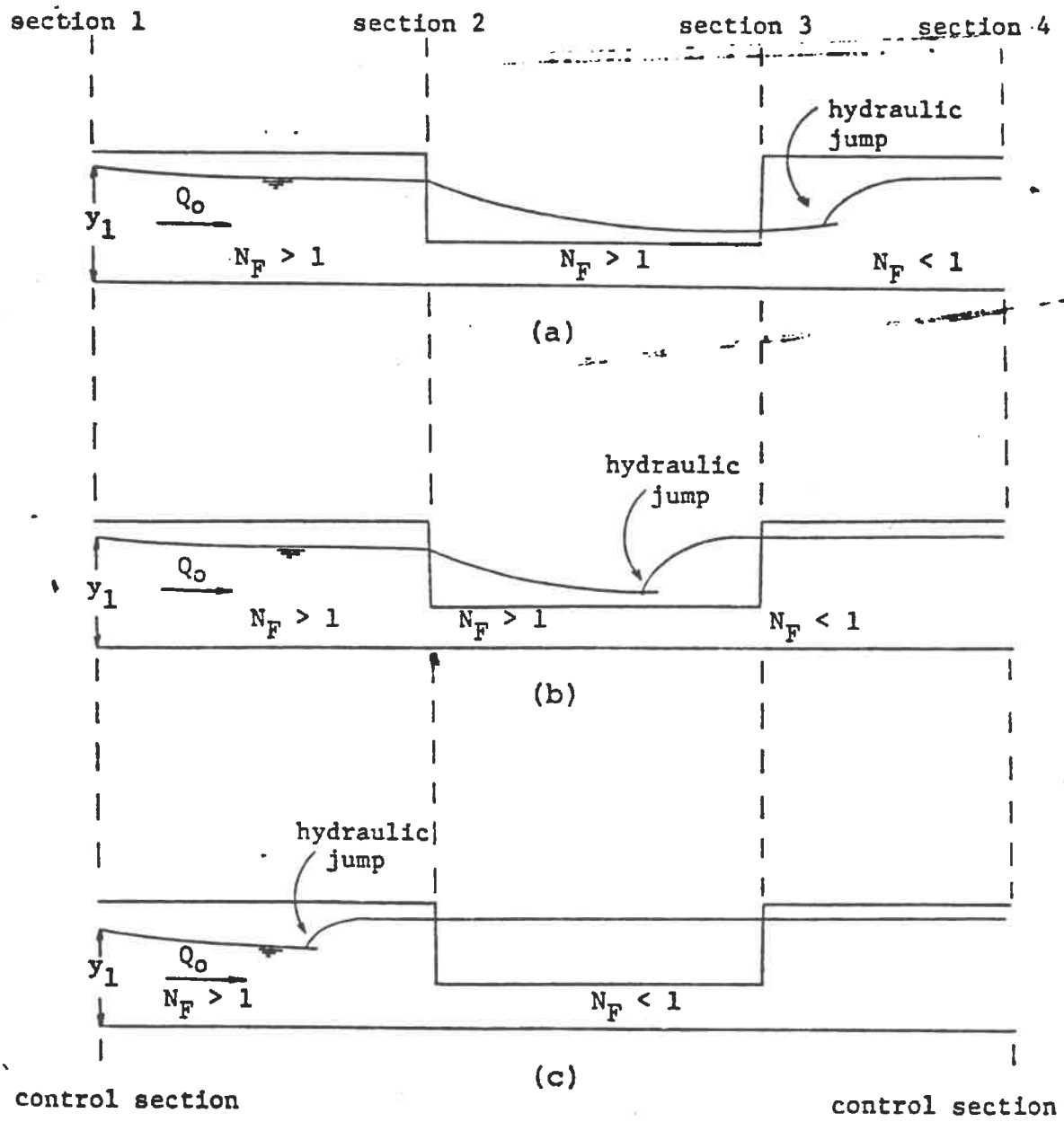

Figure 21

Flow Profiles for the Case of Nonprismatic First Reach with Control at Sections 1 and 4

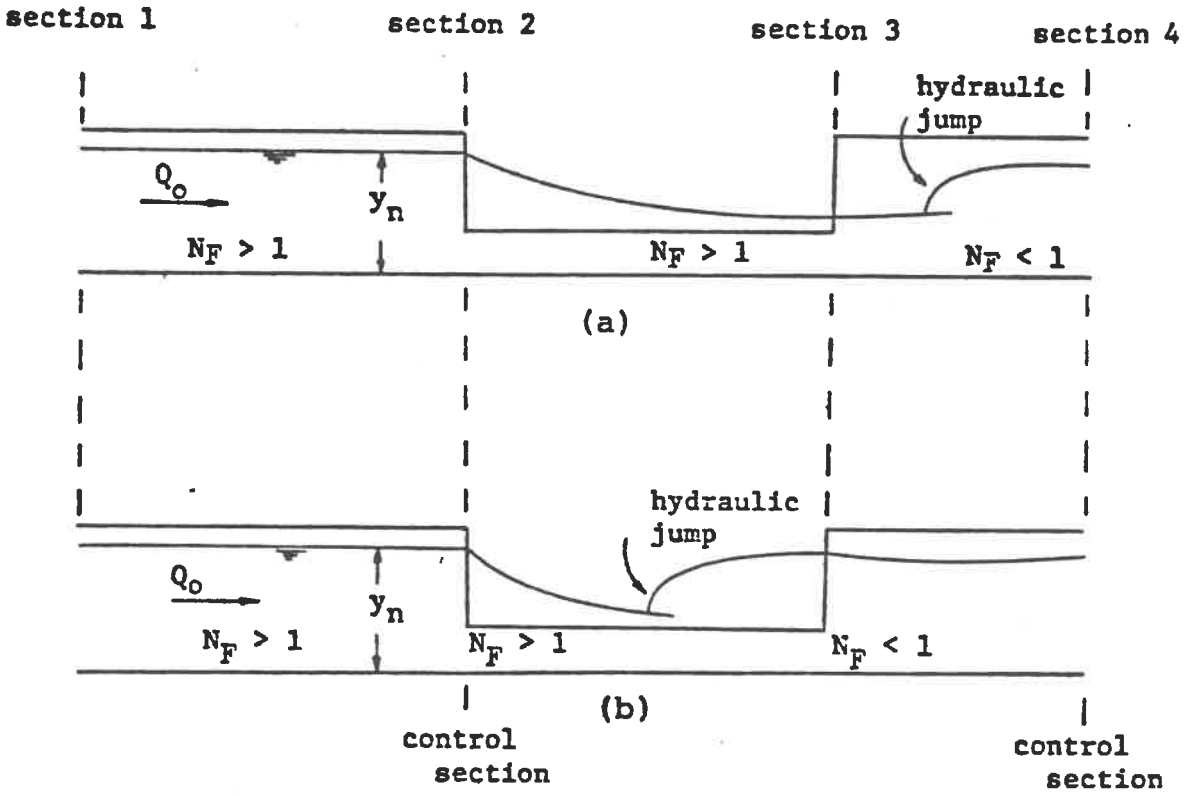

Figure 22

Flow Profiles for the Case of Nonprismatic Third Reach with Control at Section 4 and $y_c > y_n > y_w$ for the First Reach

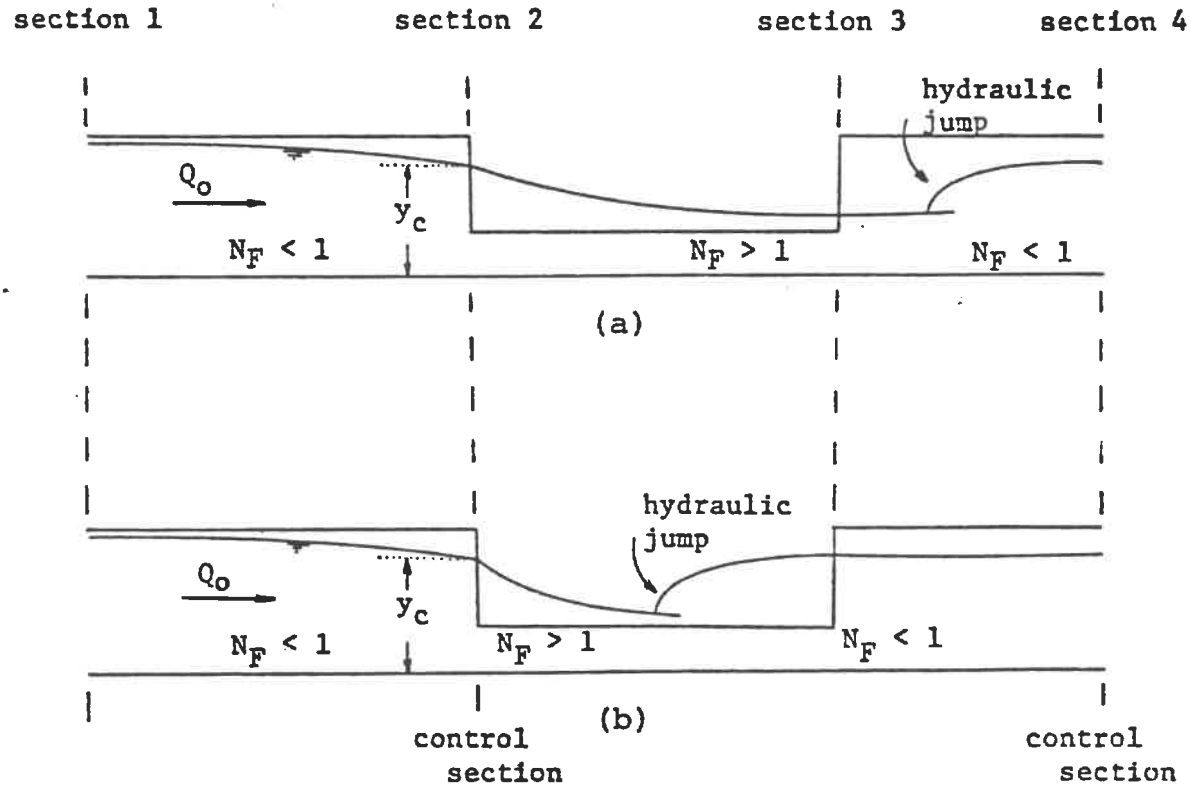

Figure 23

Flow Profiles for the Case of Nonprismatic Third Reach with Control at Section 4 and $y_n > y_c > y_w$ for the First Reach

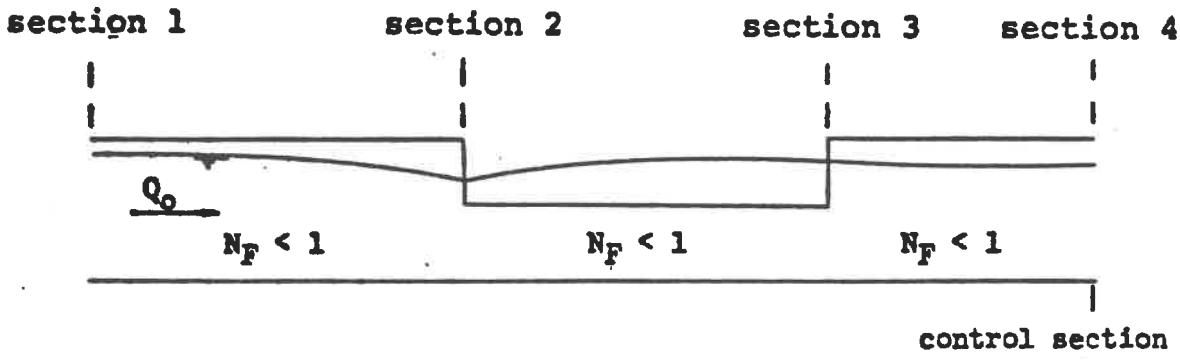

Figure 24

Flow Profile for the Case of Nonprismatic Third Reach with Control at Section 4 and $y_n > y_w > y_c$ for the First Reach

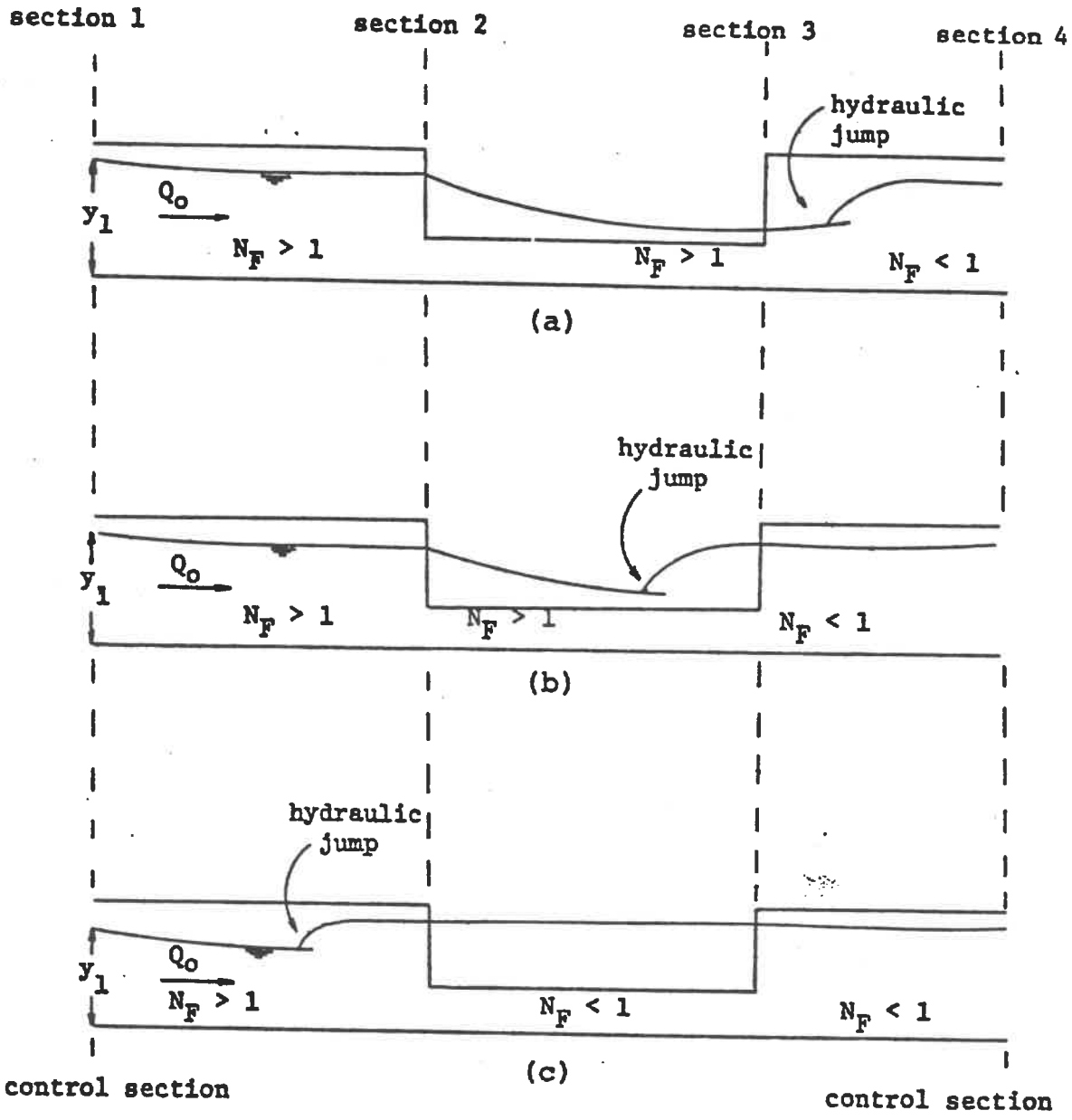

Figure 25

Flow Profiles for the Case of Nonprismatic First and Third Reaches with Control at Sections 1 and 4

B: DESCRIPTION OF THE COMPUTER PROGRAM OCFCD4A

The computer program developed for the steady numerical model consists of a main program and eight (8) subroutines. The generalized flow chart and diagram of input for this program are shown in figures 26 and 27 respectively.

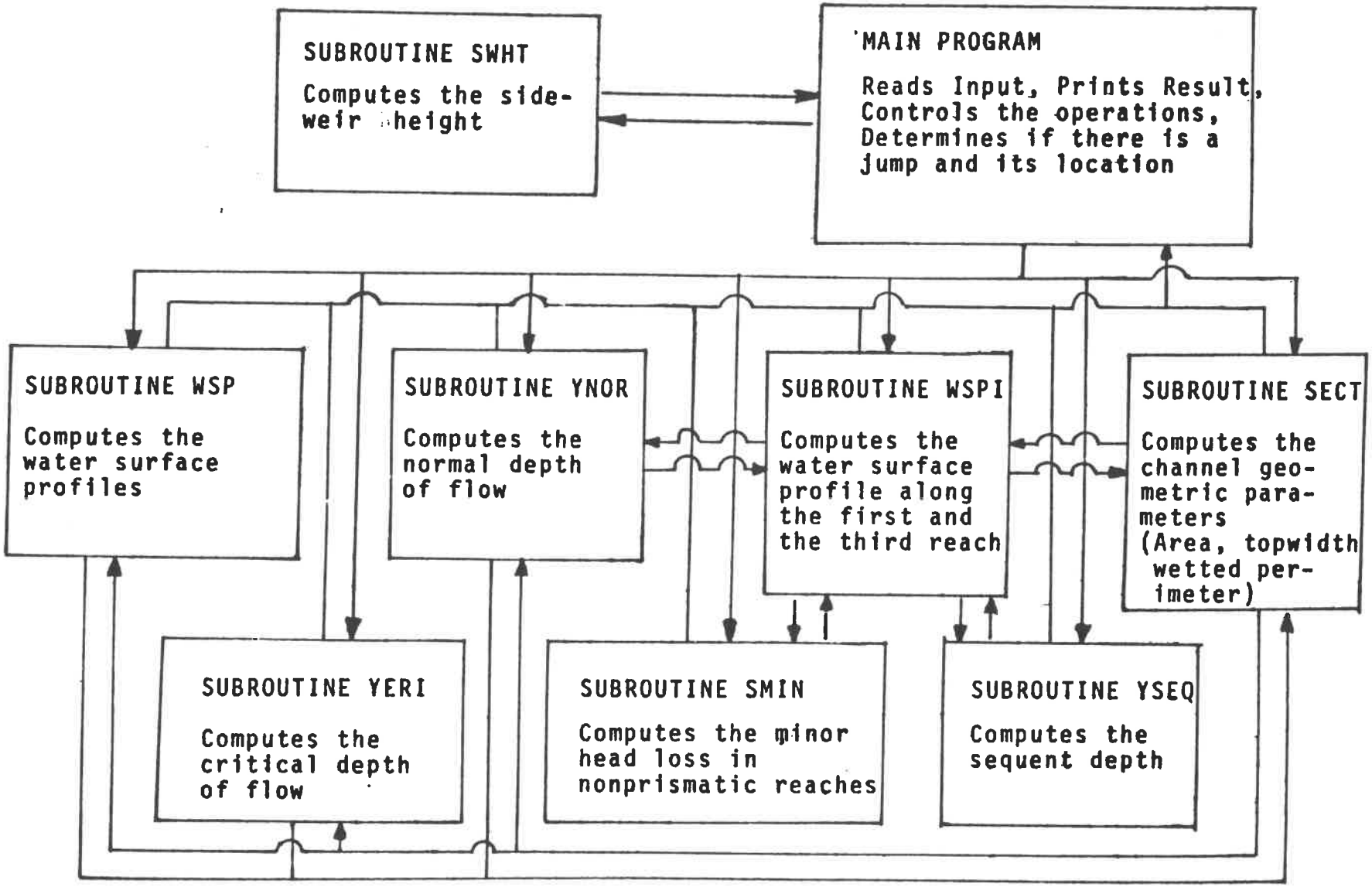

Figure 26. Generalized Flow Chart for the Steady Computer Program

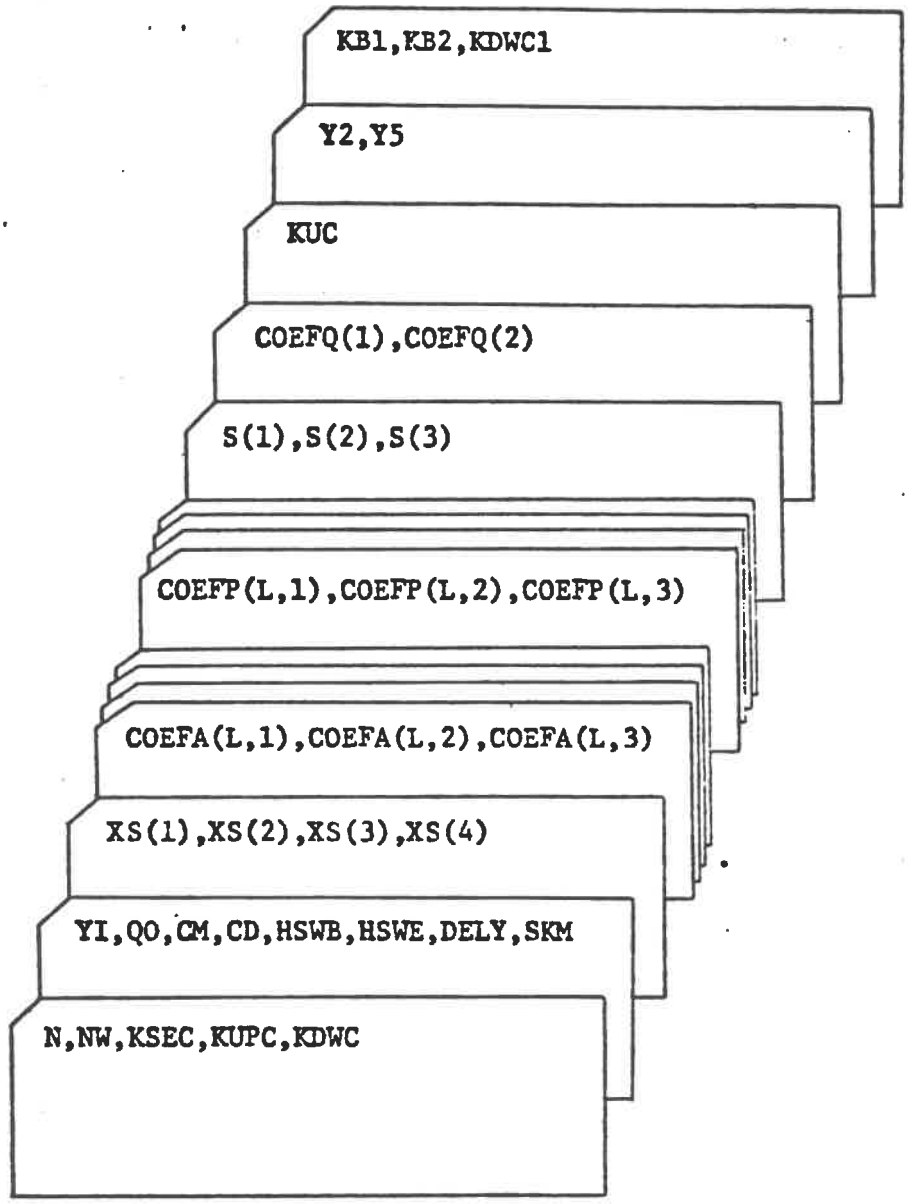

Figure 27

Generalized Diagram of Input for Computer Program

The Main Program

The main program controls the operation of the computer program and receives all input. It determines the control sections and by calling the subroutines, computes the water surface profile along the channel and prints out the results.

The Subroutines

Subroutine SWHT. SWHT computes the height of the side-weir in feet at any distance XX away from the reference section.

Subroutine WSP. WSP calculates the water surface profile, the rate of flow over the side-weir, and shows where the flow in the channel approaches critical.

Subroutine SECT. SECT computes the cross-sectional area of flow A, wetted perimeter P, top width of water section DA, second derivative of area DDA with respect to depth of flow Y and first derivative of wetted perimeter with respect to Y. For prismatic channels, the area is expressed by

$$A = COEFA(L,1)\ Y^{COEFA(L,2)} + COEFA(L,3)\ Y$$

where COEFA(L,1) is the channel side-slope at section L,

COEFA(L,2) = 2 and COEFA(L,3) is the base width at section L. For prismatic channels these coefficients are the same for all four sections. When the channel cross-section is nonprismatic the area for intermediate stations is found by interpolation.

The wetted perimeter for prismatic channels is expressed by

$$P = 2\sqrt{COEFP(L,1)^2 + 1}\; Y^{COEFP(L,2)} + COEFP(L,3) - NW\ H\sqrt{COEFP(L,1)^2 + 1}$$

where COEFP(L,1) is the side-slope at section L, COEFP(L,2) = 1 and COEFP(L,3) is the base width at section L. For prismatic channels these coefficients are the same for all four sections. The wetted perimeters for intermediate stations are found by interpolation in nonprismatic cases.

Subroutine YNOR. YNOR calculates the normal depth of flow YN (using Newton-Ralphson iteration method) for any reach when the discharge and the slope of the reach are known.

Subroutine YCRI. YCRI calculates the critical depth of flow YC by Newton-Ralphson iteration method.

Subroutine YSEQ. YSEQ computes the sequent depth YS based on the momentum principle by applying Newton-Ralphson iteration method.

Subroutine WSP1. WSP1 calculates the water surface profile along reaches 1 and 3 in cases where there are upstream and/or downstream control sections. WSP1 uses the same numerical iteration process as in WSP.

Subroutine SMINOR. SMINOR calculates the slope of the minor loss SM for the nonprismatic reaches of the channel. In the weir reach and in cases where a hydraulic jump is expected to occur, SM = 0. At the beginning SMINOR assumes that the depth of flow at the end of the transition to be equal to the depth at its beginning in order to find an approximate value for SM which is used to start the iteration process.

NOTATIONS USED IN THE COMPUTER PROGRAM

A	Cross-sectional area
AF	Correction factor for kinetic energy
AA1	Cross-sectional area at the beginning of a nonprismatic reach for a certain depth of flow Y
AA2	Cross-sectional area at the end of a nonprismatic reach for a certain depth of flow Y
A1	Cross-sectional area at the beginning of a step for a certain depth of flow Y
A2	Cross-sectional area at the end of a step for a certain depth of flow Y
CD	Nondimensional coefficient of discharge
CM	Manning's coefficient of roughness
CMM	= $CM^2/(1.486)^2$
COEFA(L,1)	Channel side-slope at section L (1 vertical on COEFA(L,1) horizontal)
COEFA(L,2)	Area coefficient at section L; equals 2
COEFA(L,3)	Base width of channel at section L
COEFP(L,1)	Channel side-slope at section L
COEFP(L,2)	Wetted perimeter coefficient; equals 1
COEFP(L,3)	Base width of channel at section L
COEFQ(J)	Coefficients for discharge calculation at section 4 when stage-discharge relation is given at this section (KDWC1 = 1)
DA	First derivative of cross-sectional area with respect to Y (top width of water section)
DADX	= (A1 - A2)/DX, partial derivative of A with respect to X when Y is constant

DDA Second derivative of A with respect to Y

DELY Increment in depth used to find the discharge downstream of side-weir in case of a rising profile

DIF Distance of a station from the beginning of the reach divided by the length of the reach

DP First derivative of wetted perimeter with respect to y

DQDX = $(2/3)CD\ NW\ \sqrt{2G}\ H^{1.5}$, discharge over side-weir per unit length

DX Incremental distance

DYDX = dy/dx

E Specific energy

E13 = 1/3

E23 = 2/3

E43 = 4/3

FN Froude number

G Acceleration due to gravity

H Height of water above the weir crest; equals 0 if Y < YW

HSWB Height of weir at the beginning of reach 2

HSWE Height of weir at the end of reach 2

HWX Height of weir at a distance X away from the reference section

I Identifies stations

J Number of reaches

J1 = J + 1

KB1 Code for identifying the first reach; equals 1 if first reach is prismatic and equals 2 if first reach is nonprismatic

KB2 Code for identifying the third reach; equals 1 if third reach is prismatic and equals 2 if third reach is nonprismatic

KDWC Code for identifying section 4; equals 1 if section 4 is not a control section and equals 2 if section 4 is a control section

KDWC1 Code for identifying the type of control at section 4; equals 1 if stage-discharge relation is known and equals 2 if depth of flow is known

KSEC Code for identifying channel cross-section; equals 1 if it is rectangular and equals 2 if it is not rectangular

KS3 Code for identifying the slope of the third reach S(3); equals 1 if S(3) is mild and equals 2 if S(3) is steep

KUC Code for identifying the type of control at section 1; equals 1 if depth of flow is known and equals 2 if critical depth is known

KUPC Code for identifying section 1; equals 1 if section 1 is not a control section and equals 2 if it is a control section

L Number of sections

L1 = L + 1

NW Number of side-weirs; equals 1 if side-weir is on one side and equals 2 if side-weirs are on both sides

P Wetted perimeter

PMF Pressure plus momentum

Q Discharge

QO Discharge in the first reach

QI(I) Discharge at station I

S(1) Bed slope of the first reach

S(2) Bed slope of the second reach

S(3) Bed slope of the third reach

SCRI Critical slope

SE Friction slope

SIGN Code for identifying the direction of computations; equals 1 if computations proceed downstream and equals -1 if computations proceed upstream

SKM Head loss coefficient due to linear expansion or contraction

SM Slope of minor loss due to change in cross-section of channel along a reach

SO Bed slope

TERM = $1 - AF\ V^2\ DA/AG$

XSB Distance of the beginning of a reach from the reference section

XSE Distance of end of a reach from the reference section

XX Distance of a station from the reference section

X(I) Distance of Ith station from the reference section

XS(1) Distance of section 1 from the reference section

XS(2) Distance of section 2 from the reference section

XS(3) Distance of section 3 from the reference section

XS(4) Distance of section 4 from the reference section

V Mean velocity of flow

Y Depth of flow

Y2	Depth of flow at section 1 when KUPC = 2
Y5	Depth of flow at section 4 when KDWC1 = 2
YC	Critical depth of flow
YI	Depth of flow for first trial for computation of normal depth in the first reach
YN	Normal depth of flow
YS	Sequent depth
YSI(I)	Sequent depth at the Ith station

C: EXAMPLES ON THE APPLICATION OF THE COMPUTER PROGRAM OCFCD4A

Three examples are carried out to illustrate the use of the computer program and its application for design purposes.

Example 1. A 1000 ft. concrete-lined rectangular channel with a base width of 50 ft. and a bed slope of 0.0009 is considered. The side-weir on one side of the second reach between stations 1+00 and 2+00 is 3.00 ft. high. The discharge in the first reach between stations 0+00 and 1+00 is 2500 cfs. Coefficient of discharge CD = 0.47 and Manning's coefficient of roughness CM = 0.013.

Required: The discharge downstream of the side-weir and the water surface profile along the channel.

Solution: In this application there are no boundary controls and the channel is prismatic. The computer output indicates that flow is subcritical along the first reach, goes through critical at the beginning of the side-weir and becomes supercritical along the side-weir reach. A jump is observed in the side-weir and flow becomes subcritical downstream of the side-weir. The resulting water surface profile is shown in figure 28.

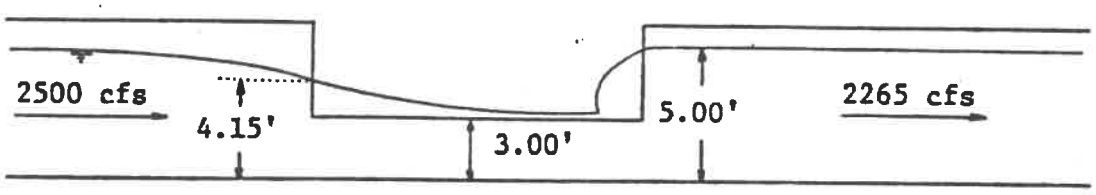

Figure 28

Water Surface Profile for Example 1

Example 2. The discharge in the first reach between stations 0+00 and 1+00 of a 1000 ft. long concrete-lined rectangular channel is 1900 cfs and the height of the side-weir between stations 1+00 and 3+00 is 12.0 ft. The channel has a constant bed slope of 0.002 and is prismatic along the first and second reaches with a base width of 10.00 ft. The base width expands linearly along the third reach from 10.0 ft. at station 3+00 to 15 ft. at station 10+00. Coefficient of discharge CD = 0.47, Manning's coefficient of roughness CM = 0.013 and the minor loss coefficient for the third reach SKM = 0.15. There is a 6.0 ft deep sluice gate opening along the base width at station 10+00 with a flow coefficient of 0.56. The stage-discharge relation at station 10+00 is expressed by

$$Q = 401.5\ y^{1/2}$$

Required: The discharge downstream of the side-weir and the water surface profile along the channel.

Solution: In this application the third reach is non-prismatic with a downstream control at section 4. The computer output indicates that the flow draw down from normal depth to 12.27' at the beginning of the side-weir and a rising profile is observed along the side-weir. Flow downstream of the side-weir is subcritical. Water surface profile for this application is shown in figure 29.

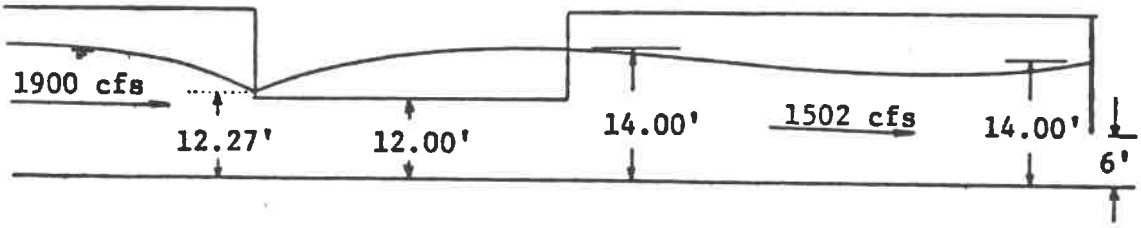

Figure 29

Water Surface Profile for Example 2

Example 3. The discharge in the first reach between stations 0+00 and 0+20 in a concrete-lined rectangular channel is 1440 cfs. The base width of the channel expands from 10.0 ft. to 30.0 ft. along the first reach. The depth of flow at station 0+00 is 5.32 ft. There is a 4.0 ft. high side-weir on one side of the prismatic second reach which is between stations 0+20 and 0+45.90. The base width of the third reach contracts linearly from 30.0 ft. at station 0+45.90 to 10.0 ft. at station 65.90. The control at station 0+65.90 is a 6.0 ft. diameter pipe. The slope of the channel is constant at 0.0049.

Required: Check that this design would lead to a downstream discharge of less than 460 cfs and find the corresponding water surface profile.

Solution: In this application both the first and the third reaches are nonprismatic and controls are imposed on both upstream and downstream ends. Computer output indicates that a jump occurs in the first reach and flow becomes subcritical along the side-weir and the reach downstream of side-weir. Water surface profile for this application is shown in figure 30.

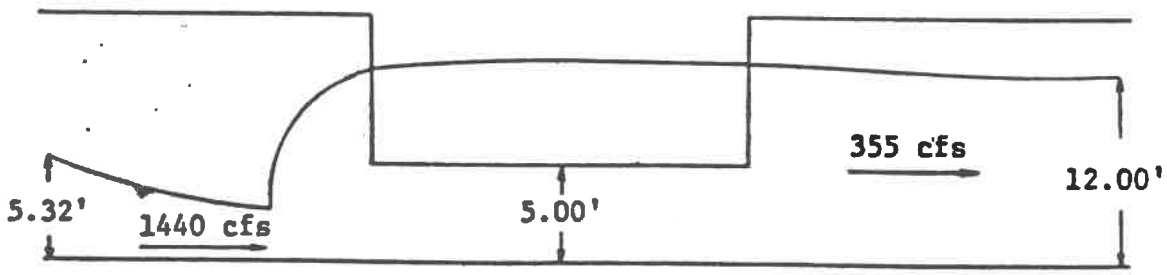

Figure 30

Water Surface Profile for Example 3

D: DESCRIPTION OF THE COMPUTER PROGRAM OCFCD4B

The computer program for the calculation of unsteady spatially-varied flow in an open channel with side-weirs is written in FORTRAN IV language and consists of a main program and five (5) subroutines. These subroutines are BDARY, INTER, MSIMQ, SECT and ARRAI. The generalized flow chart and the diagram of input for this program are shown in figures 31 and 32 respectively. A brief description of the main program and each of the subroutines is given in the following:

THE MAIN PROGRAM

The purpose of the main program is to control the operation of the whole computer program, to read necessary input data and to write output results. The principal input data fed into the main program include the number of sections, the location of each section, the slope of the channel, the initial water depth and flow rate at each section, the coefficient of roughness (Manning's Coefficient) of the channel, the coefficients controlling geometric characteristics of channel shape, the data controlling upstream and/or downstream boundary conditions, the height and the location of the side-weir and the appropriate coefficient of discharge of the side-weir.

The main program also controls the printing of calculated results at each specified time interval including the

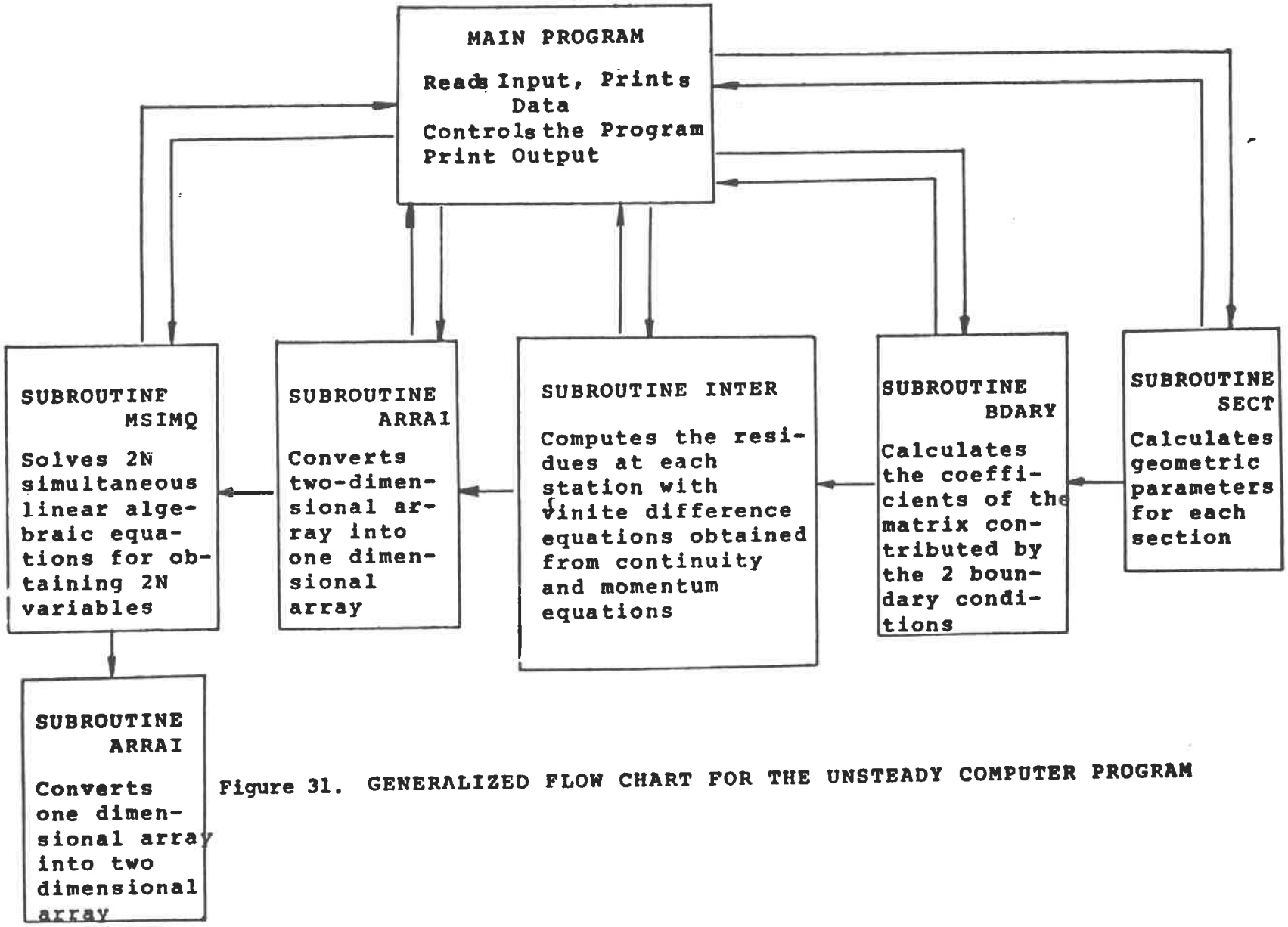

Figure 31. GENERALIZED FLOW CHART FOR THE UNSTEADY COMPUTER PROGRAM

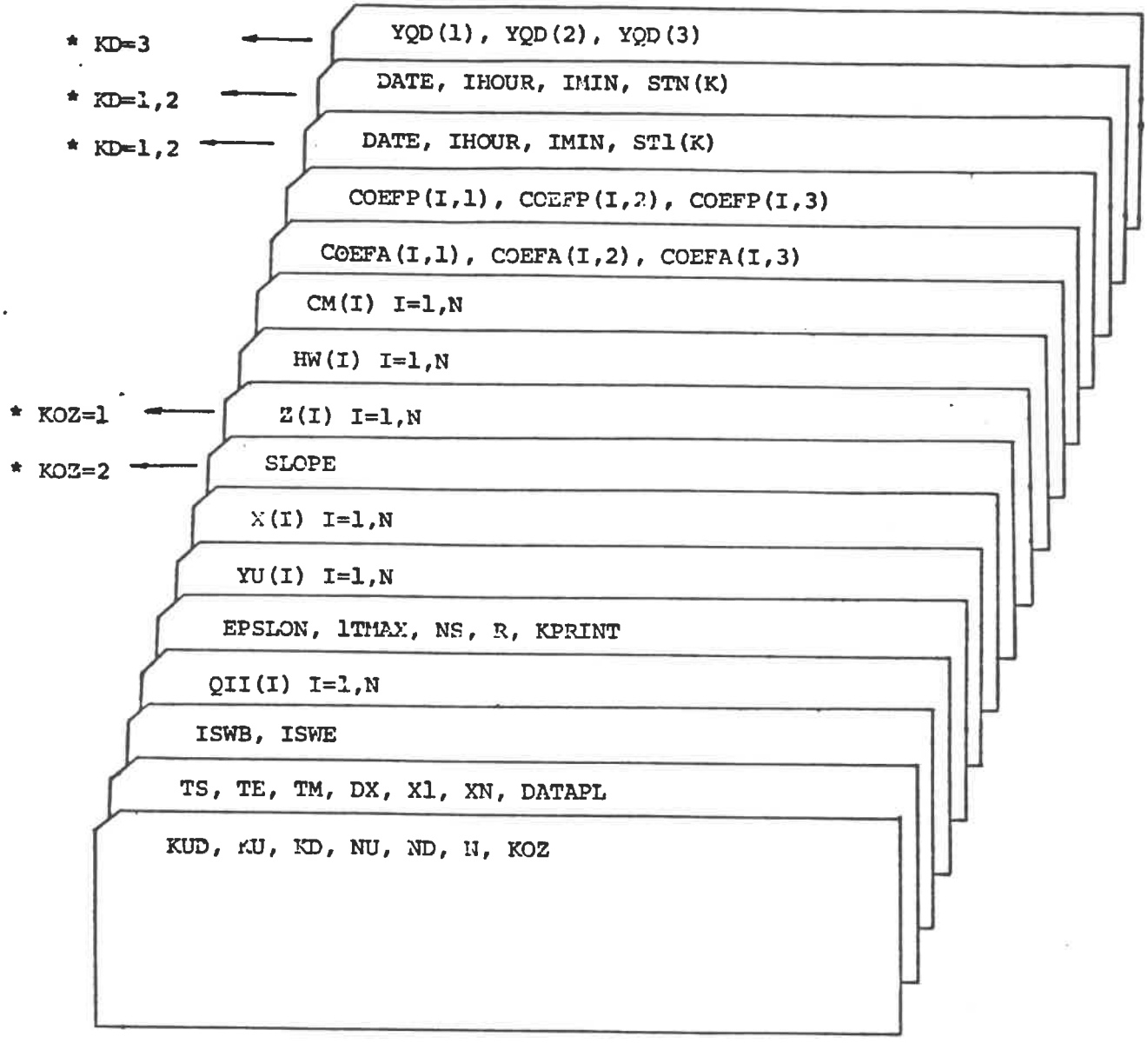

Figure 32. Generalized Diagram of Input for the Computer Program

* Needed for the conditions shown

water depth, the velocity, the discharge, the lateral discharge over the side-weir, the froude number at each section, the volume of water discharging from the side-weir between two adjacent time steps and the total volume of side-weir discharge.

SUBROUTINE BDARY

This subroutine is used for computing upstream and/or downstream boundary data at each time-step. The data then are used for computing residues and for obtaining elements of the coefficient matrix contributed by the boundary conditions. For the case where the flow at the beginning section of the side-weir is supercritical and the height of the side-weir is less than the critical depth corresponding to the initial flow in a prismatic channel, flow is controlled at the upstream side and thus two upstream conditions may exist. These two upstream conditions may consist of a stage or discharge hydrograph (elevation or discharge versus time) and a uniform flow relationship. For the case where flow is subcritical along the channel with a side-weir, one upstream and one downstream boundary condition may exist and the upstream boundary condition may be given as a hydrograph while the downstream boundary condition at the end of the channel may be a uniform flow relationship.

SUBROUTINE INTER

This subroutine is used for computing necessary data for all the interior sections which are sections other than those where the boundary conditions are specified. In this subroutine equations of continuity and momentum governing the unsteady spatially-varied flow with side-weirs in an open channel are transformed into the finite difference forms. Residues and elements of the coefficient matrix contributed by every subreach of the channel are computed. Newton-Raphson's method is then applied to calculate the flow parameters at a future time level when the flow parameters at a present time level are given.

SUBROUTINE SECT

This subroutine is used to compute several parameters which characterize the geometric properties of all the channel subreaches. These parameters include the cross-sectional area, the wetted perimeter, the top width and others.

SUBROUTINE ARRAI

This subroutine is used for changing a two-dimensional array into a one-dimensional array and vice versa. This process is required in solving simultaneous linear algebraic equations when the number of equations is not specified in the Dimension Statement of the computer program.

SUBROUTINE MSIMQ

This subroutine is used for solving simultaneous linear algebraic equations by the Gaussian elimination method.

NOTATIONS USED IN THE COMPUTER PROGRAM

A(I) = Cross-sectional area at station I for the advanced time level

AD(I) = Cross-sectional area at the given time level

B(I) = First derivative of A(I) with respect to depth of flow

C(I) = Vector representing residues formed by continuity and momentum equations for all sections

CD = Coefficient of discharge of the side-weir (CD=0 when there is no side-weir)

CM(I) = Manning's frictional coefficient at station I

COEFA(I,J) = No. J coefficient for determining the cross-sectional area of flow at station I

COEFP(I,J) = No. J coefficient for determining the wetted perimeter of the channel at station I

CONST = 1.486 $\sqrt{SLOPE}$ / CM(N)

D(I,J) = Coefficients of a matrix for the implicit finite difference process obtained by differentiation of momentum and continuity equations with respect to unknowns Y or V for all the sections

DATAPL = Datum plane for water surface elevation

DATE = Month/Day/Year at which the initial data are given

DB(I) = Second derivative of S(I) with respect to depth of flow

DP(I) = First derivative of P(I), the wetted perimeter at station I, with respect to depth of flow

DX = Distance interval in feet between stations

DXT = DX/DT

DT = Time interval in seconds used in finite difference method

DTX = DT/DX

EPSLON = Small positive number used in the convergence test

E13 = 1./3.

E23 = 2./3.

E43 = 4./3.

F1 = Residue of the equation which satisfies the first boundary condition

FN = Residue of the equation which satisfies the second boundary condition

G = Acceleration due to gravity

G1 = $G/(1.486)^2$

HW(I) = Side-weir height at station I

I = Station number

ISWB = Station at which the side-weir begins

ISWE = Station at which the side-weir ends

ITER = Iteration Counter

ITMAX = Maximum number of iterations permitted

KD = Code for identifying the second boundary data; equals 1 if stage-hydrograph is given, equals 2 if discharge hydrograph is given, equals 3 if Q=F(YQD(J),Y) is given, equals 4 if flow is uniform and equals 5 if flow is critical.

KCZ = Code for identifying the channel bottom slope; equals 1 if channel bottom elevations are specified at each station and equals 2 if the channel bottom slope is given.

KPRINT = Control whether or not to print the iterated results. KPRINT=1 means not to print and KPRINT=2 means to print.

KU = Code for identifying the first boundary data; equals 1 if stage hydrograph is given and equals 2 if discharge hydrograph is given.

KUD = Code for controlling the type of upstream and/or downstream boundary conditions; equals 1 if there is one upstream and one downstream boundary condition, equals 2 if there are two upstream boundary conditions and equals 3 if there are two downstream boundary condition.

N = Number of stations

ND = Number of second boundary data

NS = Number of subreaches between two adjacent stations for applying Simpson's rule (Composite Integration Formula)

NU = Number of first boundary data

P(I) = Wetted perimeter at station I

PFNV = Partial derivative of FN with respect to V

PFNY = Partial derivative of FN with respect to Y

PF1V = Partial derivative of F1 with respect to V

PF1Y = Partial derivative of F1 with respect to Y

QII(I) = Initial discharge at station I

R = Ratio of difference; is 0.5 for central differences, is 0 for backward differences and is 1 for forward differences.

SLOPE = Channel bed slope

STN(J) = Second boundary data in cfs of ft given at time TN(J)

ST1(J) = First boundary data in cfs or ft given at time T1(J)

TE = Terminal time in hours

TM = Maximum computing time interval in minutes

TN(J) = Time in hours which specify the Jth second boundary data

TS = Starting time in hours

T1(J) = Time in hours which specify the Jth first boundary data

VD(I) = Velocity of water flow at station I for a given time level

VU(I) = Velocity of water flow at station I for the advanced time level

WAD(I) = Mass (equivalent) in the block between section I-1 and I for a given time level

WAU(I) = Mass (equivalent) in the block between section I-1 and I for the advanced time level

WQD(I) = Momentum (equivalent) in the block between section I-1 and I for a given time level

WQU(I) = Momentum (equivalent) in the block between section I-1 and I for the advanced time level

XN = Last station in miles

X1 = First station in miles

YD(I) = Water surface elevation at station I for a given time level

YQD(J) = Coefficients governing the relationship of Y versus Q when XD=3

YU(I) = Water surface elevation at station I for the advanced time level

Z(I) = Channel bottom elevation at station I

E: EXAMPLES ON THE APPLICATION OF THE COMPUTER PROGRAM OCFCD4B

The solution of the unsteady flow problem in an open channel with decreasing discharge in a portion of the channel reach due to side-weirs can be grouped into three types: The first type includes cases when the flow is sub-critical throughout the channel reach and the flow profile is continuous; the second type is when the flow is super-critical throughout the channel reach and the flow profile is continous; the third type is when the flow is super-critical in the upstream portion of the reach and is sub-critical in the remaining portion of the reach and the flow profile is discontinuous due to the existence of a moving hydraulic jump.

Due to difficulties arising from the existence of a moving hydraulic jump in the application of this method, the solution to the third type of problems is not available at this time. Further research is needed for obtaining any meaningful results to problems in this category. Examples for the application of the proposed method leading to the numerical solutions of the first two types of problems are given in the following:

Example No. 1 - Subcritical Case

The following data for the channel are available:

Channel shape and roughness: Concrete lined rectangular channel, 10 ft. wide, Manning's Coefficient = 0.013.

Channel slope: 0.002

Channel length: 8,000 ft. (See Figure 33)

Upstream boundary condition: A triangular shape storm hydrograph from 1900 cfs rises linearly to a peak flow of 2500 cfs at the end of the first hour and then drops down linearly to 1900 cfs at the end of the second hour (See Figure 34).

Downstream boundary condition: Flow reaches uniform at the downstream end.

Side weir: 12 ft. high and 200 ft. long starting at station 4000 ft and ending at station 4200 ft. Discharge coefficient = 0.47.

Initial condition: The water depth and discharge values at each specified section are obtained from the backwater calculation given by the steady flow computer program.

Required

Determine the discharge and the stage hydrographs at the beginning section and the end section of the side weir and at the downstream end. Determine the total amount of flow released through the side weir from the above hydrographs.

Solution

The 8000 ft. long channel reach is divided into 15 blocks or subreaches (16 sections) as shown in Figure 33. The minimum block length (ΔX) is 20 ft. while the maximum block length (ΔY) is 2000 ft. The chosen time increment is constant and equals to 0.5 minutes giving a ratio of $(\frac{\Delta X}{\Delta t})$ min = 0.67 ft/sec. and $(\frac{\Delta X}{\Delta t})$ max = 67 ft/sec..

The water depth, the discharge, the flow velocity and the Froude number at all of the 16 channel sections and at each time increment are shown in the computer printout. The discharge hydrograph as plotted from data given by the computer printout at the upstream boundary section, the beginning section of the side weir, the end section of the side weir and the downstream section are given in Figure 34. The stage hydrographs at these sections are plotted in Figure 35.

The area bounded between the hydrograph at the beginning of the side weir and the hydrograph at the end of the side weir indicates the quantity of flow discharged laterally through the side weir.

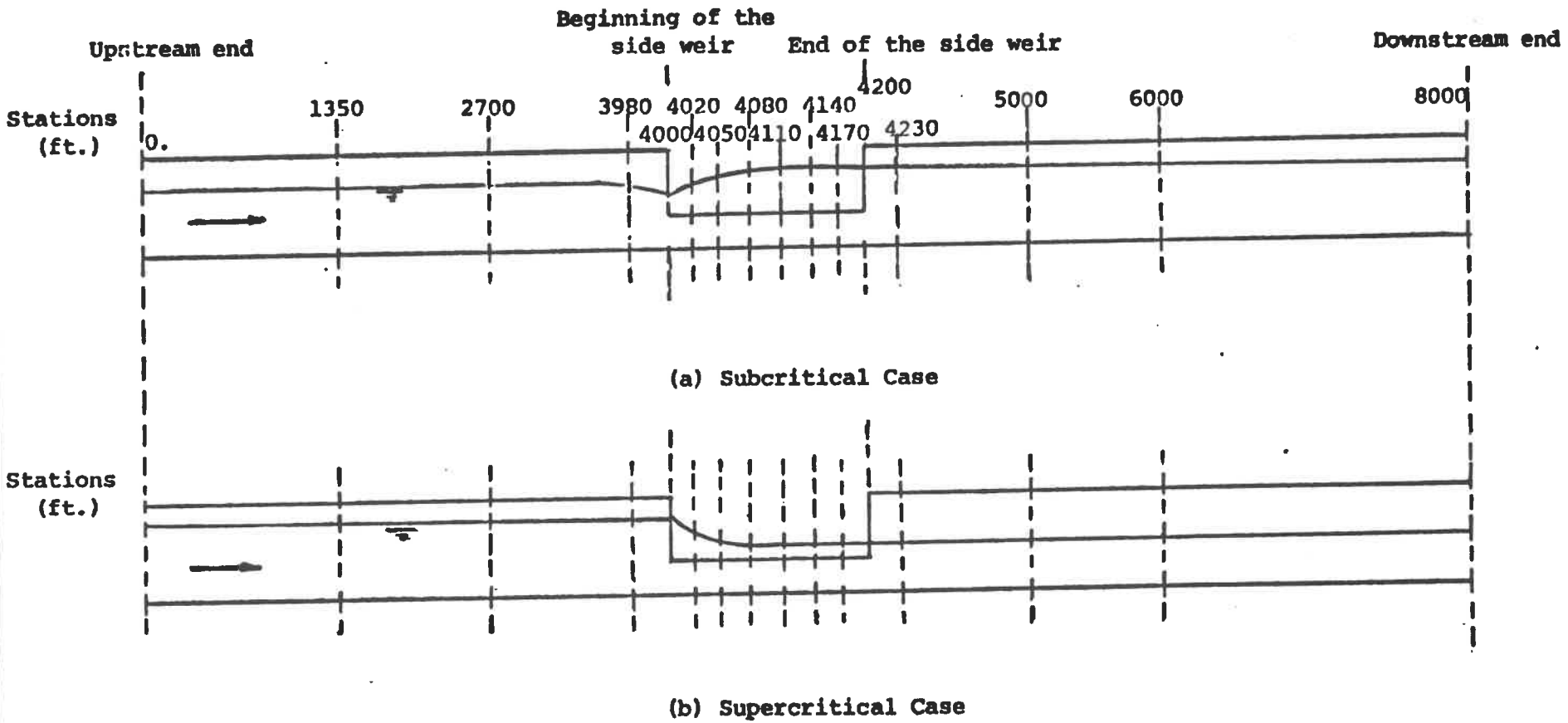

Figure 33. Schematic sketch of an open channel with a side weir

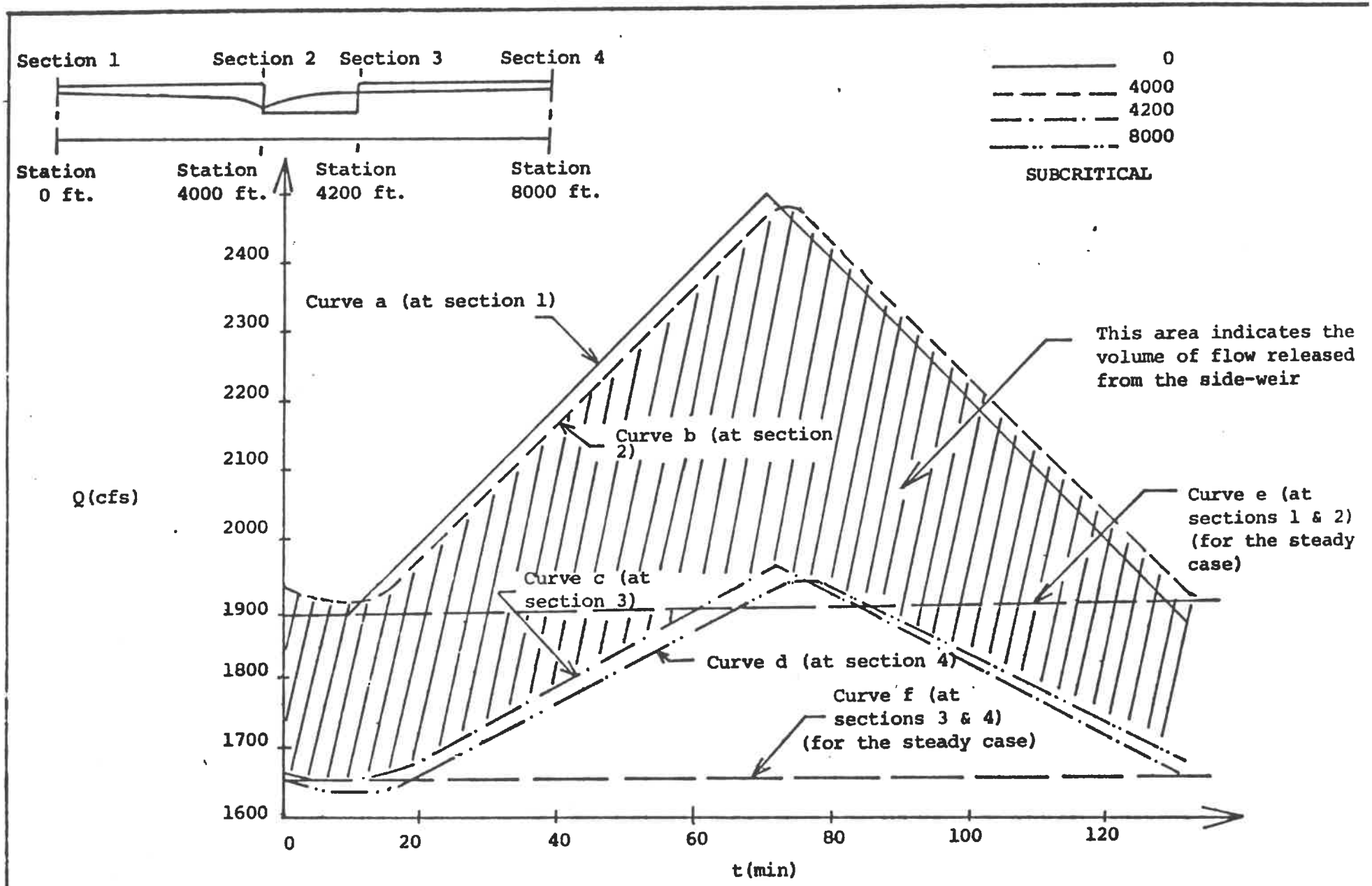

Figure 34. Discharge hydrographs at sections 1 through 4 for the 8000 ft. channel when flow is subcritical

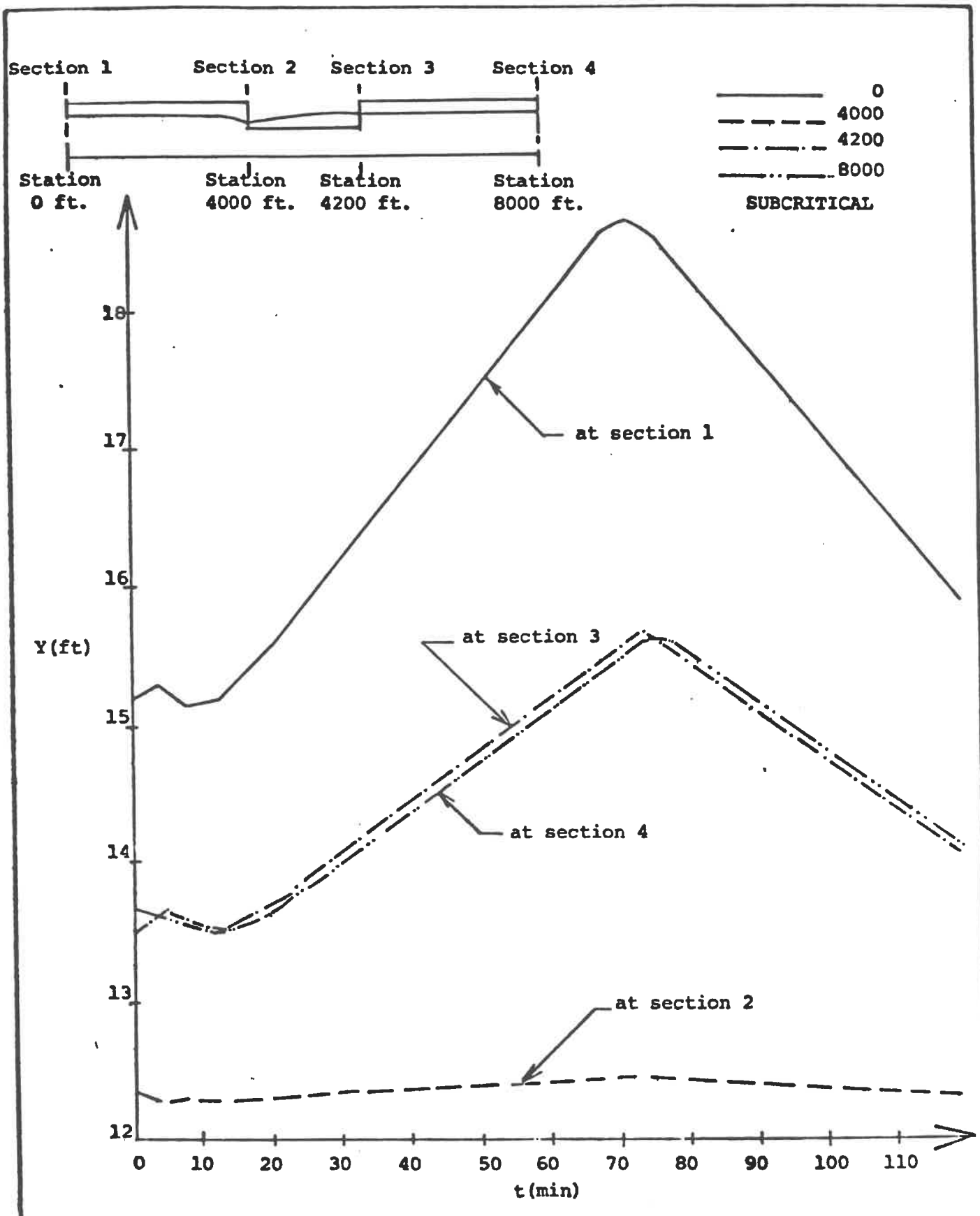

Figure 35. Stage hydrographs at sections 1 through 4 for the 8000 ft. channel when flow is subcritical

Example No. 2 - Supercritical Case

The following data for the channel are available:

Channel shape and roughness: Concrete-lined rectangular channel, 10 ft. wide. Manning's coefficient = 0.013.

Channel slope: 0.009

Channel length: 8000 ft. (See Figure 33)

Upstream boundary conditions:

(a) A triangular shape storm hydrograph from 1900 cfs rises linearly to a peak flow of 2500 cfs at the end of the first hour and then drops down linearly to 1900 cfs at the end of the second hour (See Figure 36).

(b) Flow becomes uniform at the upstream end.

Downstream boundary conditions: None.

Side weir: 2.5 ft. high and 200 ft. long starting at station 4000 ft. and ending at station 4200 ft. Discharge ccefficient = 0.47.

Initial condition: The water depth and the discharge at each specified section are obtained from the draw down calculation given by the steady flow computer program.

Required

Determine the discharge and stage hydrographs at the beginning section and the end section of the side weir and at the downstream end. Determine the total amount of flow released through the side weir.

Solution

As in Example No. 1, the channel is divided into 15 sub-reaches with 16 sections (See Figure 33). The minimum block length (ΔX) is 20 ft. while the maximum is 2000 ft. The time increment is 0.5 minutes giving a ratio of

$$\left(\frac{\Delta X}{\Delta t}\right)_{min.} = 0.67 \text{ ft/sec, and } \left(\frac{\Delta X}{\Delta t}\right)_{max.} = 67 \text{ ft/sec.}$$

Discharge and stage hydrographs are plotted based on the computer output and are shown respectively in figures 36 and 37. In figure 36 the area bounded between curves b and c represents the amount of flow discharged through the side weir for the unsteady case while the area bounded between curves e and f is the flow released through the side weir for the steady case when the flow rate at the upstream end is 2500 cfs at all time.

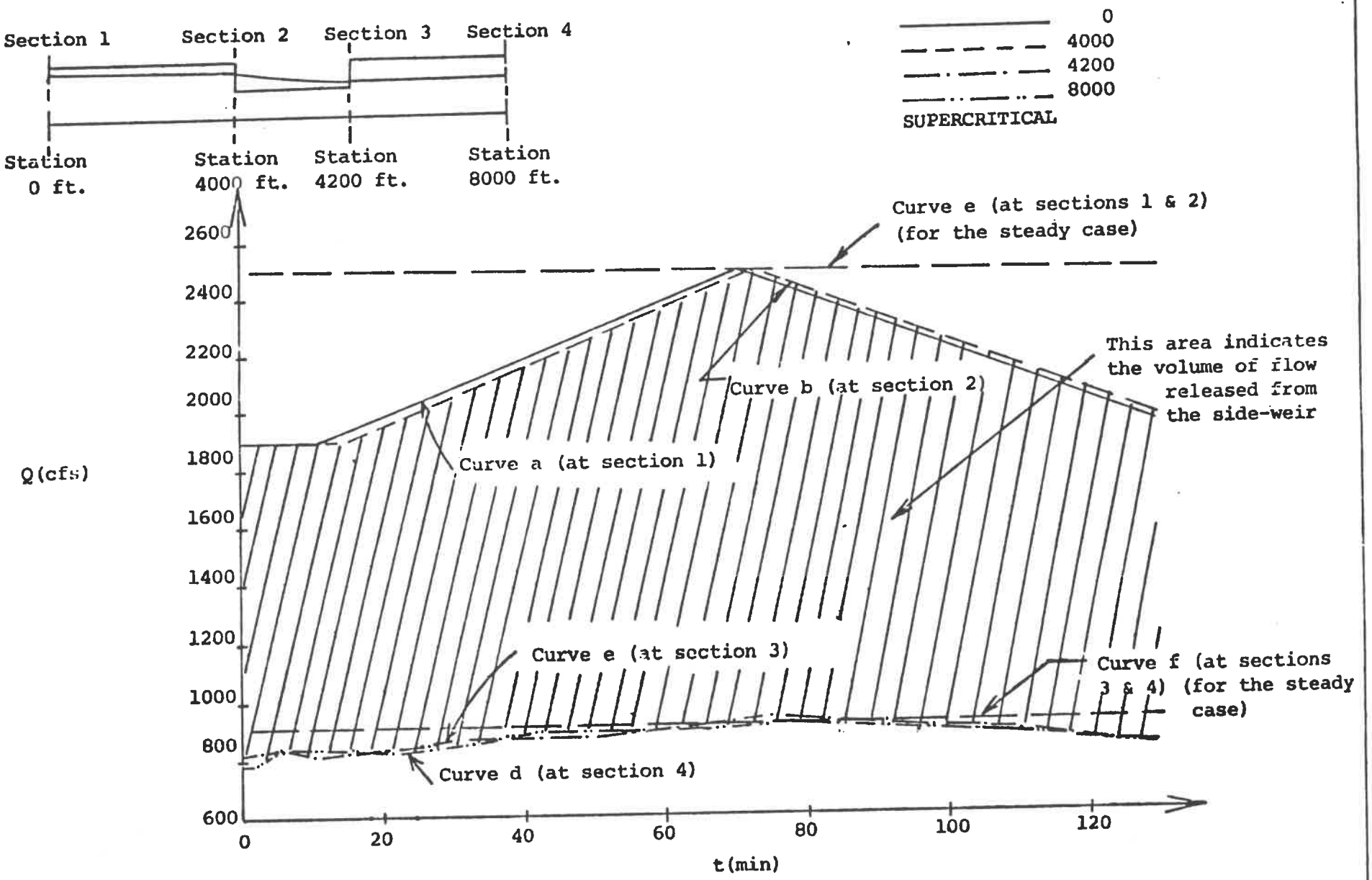

Figure 36 Discharge hydrographs at sections 1 through 4 for the 8000 ft. channel when flow is supercritical

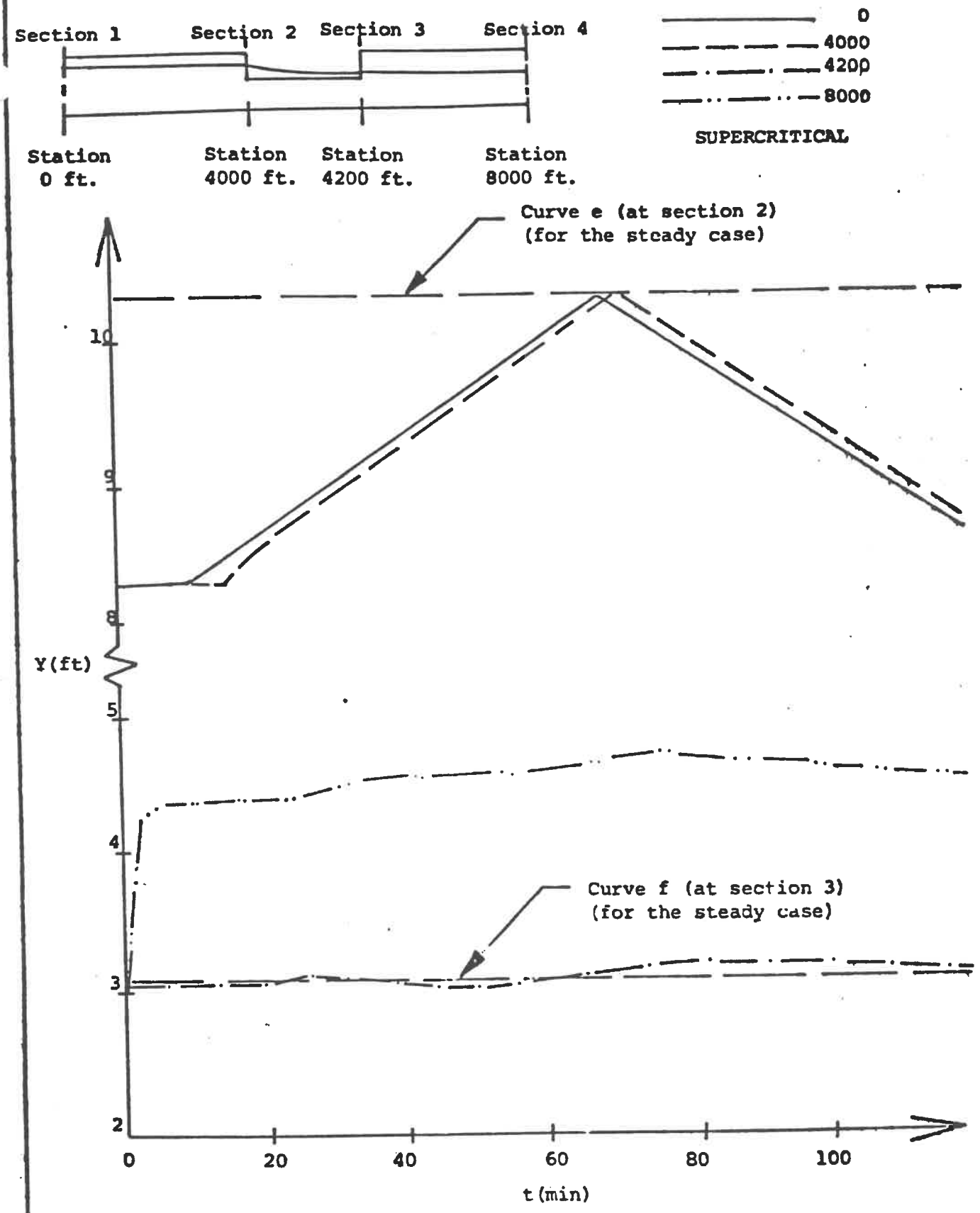

Figure 37 Stage hydrographs at sections 1 through 4 for the 8000 ft. channel when flow is supercritical

For the purpose of determining the effect of channel length to the unsteadiness of flow with decreasing discharge through a side weir, two more examples, one subcritical and the other one supercritical, are given in the following.

Example No. 3 adopts the same channel characteristics, side-weir dimensions and boundary conditions as those used in Example No. 1 with the exception that the total channel length is 52,800 ft. and the side weir starts at station 26,200 ft. and ends at station 26,400 ft. The computed discharge hydrographs and stage hydrographs of this example are shown in figures 38 and 39 respectively.

Example No. 4 uses the same data as those applied in Example No. 2 with the exception that the total channel length is 52,800 ft. and the side weir starts at station 26,200 ft. and ends at station 26,400 ft. The results of Example No. 4 are given in figures 40 and 41 .

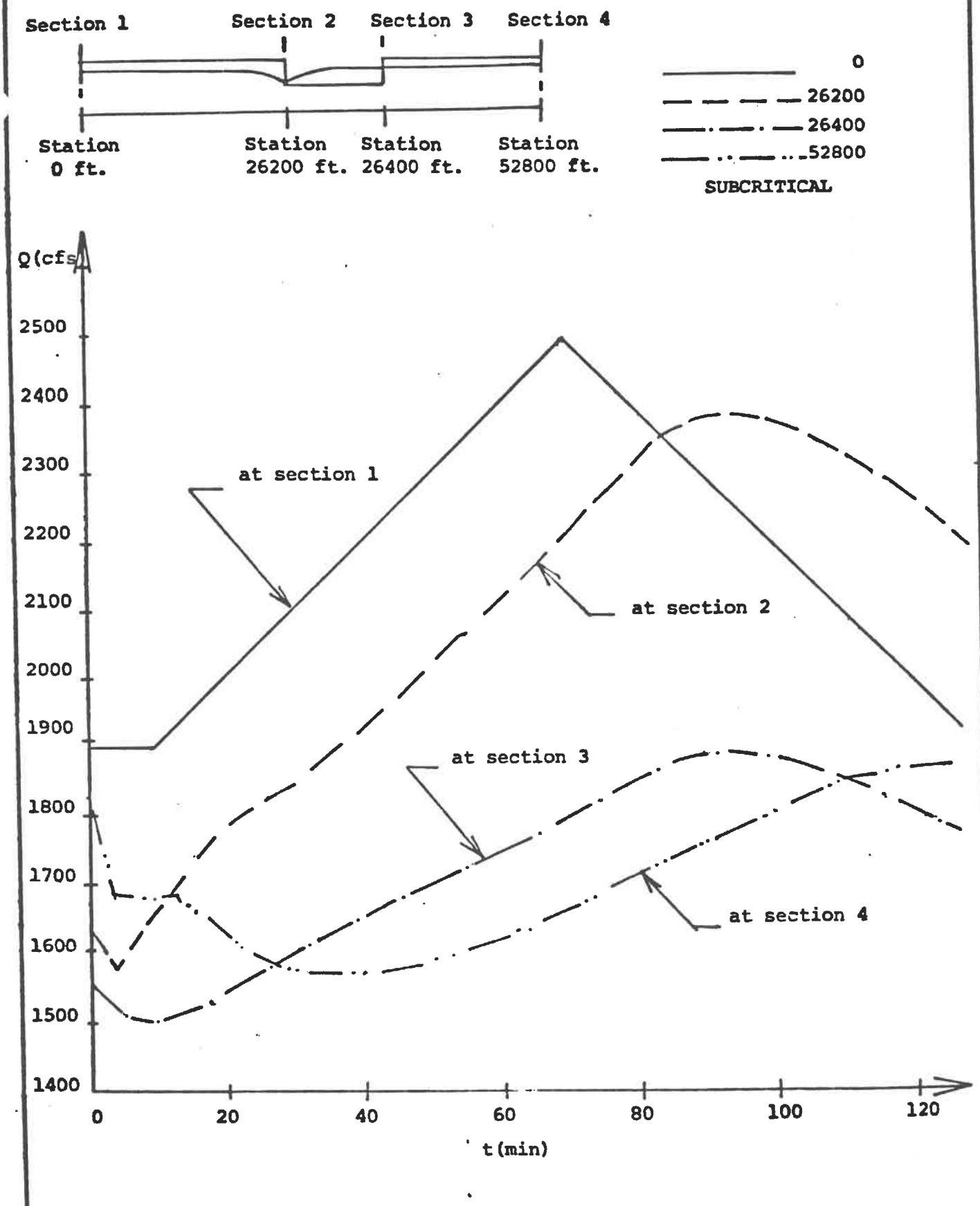

Figure 38 Discharge hydrographs at sections 1 through 4 for the 52800 ft. channel when flow is subcritical

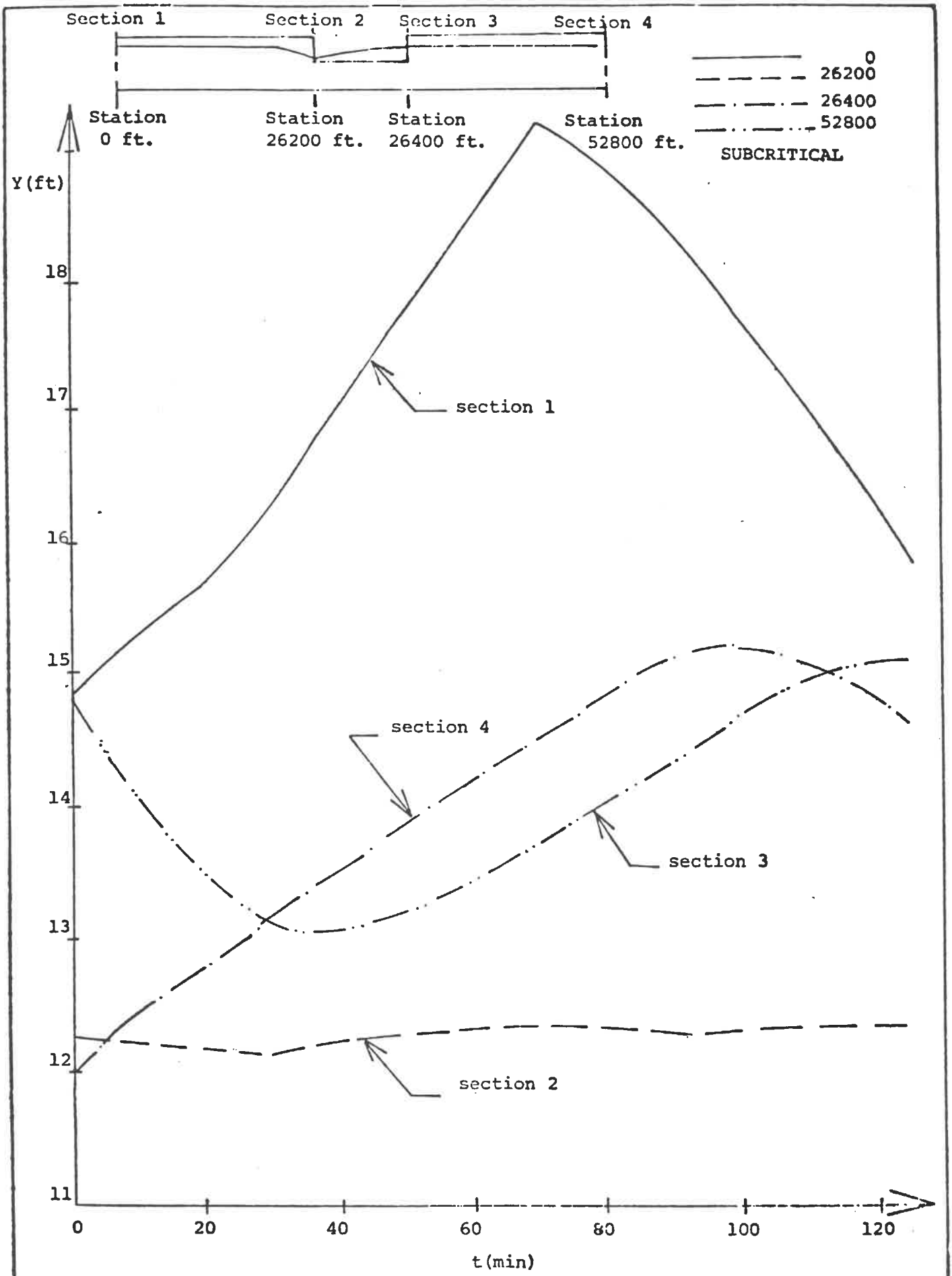

Figure 39 Stage hydrographs at sections 1 through 4 for the 52800 ft. channel when flow is subcritical

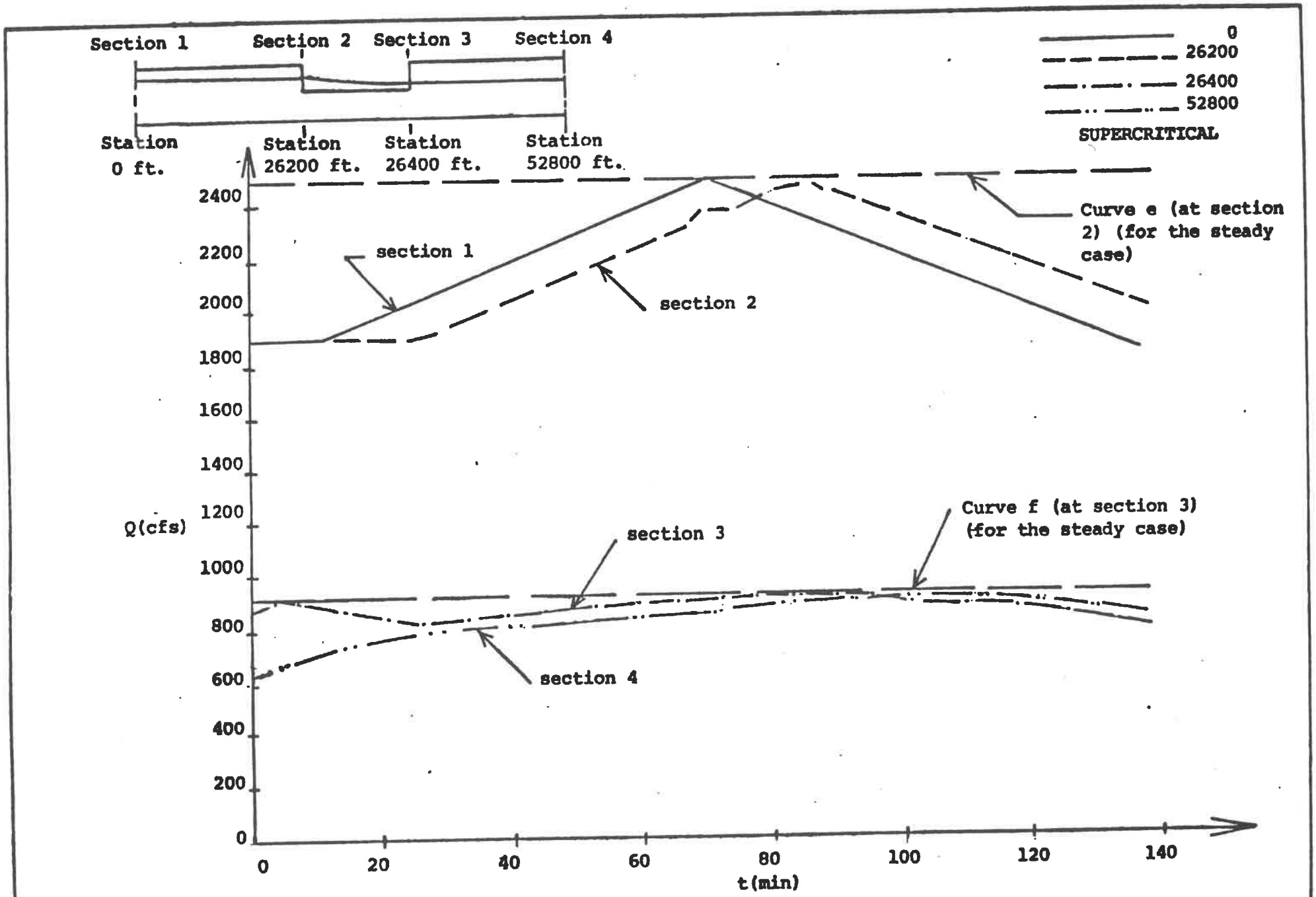

Figure 40 Discharge hydrographs at sections 1 through 4 for the 52800 ft. channel when flow is supercritical

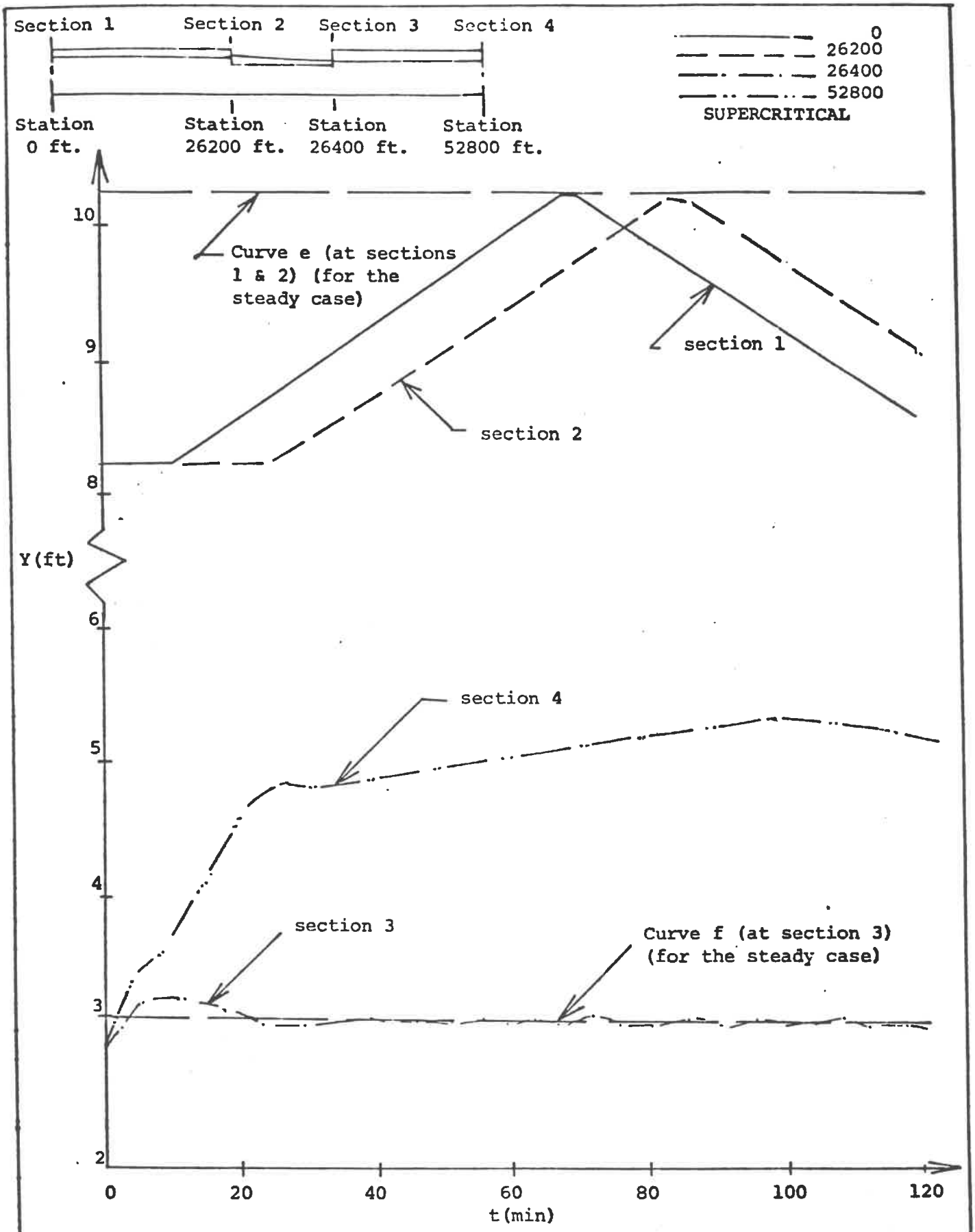

Figure 41 Stage hydrographs at sections 1 through 4 for the 52800 ft. channel when flow is supercritical

The stage and discharge hydrographs given in figures 36, 37, 40 and 41 suggest that for a channel with supercritical flow the stage or the discharge at the end of the side-weir remains almost constant regardless of the shape of the upstream hydrograph. Also for a channel with supercritical flow it is found that the subsidence of the stage or the discharge along the channel reach between the upstream end and the beginning of the side-weir is very little. Increasing the length of the channel upstream, will only delay the time that the peak discharge or the peak stage reaches the beginning of the side-weir but will not substantially increase the subsidence of either the stage or the discharge at the beginning of the side-weir. The above findings together with the result from a comparison of unsteady and steady solutions given in figures 36, 37, 40 and 41 suggest that, for a channel with supercritical flow, the steady case solutions based on different upstream discharges could be used to simulate the solution of the corresponding unsteady flow case with satisfactory results.

For the subcritical flow case the unsteady flow solution as given in figures 34, 35, 38 and 39 noticeably deviates from the corresponding steady flow solutions. The discharge along the channel reach between the upstream end and the beginning of the side-weir may subside an appreciable amount; the degree of subsidence increases with the length of the

channel reach. Therefore it may be concluded that it is not advisable to predict the unsteady flow solution of a channel with subcritical flow from the steady state solution when the hydrograph is relatively steep.

The computer program developed for this study has been run on a CDC 3150 computer facility at CSULB campus. As predicted, the implicit finite difference method as adopted in this study always provides stable results. It is shown, however, that scattering numerical values between adjacent sections or between adjacent time levels sometimes do occur when the ratio of the block length (Δx) and the time increment (Δt) is large. Based on numerical experiments, it is found that for the block length (Δx) in the range of 20 to 2000 feet, the time increment (Δt) of one minute gave unacceptable scattering in the results. Reducing (Δt) to half a minute reduced the scatter to an acceptable range.

REFERENCES

(1) Mostafa, M.G., Current Theories and Needed Research for Canal Protection by Diversion of Excess Flood Waters to Retarding Basins, Report prepared for Orange County Flood Control District, October 15, 1972.

(2) De Marchi, G., "Saggio de Teoria del Funzionamento degli Stramazzi Laterali" (Essay on the Performance of Lateral Weirs), L'Energia Elettrica, Milano, 11, November 1934.

(3) Eichert, B.S., "Survey of Programs for Water-Surface Profiles," Journal of the Hydraulics Division, American Society of Civil Engineers, February 1970.

(4) Smith, K.V.H., "Computer Programming for Flow over Side-Weirs," Journal of the Hydraulics Division, American Society of Civil Engineers, March 1973.

(5) Amein, M. and Fang, C.S., "Implicit Flood Routing in Natural Channels," Journal of the Hydraulics Division, American Society of Civil Engineers, December, 1970.

(6) Collinge, V.K., "The Discharge Capacity of Side Weirs," Proceedings, Institution of Civil Engineers, London, 6:288-304, 1957.

(7) Prasad, R., "Numerical Method of Computing Flow Profiles," Journal of the Hydraulics Division, American Society of Civil Engineers, 96:75-86, January, 1970.

(8) Baltzer, Robert A., and Chintu Lai, "Computer Simulation of Unsteady Flows in Waterways," Journal of the Hydraulics Division, American Society of Civil Engineers, July 1968.

(9) Chu, H.L., A Consistent Implicit Numerical Formulation of Flood Routing Method and its Application in Natural Channels and Reservoirs, Technical Report, Department of Civil Engineering, North Carolina State University, 1971.

(10) Weisz, D.M., Experimental Investigation of Flow Over Side-Weirs in a Rectangular Open Channel, Thesis in partial fulfillment of the degree of M.Sc.C.E., CSU Long Beach, August 1973.

(11) Liu, K.L., Experimental Investigation of Flow Over Side-Weirs in a Rectangular Open Channel: Phase II, Report on a Directed Study in partial fulfillment of the degree of M.Sc.C.E., CSU Long Beach, May 1974.

(12) Kayiran, O.Z., Mathematical Model for Spatially-Varied Flow in Open Channels with Side-Weirs, Thesis in partial fulfillment of the degree of M.Sc.C.E., CSU Long Beach, January 1974.

(13) Tults, H., "Flood Protection of Canals by Lateral Spillways," Journal of the Hydraulics Division, American Society of Civil Engineers, 82:1077, 1-14, October 1956.

(14) Frazer, W., "The Behaviour of Side Weirs in Prismatic Rectangular Channels," Proceedings, Institution of Civil Engineers, London, 6:305-328, February 1957.

(15) Ackers, P., "A Theoretical Consideration of Side Weirs as Storm-Water Overflow," Proceedings, Institution of Civil Engineers, London, 6:250-269, February 1957.

(16) Hulsing, H., Smith, W. and Cobl, E.D., Velocity-Head Coefficients in Open Channels, U.S. Geological Survey, Water Supply Paper 1869-C, Washington, D.C., 1966.